Thermal Remote Sensing and the Exergy Destruction Principle Applied to Precision Agriculture

by

Reece Lawrence

A thesis
presented to the University of Waterloo
in fulfillment of the
thesis requirement for the degree of
Master of Applied Science
in
Mechanical and Mechatronics Engineering

Waterloo, Ontario, Canada 2016

Author's declaration

I hereby declare that I am the sole author of this thesis. This is a true copy of the thesis, including any required final revisions or corrections, as accepted by my examiners.

I understand that my thesis may be made electronically available to the public.

Abstract

The objective of this thesis is to investigate the application of exergy analysis for classifying the health and maturity of ecosystems as defined by the exergy destruction principle and to determine its suitability as a tool within the precision agriculture industry. In doing so, this thesis presents some initial background information of precision agriculture but then heavily focuses on the core principles of exergy theory, starting with a general thermodynamical background, followed by a review of solar exergy, and concluding with a thorough review of the exergy destruction principle. Finally, the experiments which were conducted as part of the field work for this thesis will be presented and discussed.

Through the investigation of the interaction of exergy with living (and non-living) systems, a connection becomes clear between ecosystem development (complexity) and exergy destruction. As illustrated in principle with the Bénard cell, as systems become more complex they require increasing amounts of work potential in order to maintain structure. Conversely, as part of the redeveloped second law of thermodynamics, it is shown that any system which is imparted with a gradient will organize itself as to mitigate the effect.

By identifying the importance of surface temperature to the exergy flows of an ecosystem via the exergy destruction principle, it allows for various characterizations of both health and maturity to be inferred through thermal remote sensing. With applications for precision agriculture in mind, the effectiveness of utilizing remotely sensed surface temperature in order to infer crop health (stress) and crop complexity (yield) is tested and discussed.

Based on initial trials in both realistic field and controlled greenhouse conditions, there appears to be a statistically significant correlation between surface temperature and stress artificially induced in both the nitrogen and weed trials in corn and wheat. Yield also appears to be correlated with surface temperature, as was suggested by previous research. These results suggest that thermal remote sensing of temperatures can be utilized in a precision agriculture management regime in order to actively identify, and possibly quantify the effect of stress on crops.

Acknowledgements

I would like to thank the following people for their input and contributions throughout the entirety of the research that went into this thesis. First, my advisor and mentor Professor Roydon Fraser, I would like to thank you for sticking with this idea throughout the years and finally taking a chance on me to pursue a research topic that was outside of the norm. Your tireless pursuit of engineering excellence and enabling me to think outside of the box will be something I take with me long after. Second, I would like to thank my co-advisor Professor Clarence Swanton, much like Professor Fraser you stuck with this idea through thick and thin and only through your perseverance is this research finally realized. Your passion for your craft is truly remarkable and I thank you for taking me in as one of your students. To both of you, this thesis is as much yours as it is mine.

Finally, I would like to thank the entire field staff at the University of Guelph who laid down the groundwork so that our trials and experiments ran smoothly. Specifically I would like to thank Peter Smith and Dietmar Scholz, you guys went above and beyond to help me whenever I needed it and did countless work behind the scenes without recognition.

Table of Contents

List of Tables

List of Figures

Chapter 1. Introduction

1.1 Introduction

The overall objective of this thesis is to investigate the application of exergy analysis for classifying the health and maturity of ecosystems as defined by the exergy destruction principle, and to determine its suitability as a tool for use within the agriculture industry. Exergy is a product of the first and second laws of thermodynamics and represents the quality of energy, or more specifically the ability of a system to perform useful work. While exergy has been predominantly used within the confines of engineering optimization, it is starting to find considerable use in a diverse range of non-engineering disciplines such as ecology, biology and sustainability (Jørgensen et al., 1995; Jørgensen, 2006;Jørgensen, 2008; Rosen and Dincer, 2005; Schneider and Kay, 1994; Wall, 1977; Kay, 1991; Kay, 2000; Maes et al., 2011; etc).

The first attempt to utilize the fundamental laws of science to understand the underpinnings of life and why biological processes occur as they do was theorized by Erwin Schrödinger in 1944 with his short book: What is Life? (Schrödinger, 1944). In this work it was theorized that life existed due to two fundamental processes, first being "order from order" and the second being "order from disorder". Schrödinger predicted that there was something at play in the human gene which transferred various traits onto ones kin, representing his first "order from order" process, which was later confirmed to be the case in 1953 when the molecular structure of Deoxyribonucleic acid (DNA) was identified by Watson and Crick.

The second premise, "order from disorder" was Schrödinger's attempt at combining biology with thermodynamics in order to better explain why living systems behave the way they do. Specifically, Schrödinger noted that in apparent contradiction with the second law of thermodynamics, ecosystems and seemingly all living things continue to exist in very ordered and complex states. This observation lead Schrödinger to the realization that ecosystems could not be studied by assuming they were simple closed systems, but in fact, must be treated as open systems that freely exchange energy and matter with their surroundings and operate in a state of far from equilibrium.

While thermodynamics in the "classic" sense was utilized to predict or model how a system would come into equilibrium given a certain change in conditions, this framework needs to be reworked when examining systems which exist in a constant "far from equilibrium" state. It will be shown through an extension of the thermodynamic laws described by Hatsopoulos, Keenan and Kestin that these thermodynamic systems are maintained and thus described via the gradients which are imparted upon them from their surroundings (Hatsopoulos and Keenan, 1965; Kestin, 1966).

Through this restated version of the second law it becomes clear that when any system is moved away from equilibrium, it will take advantage of all processes available to it, and even develop new processes, in order to resist any further movement. Schneider and Kay were the first to propose how this restated version of the second law could be applied to complex

structures, such as ecosystems, which operate in far from equilibrium conditions due in part to the exergy it receives from the sun (Schneider and Kay, 1994). This restated version of the second law of thermodynamics came to be known as the exergy destruction principle and is stated below in its entirety.

> ***A system exposed to a flow of exergy from outside will be displaced from equilibrium. The response of the system will be to organize itself so as to degrade the exergy as thoroughly as circumstances permit, thus limiting the degree to which the system is moved from thermodynamic equilibrium. Furthermore, the further the system is moved from equilibrium, the larger the number of organizational (i.e. dissipative) opportunities which will become accessible to it and consequently, the more effective it will become at exergy degradation. This is the exergy degradation principle for nonequilibrium thermodynamic situations. (Kay, 2000)***

A full breakdown of the exergy destruction principle and how it can be specifically applied to agriculture is presented in Section 5.3.

The exergy destruction principle represents an important philosophical shift in the attempt to quantify ecosystem health and complexity, and represents the theoretical basis for the work presented in this thesis. It will be hypothesized just how crucial exergy is to modeling and quantifying far from equilibrium systems. Specifically, it will be theorized how exergy theory can be applied to measure the maturity of various land types and the degree with which a crop is effected by stress.

Through the exergy destruction principle it is hypothesized that healthy plants will optimize their surface temperature in relation to their environment in order to maximize the incoming solar exergy (Section 5.5). It is also hypothesized that stress hampers a plants ability to destroy or utilize the incoming exergy, thus making it more susceptible to the incoming solar exergy gradient which pushes it farther away from equilibrium. Agricultural crops are a well suited subject to test this hypothesis as it provides more control over other variables such as stress (nitrogen) and invasive plants (weeds). The trials conducted in this thesis are described in Chapter 6.

1.2 Model Assumptions

Ecosystems are complex thermodynamic systems which exchange matter and energy with their surroundings. As a function of a plants complexity, it is difficult to trace and quantize all the energy and exergy flows which plants utilize. The exergy destruction principle examines plants as a thermodynamic "black box", therefore internal functions and processes do not need to be known. A system diagram visualizing these flows is shown in Figure 1-1.

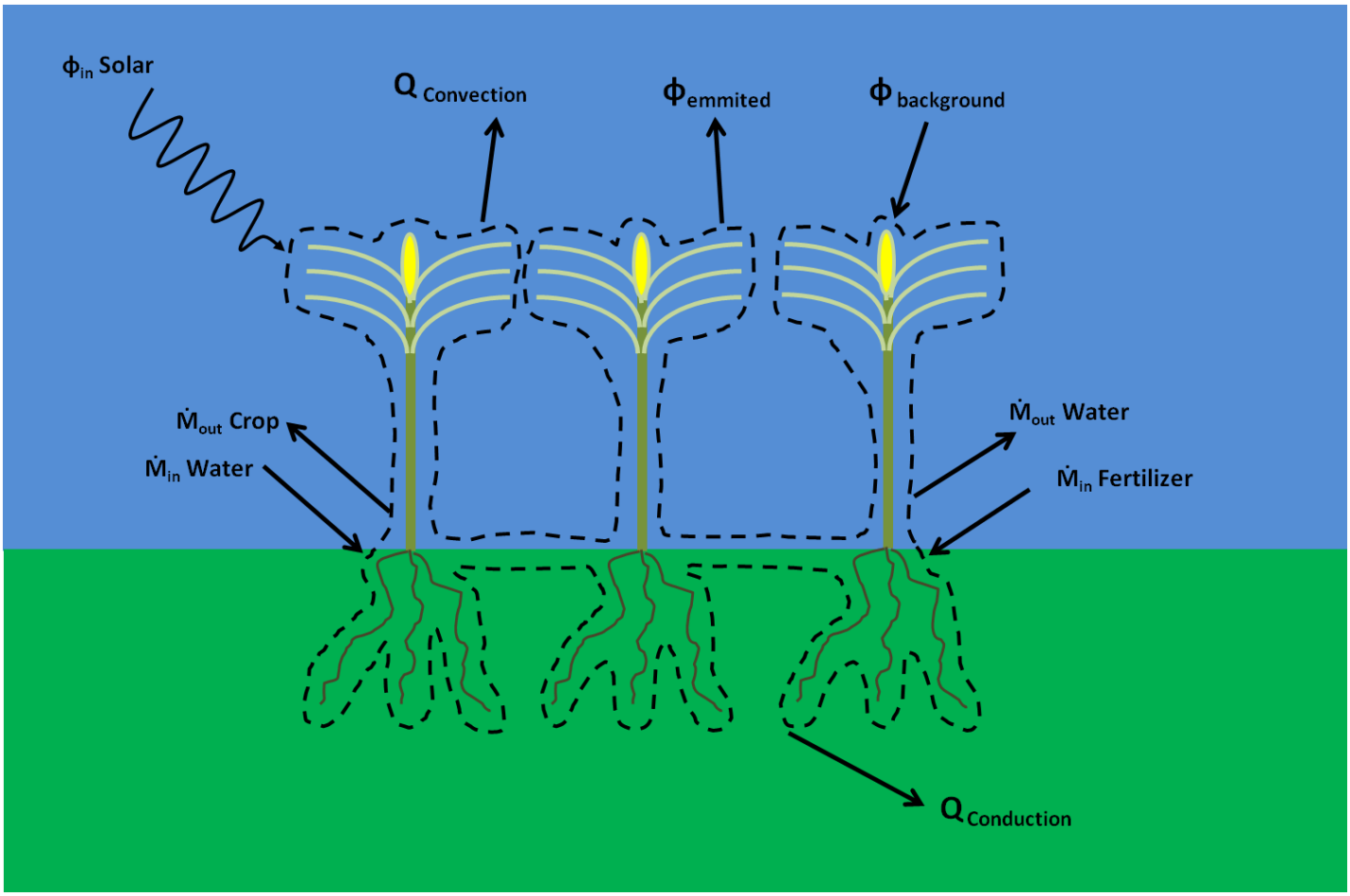

Figure 1-1 Inflows and outflows in corn

where $\dot{M}$ represents the mass flow, Q represents the convective or conductive heat transfer, and ϕ represents the radiative flux, where exergy flows are associated with all energy flows. It is important to note that ϕ is not the net radiation energy transfer, but the flux in a given direction, either into or out of the system. This is important because, as shown in Chapter 5, the exergy destruction principle hypothesizes in part that plants will strive to maximize the amount of exergy available to them. As a consequence, the characterization of **incoming** exergy flows are hypothesized to possibly be sufficient to characterize the health and operation of plants. That is, **only the incoming exergy flows are being considered in this research.** As an outcome

of this hypothesis, measuring the dominate exergy inputs into the system becomes crucially important when inferring the health of plants. Explained in detail in Chapter 4, the exergy content of the incoming solar radiation is largely a function of plant **surface temperature**, which a plant can inherently change or manipulate. And as shown in Chapter 5, solar radiation dominates the exergy inputs into agricultural ecosystems.

1.3 Research Objective

While remaining consistent with the overall objective of **investigating the application of exergy analysis for classifying the health and maturity of ecosystems as defined by the exergy destruction principle**, the research presented in this thesis covers two main sub-objectives:

- Build off of and confirm findings from previous experiments in the exergy theory field
- Determining the feasibility and effectiveness of exergy theory for identifying stress in agricultural crops for use within the precision agriculture sector.

Various experiments conducted in past years (Luvall and Holbo, 1991; Akbari, 1995; Maes et al., 2011) have investigated the suitability, either directly or indirectly, of exergy theory to be utilized as a key ecosystem indicator. The work in this thesis will further elaborate on those results and bring clarity to what exergy represents in an agricultural context and how it should be properly applied to generate useful results.

While exergy theory can be applied to all types of ecosystems (natural regenerating forests, tilled fields, agricultural crops etc) the trials and results conducted in this thesis will focus on the applicability of exergy theory for use in the agricultural sector and thus mainly cover ecosystems such as tilled cash crops.

1.4 Scope of work

The work presented in this thesis focuses primarily on the application of exergy theory to agricultural corn crops grown both in a typical outdoor setting and a more controlled greenhouse environment. In these trials the corn was subjected to various degrees of stress via either variable initial nitrogen rates (0, 0.5X, 1X, 2X where X is the standard nitrogen rate given in Kg/Hectare applied post planting) or timed weed removal (an analog weed of wheat was utilized and removed at specific corn leaf stage). While corn was the main crop studied in the presented trials, variable nitrogen rate wheat was also investigated, again using the same nitrogen application regime of 0, 0.5X, 1X and 2X.

Surface temperature was the main observable measured in all trials with the majority of data being collected via a thermal imaging camera (640 x 480 resolution and 7.5 to 14 micron spectral range). Thermocouples (Type T) were also utilized in a number of trials to provide longer duration measurements from a consistent and single location on the plants.

Chapter 2. Precision Agriculture

A crucial component to the theoretical framework presented in this thesis is the technology, infrastructure, or "management technique" which allows the theory to be put into action, all of which fall under the umbrella term of precision agriculture. Specifically, precision agriculture or precision farming describes whenever agricultural information is gathered with regards to its geographical position, through use of GPS or other spatial monitoring. Some typical examples of precision agriculture include: yield mapping, variable spraying of herbicides or pesticides, and targeted irrigation. The objective of this chapter is to investigate the concept and background of precision agriculture, outline the popular applications and introduce the importance of remote sensing as it pertains to crop management.

2.1 Background

At its core, precision agriculture represents the binding of Geographical Information Systems (GIS) with spatial tools (location) in order to make more efficient and effective farming decisions. With the increased costs associated with farming chemicals, the growing environmental concerns over chemical runoff, and the increased weed resistance due to blanketed spraying of herbicides, it is no surprise that farmers are turning to new innovative methods to deal with these challenges. Through the use of precision agriculture, chemical applications can become targeted, and only applied where the data suggests it is needed. This essentially eliminates "blanketed" applications from a farmers crop management regime and

has a dual benefit of reducing the waste or negative environmental effects while also cutting costs.

It should also be noted that precision agriculture as a whole is not specifically a "technology", but rather a crop management technique that employs tools and analysis in order to make more informed agricultural decisions. This management strategy can be broken down into four stages (Adl, 2014):

1. **Geo-location of data**

   "enables the farmer to overlay information gathered from analysis of soils and residual nitrogen, information from previous crops etc."

2. **Characterizing variability**

   "investigating variability in data due to climate conditions, soils, cropping practices etc."

3. **Decision making: 2 ways for dealing with variability**

   "Farmers can choose to deal with variability in two ways: Predictive (using static indicators such as history) or Control (using indicators that are updated regularly during the growing cycle such as remotely sensed data)"

4. **Implementing practices to address variability**

   "Application of crop management decisions"

The following sections will highlight examples of two of these stages which are most pertinent to the work presented in this thesis. First, yield mapping will be explained as it represents the origin of precision agriculture as a whole, and can be used as an example of stage 1. Next

examples of various crop management decisions such as targeted irrigation and chemical application will be investigated, which can be used to illustrate stage 4 and the applicability of thermal remote sensing as a tool for precision agriculture.

2.2 Yield Mapping

The first commercially available yield monitor ("Yield Monitor 2000") was developed in 1992 by Al Meyer and represented the shift in precision agriculture from being a management tool which only "early innovators" utilized to something which the "early majority" could adopt (Risius, 2014; Brase, 2005). A brief timeline of the early days of precision agriculture is shown below:

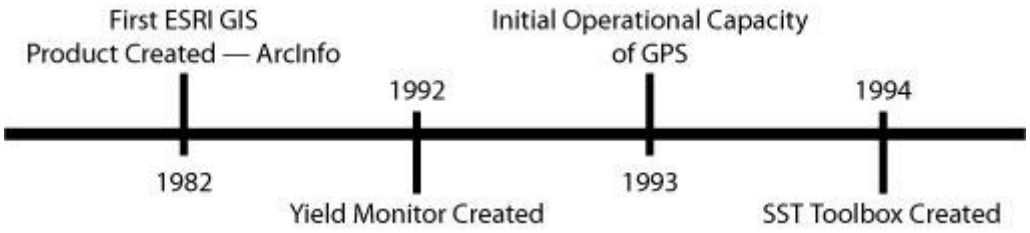

Figure 2-1 Precision Agriculture in the 1990's
Source: Brase, 2005

By combining these newly available yield monitors with the increasingly reliable Global Positioning System (GPS), yield maps could be formulated in order to provide the user with yield variability data throughout their fields. By creating these yield maps and overlaying them with satellite images or other metrics one could start to visualize problem areas in their field

(stage 1). This would only be added and expanded with the increasing use of high level statistical software which could run models over multiple years of historical data in order to draw more meaningful conclusions. An example of yield maps of a single field over a number of years is shown below, with red representing lower than average yields and green representing higher.

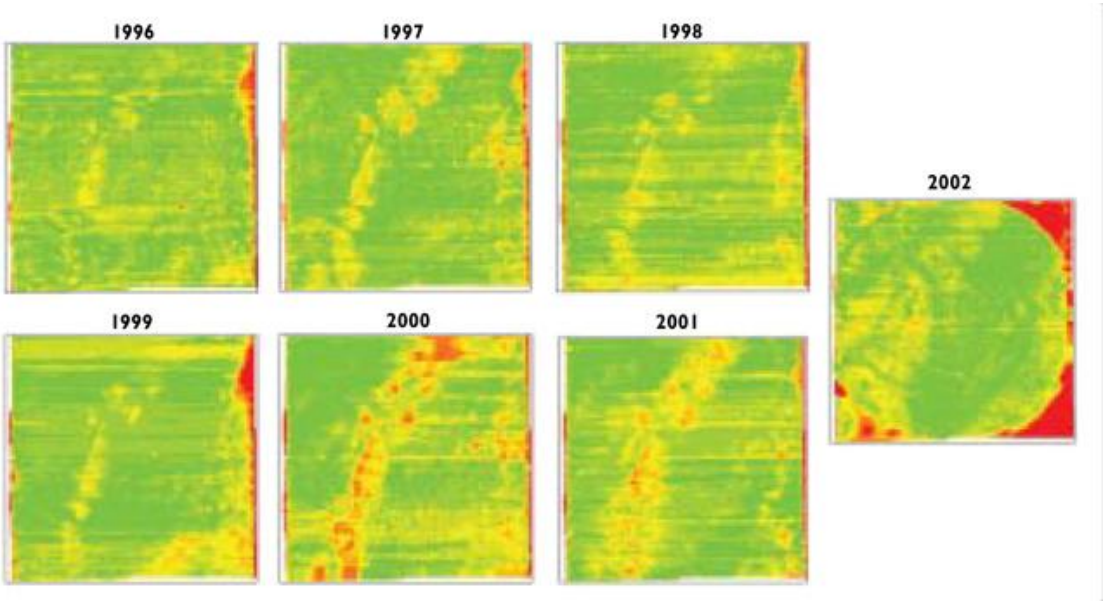

Figure 2-2 Agricultural yield map of corn over 7 years
Source: Nebraska Crop Watch

Yield maps can be in essence taken as the final results of all crop management techniques that are utilized throughout the growing season and cannot be used as an active crop management regime as it inherently represents a lagging indicator. Even though they represent a lagging indicator, yield maps still provide the basis for dealing with crop variability in a predictive way (stage 3) and represent a staple and important part of the precision agriculture management

regime. Various techniques employed to address this identified variability (stage 4) will be investigated next.

2.3 Variable Spraying

Through utilization of static variability indicators which are regularly updated throughout the growing season (control approach to stage 3), one is able to generate real time variability data (whether it be weed outbreaks, or water stress) through remote sensing or sampling (Adl, 2014). This data can then be utilized in order to reactively address any issues in real time through the targeted application through spraying of chemicals or water (stage 4).

2.3.1 Irrigation

Irrigation is currently the largest user of the world's freshwater supply and accounts for approximately 70% of the total withdrawal which is used to produce 30% - 40% of the world's food crops (Bastiaanssen et al., 2000). Targeted irrigation enables effective and efficient use of the water by monitoring the crops and only irrigating when and where it is needed, reducing the amount of water needed and also the runoff. Usually the degree of water stress is measured via thermal remote sensing, largely hyperspectral over the IR wavelengths which is then monitored in order to ensure that minimum stress levels are kept through use of scheduled and targeted irrigation (Pinter et al., 2003). Figure 2-3 shows an example of a false-color hyperspectral image which was taken over a corn field where water stress was induced in certain areas.

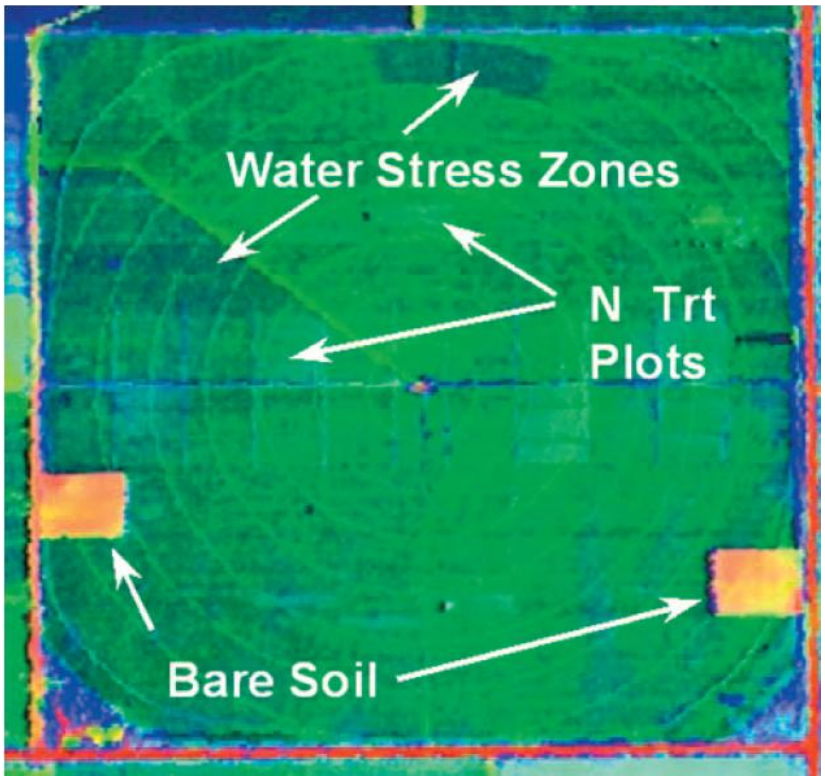

Figure 2-3 Hyperspectral water stress image of corn
Source: Pinter et al., 2003

This image is composed of 224 bands in the wavelengths between 370nm and 2510nm and clearly identifies the zones where water has been scaled back ("Water Stress Zones"). While utilizing remote sensing to schedule irrigation is still largely in the stage of early innovators and researchers, it shows significant promise as the need for more crops competes with the finite amount of freshwater available (Pinter et al., 2003; Bastiaanssen et al., 2000).

2.3.2 Chemical Spray

Similar to irrigation, chemicals such as: nitrogen, herbicides or pesticides can be applied to crops in a targeted way. While detecting heat stress in plants is somewhat straightforward thanks to thermal remote sensing, detecting patches or low nitrogen or weed outbreaks is decidedly more difficult and the topic of continued research within the precision agriculture industry. However, remotely monitoring the reflectance of the field and locating variabilities has been shown to be useful in identifying foreign plant species (weeds) and forms of mold which can then allow for the targeted application of herbicides and pesticides (Pinter et al., 2003).An example of this reflectance difference is shown in the Figure below:

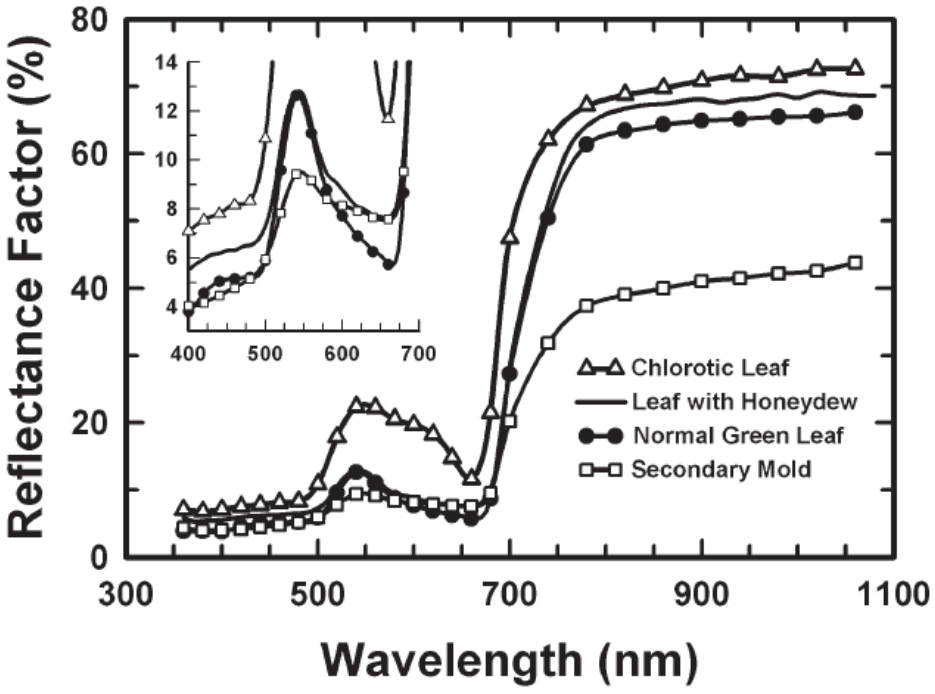

Figure 2-4 Reflectance variabilities in cotton leaf
Source: Pinter et al., 2003

In Figure 2-4, honeydew is a harmful fungus which grows on the surface of the cotton leaf, and a chlorotic leaf occurs when the plant is producing insufficient amounts of chlorophyll due to a nitrogen deficiency. By utilizing this remotely sensed data in a precision agriculture management regime, the user can increase the effectiveness of the application treatments while also reducing the negative effects associated with chemical applications.

2.4 The need for remote sensing

Of clear importance to precision agriculture, as illustrated in the previous two treatment examples, is the need to remotely sensed data in order to identify potential crop variability and to drive informed decision making. While the implementation of various solutions to deal with variability is no doubt a pillar of precision agriculture (stage 4), they require accurate remotely sensed data in order to be truly effective (stage 3). Remote sensing enables large amounts of data to be gathered either via ground (tractors, etc) or via the air (drones, satellites, etc) in a short amount of time so that any identified variability can be rectified as soon as possible. The utilization of thermal remote sensing, specifically with regards to measuring surface temperature, will be the critical tool utilized to provide the informational input for the theory presented in this thesis.

The theoretical importance of temperature to precision agriculture as it relates to agricultural crop exergy flows is presented in the next 3 chapters. Chapter 3 defines exergy, Chapter 4

identifies the most critical exergy flow, solar exergy, and Chapter 5 applies exergy theory to an agricultural crop via the exergy destruction principle.

Chapter 3. Background

Given the objective of this research to investigate the application of the exergy destruction principle to precision agriculture, it is necessary to first develop and expand upon the meaning of exergy. The purpose of this chapter is to define exergy as a thermodynamic pseudo property, as opposed to a pure thermodynamic property, and thus provide the foundation for thermodynamically linking an ecosystem to its environment. Exergy, as it will be more thoroughly defined below, is a measure of energy quality, and represents the ability of a given system to perform useful work (Cornelisson, 1997; Rosen and Dincer, 2001). Ecosystems are complex thermodynamic systems which exchange energy and matter with their surroundings and constantly adapt and evolve over time. It will be proposed in this chapter how exergy can quantify the thermodynamic relationship ecosystems have with their surroundings and lay the foundation for how it can be utilized to monitor health and development over time.

3.1 Exergy

3.1.1What is exergy

While energy is ubiquitously described in terms of form (kinetic, etc) or magnitude (joules etc) it is energy's third and lesser known characteristic, energy quality, which will be utilized throughout this thesis. Energy form and magnitude are rather straight forward terms which derive their roots from the first law of thermodynamics. Energy quality on the other hand, is remarkably harder to conceptualize, no doubt because it is not a property inherent to a system,

but rather a pseudo-property which derives its value by comparing properties of a system to that of its surroundings.

It should be noted that from here on throughout, energy quality will be interchangeably referred to as its more specialized term “exergy” (Wall, 1977; Cornelissen, 1977; Rosen and Dincer, 2001; etc).Exergy was first coined by Z. Rant (1973) in which he stated that the term should be utilized to denote “*technical working capacity”*. This broad definition of exergy was then further refined by Baehr (1965) in which he stated:

Exergy is that part of energy which is convertible into all other forms of work.

In this thesis, exergy will be primarily defined based on the work of Fraser and Kay (2003) which stated the definition as:

The maximum useful to-the-dead-state work

where “useful” work can be thought of as the work required to lift a weight or to turn a shaft. On a more technical level, useful work can be derived by taking the total work which a system performs and subtracting out the expansion work which the system does to the surrounding environment $P_o\Delta V$ (Atkins, 2001). The dead state is also defined by Fraser and Kay as occurring when a system is in thermodynamic equilibrium with its reference environment, where the reference environment is the non-immediate environment which maximizes a systems exergy.

Wall (1977) similarly describes exergy in the context of "energy quality" where he describes exergy as:

> *The exergy of a system in a certain environment is the amount of mechanical work that can be maximally extracted from the system in this environment*

Since exergy represents the maximum amount of work that can be extracted from a system as it is brought fully into equilibrium with its surrounding environment, it stands that fundamentally exergy is also a measure of how far away a system is from equilibrium.

For the purpose of this thesis the above definitions are within reasonable agreement and are taken to be equivalent, however all further references towards exergy unless explicitly stated otherwise, will be in reference to the definition presented by Fraser and Kay (2003).

3.1.2 The reference state

Since exergy derives its value based on how thermodynamically far away from equilibrium a system is with its environment, and given the fact that exergy is meaningless without a reference state, it is important to clearly identify what constitutes both the system and the environment or surroundings (Valero, 2006). It is common engineering practice to define the "system" as the region of interest, or more specifically as defined by Reynolds and Perkins (1977):

A system might be a particular collection of matter, such as gas in a bottle. Or it might be a region of space, such as the bottle and whatever happens to be in it at the moment. ...

Conversely, anything that hasn't been assigned to the "system" is defined as the "environment" or "surroundings".Since the "environment" is often extremely large it is common to then create subdivisions based on proximity to the identified system, such as creating an "immediate environment" which is in direct contact with the system boundary. Shown below is an example control mass boundary diagram taken from Fraser and Kay (2003) which shows how to properly divide all the regions and sub-regions present in most thermodynamic applications.

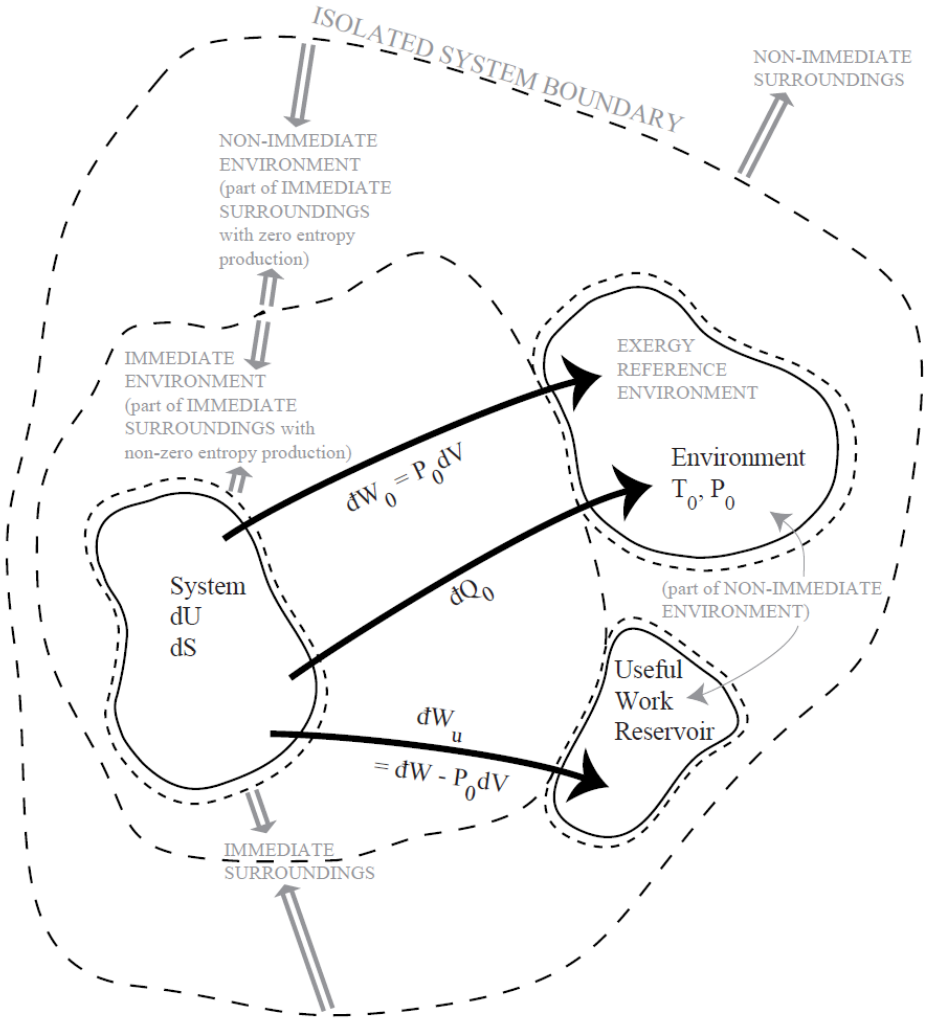

Figure 3-1 Control mass boundary layer diagram
Source: Fraser and Kay, 2003

It should be stated that the reference environment, with which exergy inherently derives its value from, can be arbitrarily chosen by the user, which means that exergy can be calculated with respect to any number of different reference states, such as the immediate environment or non-immediate environment. While these all represent valid exergy calculations, under the definition presented by Fraser and Kay, where exergy represents the *maximum to-the-dead-*

state work, the reference state should always be selected which maximizes the exergy calculation (Fraser and Kay, 2003).

3.1.3 Defining equilibrium

Of equal importance to defining the proper reference state is defining what criteria must be met in order to say that a system has reached equilibrium with a given reference environment. The most basic and general statement of thermodynamic equilibrium, provided by Fraser and Kay (2003) can be defined as:

> *A system in thermodynamic equilibrium is macroscopically identifiable by the absence of all force and thermodynamic property gradients.*

While this definition is somewhat straight forward and obvious for most closed systems, it has to be modified when examining systems which operate in an environment whose intensive thermodynamic properties (pressure, temperature etc) are unaffected by the system. This is of crucial importance when examining systems which operate in much larger surrounding environments such an ecosystem interacting with the surrounding atmosphere.

This is where Fraser and Kay (2003) introduced the concept of a "stable-equilibrium environment" which is defined as follows:

> *A **stable-equilibrium environment** is a non-immediate environment system which may interact with the system, whose intensive properties are unaffected by the system (e.g.,*

temperature, pressure, specific internal energy, chemical concentrations), whose extensive properties may change (e.g., internal energy, volume, entropy, mass), and which is in thermodynamic equilibrium. The atmosphere, river water, and lake water are often modelled as stable-equilibrium environments.

This stable-equilibrium environment provides the basis to define a "stable-equilibrium dead state" which occurs once the system in question reaches equilibrium with the stable-equilibrium environment. Since exergy is taken as the ***maximum*** useful to-the-dead state work, Fraser and Kay (2003) then go one step further and define a "stable-equilibrium reference environment" which utilizes the stable-equilibrium environment defined above, with the exception that it is specifically selected to maximize a systems exergy calculation.

While the stable-equilibrium reference environment provides a good basis for most exergy applications, it is noted by Fraser and Kay (2003) that this definition must be generalized to include the possibility that the reference environments properties may change over time as it interacts with the system. This issue of potentially changing conditions of the reference environment is also addressed by Wall (1977) where he suggests using either "global" standard environments, such as standard atmospheric pressure with a standard sea level etc., or using "local" standards and utilizing some sort of averaging to deal with fluctuations in property values.

3.2 Exergy as a measure of energy quality

Energy quality, while not usually stated as an explicit measure, is extremely valuable as an implicit tool to visualize what exergy actually represents when investigating thermodynamic systems. In this sense, most energy flows can be expressed as generally "high quality" or "low quality" which can then be translated into "high exergy content" or "low exergy content". The way in which energy is transferred into or out of a system into the surroundings has a large effect on the quality of energy. The exergy content of various forms of energy are shown below in Table 3-1 where the quality index represents an approximation of exergy content as a percentage of energy content.

	Form of energy	Quality index (Percentage of exergy)
Extra superior	Potential energy[1]	100
	Kinetic energy[2]	100
	Electrical energy	100
Superior	Nuclear energy[3]	almost 100
	Sunlight	95
	Chemical energy[4]	95
	Hot steam	60
	District heating	30
Inferior	Waste heat	5
Valueless	Heat radiation from the earth	0

[1] e.g. highly situated water resources
[2] e.g. waterfalls
[3] e.g. the energy in nuclear fuel
[4] e.g. oil, coal, gas or peat

Table 3-1 Exergy content of various energy forms as a percentage of exergy
Source: Wall, 1977

While Table 3-1 might be simplistic, it highlights just how much of an effect various forms can have on energy quality, especially when comparing those of "extra superior" or high quality energy forms with that of "inferior" or low quality energy forms.

By utilizing the qualitative information presented in Table 3-1 and applying that to the energy interactions which the earth undergoes, it becomes clear why exergy is not a conserved quality. One can assume that the earth is mainly receiving energy in the form of shortwave radiation emitted from the sun, which is of a very high energy quality or high exergy content. Some portion of this incoming radiation would be reflected by the surface of the earth back into the surroundings, however the rest of the incoming radiation would be absorbed and enter the thermodynamic fold of plants and matter on earth. This incoming high quality energy would either be simply absorbed by inert materials like rocks and soil or be utilized by living processes which need the high exergy content of the suns radiation to fuel their biological processes (Fraser and Kay, 2003; Wall, 1977; Schneider and Kay, 1994; etc).

While the interaction of exergy with biological processes will be explained in full in later chapters, one doesn't need to understand what the specifics are in order to realize the effect that they have on exergy flows. This is why exergy theory is often described as a "black box" principle, as information about the system ("box") can be inferred by measuring the exergy flows in and out of the system without needing to know or understand what's actually happening inside of the box. For example, the exergy flows entering the earth are

predominantly shortwave radiation from the sun while the exergy being re-radiated is almost entirely longwave heat radiation. Without knowing any of the inner workings, or peeking into the "box", an observer who's measuring these flows can still gain information about how the planet is functioning. This concept is shown in Figure 3-2:

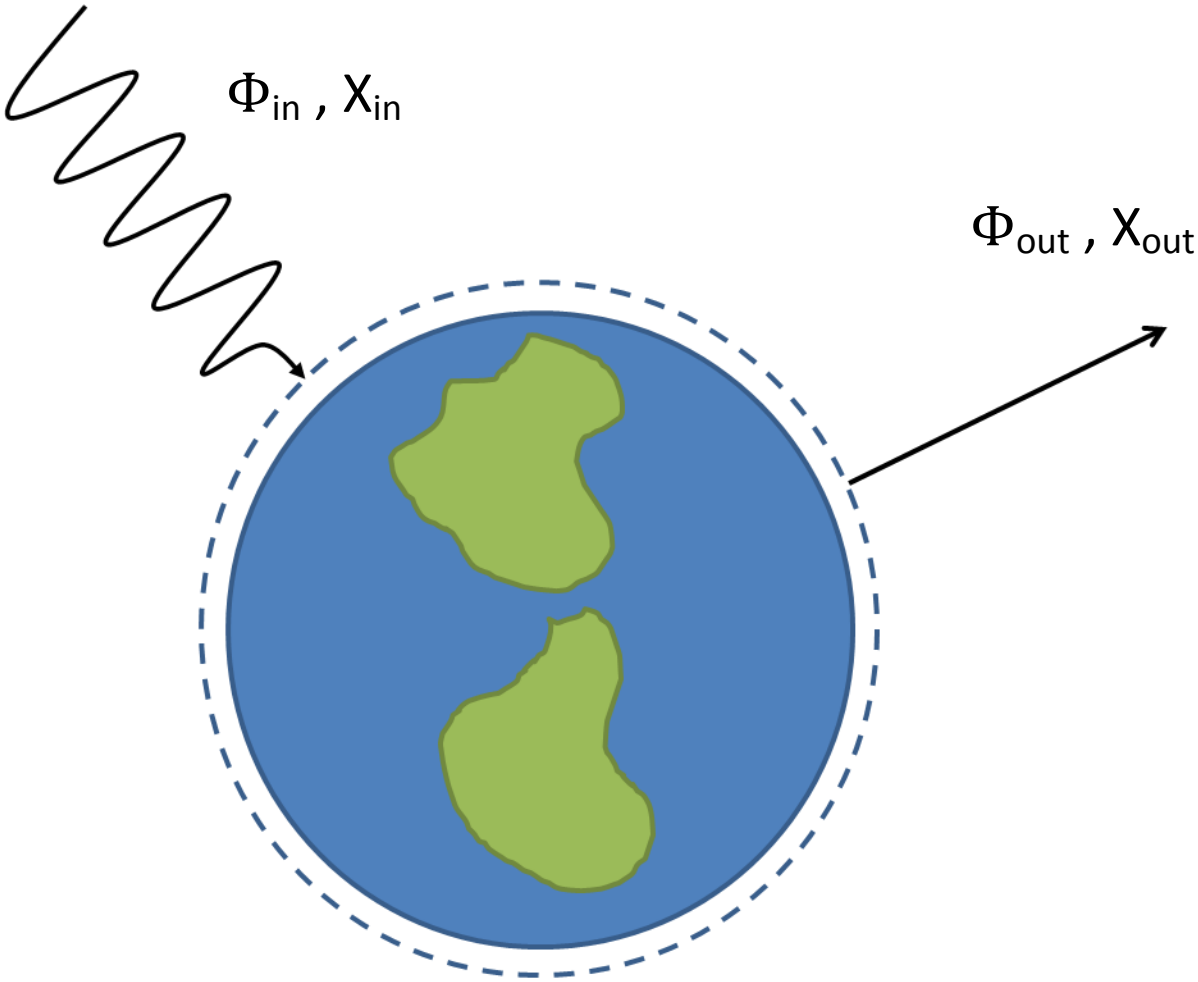

Figure 3-2 Energy and exergy inflows and outflows for the Earth

Where Φ represents the energy flux both incoming ($_{in}$) and outgoing ($_{out}$) and X represents the exergy flux both incoming ($_{in}$) and outgoing ($_{out}$) for the earth, and the boundary layer is denoted by the dashed line.

The earth receives high quality energy via the suns shortwave radiation, interacts with the radiation in some way, either absorbing it and simply re-radiating it, as is the case for inert objects, or utilizing it in some way through various biological processes, and eventually re-radiating it into the atmosphere as low quality, longwave waste heat. This degradation of work quality is a manifestation of the second law of thermodynamics and is present in any real system or process, however it should be stated for completeness that it is possible to locally increase the quality of energy albeit at the cost of decreasing the quality of the surroundings and thus the entire system as a whole(Wall, 1977; Schneider and Kay, 1994).

Energy and matter are simply carriers of energy quality, where different forms of energy have the potential of providing a system with more useful work than others and are thus classified as being of a higher quality. It's energy quality, and not energy itself, which is consumed throughout the thermodynamic process and accounts for the inherent irreversibilities as energy is transferred from different forms. This is shown visually in Figure 3-3.

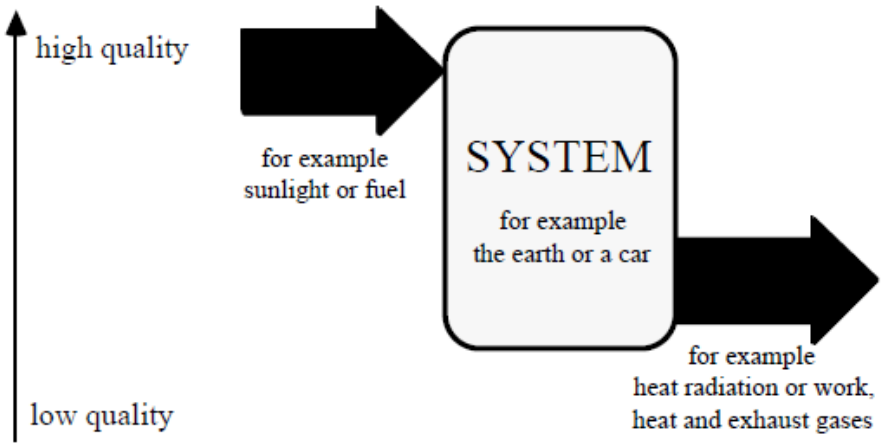

Figure 3-3 Exergy flow of energy and matter showing degradation of energy quality
Source: Wall, 1977

3.3 Mathematical description of exergy

While utilizing a qualitative approach to describing exergy is useful for visualizing the concept of energy quality, it is also necessary to understand the quantitative model of exergy which is fundamentally rooted in the first and second laws of thermodynamics.

3.3.1 Modeling assumptions

While there are a number of different exergy equations for the various types of systems, only the "control mass, non-flow" exergy equation will be presented here. Also, the dead state will be chosen to be the stable-equilibrium dead state explained in Section 3.1.3. The major underlying assumption inherent to the following model is that the derived value of exergy will

assume that all constituents are taken into chemical equilibrium as well as thermal and mechanical equilibrium.

It should be noted that the thermal-mechanical dead state is often used in most engineering literature and practical problems, where the exergy potential of bringing all the constituents into chemical equilibrium isn't included (Bejan, 1997; Cengal and Boles, 1998; Wark and Richards, 1999; Fraser and Kay, 2003). The reason that chemical equilibrium is rarely taken into account is due to the fact that almost always the gradients of chemical constituents post reaction (combustion, exothermic reactions etc) are so small that it is either not possible or not economically viable to recover the useful work potential.

It is even argued by Jørgensen (2006) and Susani et al. (2006) that for exergy analysis of resources the changes in value for thermal-mechanical exergy are in fact much less important than that of the exergy associated with chemical gradients. This led to the concept of "eco-exergy" where the system is assumed to maintain constant temperature and pressure with its reference environment and instead focus on the "chemical-physical" exergy content and also the "info-exergy" of the system which represents the inherent information that a system contains. While somewhat out of the scope of this thesis, it can be shown that exergy, through its connection with entropy, can be utilized as a measure of complexity and information, something which eco-exergy takes full advantage of (Susani et al., 2006).

While eco-exergy is already widely utilized for ecological modeling, especially within the aquatic ecology sector (Jørgensen, 1988), the major flaw as it pertains to larger ecosystems (amazon rainforest) which was identified by Fraser and Kay (2003), is that the ecosystem itself is able to effect the surrounding environment to such a degree that the assumption of both the system and the surrounding environment maintaining a constant temperature and pressure is no longer valid. Thus, Fraser and Kay presented the concept of utilizing a stable-equilibrium reference environment to calculate exergy (defined in 3.1.3).

3.3.2 Combining the first and second laws

The following derivations will be presented while assuming a non-reactive, control mass system which is depicted in Figure 3-1 and will primarily follow the work of Fraser and Kay (2003). Much like all thermodynamic relations, exergy can be constructed via a combination of the first and second law of thermodynamics, stated below for completeness.

$$\text{First Law: } dU = -đW - đQ_o \quad (3\text{-}1)$$

$$\text{Second Law: } đP_s = dS_{system} + dS_{Immediate\ Environment} \quad (3\text{-}2)$$

$$đP_s = dS + \frac{đQo}{To} \quad (3\text{-}3)$$

Where U is the internal energy of the system (kJ), W is the work output of the system (kJ), Q_o is the heat transfer between the system and the environment (kJ), P_s is the entropy produced in both the system and immediate environment (kJ/K), T_o is the temperature of the environment

(K) and S is the entropy of the system (kJ/K). Also of note, the differential symbol "đ" denotes an inexact differential (path dependant) whereas the differential symbol "d" denotes an exact differential (state and not path dependant such as temperature, entropy).

Through the common heat transfer term, both the first and second law equations can be combined and rearranged to solve for the work output of the system:

$$đW = -dU + T_o dS - T_o đP_s \quad (3\text{-}4)$$

Here “W” denotes the "actual work" of the system, and does not represent the "useful work" which exergy describes. Useful work is calculated by taking the actual work and subtracting the expansion work done by the system onto the surrounding environment which can be represented by $P_o \Delta V$ where ΔV represents the change in volume of the system and P_o represents the pressure of the surrounding environment (Atkins, 2001).

Subtracting the expansion work ($P_o \Delta V$, or in differential form $P_o dV$) from equation (3-4) will produce the useful work of the system; however it still does not represent the *maximum* useful work, which is required by the stated definition of exergy. The maximum amount of useful work will only occur when entropy production is minimized; this is represented mathematically by zeroing the entropy production ($đP_s$) differential term in equation (3-4). Doing so gives the mathematical description of the maximum useful work which a system can perform (Fraser and Kay, 2003):

$$đW_{Useful,\ Maximum} = -(dU + P_o dV - T_o dS) \quad (3\text{-}5)$$

Finally, given that the presented definition of exergy is "*the maximum useful to-the-dead-state work",* equation (3-5) must be integrated from the systems current state to that of the dead state in order to give the complete and final mathematical definition of exergy which is shown below:

$$\text{Exergy} = \int_{Current\ system\ state}^{Stable-Equilibrium\ Dead\ State} đW\, useful, maximum$$

$$\text{Exergy} = W_{Useful,\ Maximum\ to\text{-}the\text{-}dead\text{-}state}$$

Applying the integration above to equation (3-5) will finally produce the final exergy equation for a control mass system which is shown below in equation (3-6). Note that in common engineering nomenclature exergy is almost always denoted by the letter X.

$$X_{cm} = (U + P_o V - T_o S) - (U_o + P_o V_o - T_o S_o) \quad (3\text{-}6)$$

In equation (3-6) U represents the internal energy, V represents the volume, S represents the entropy and anything denoted with an "$_o$" represents the value of that property when the system reaches equilibrium with its surroundings. As a condition of a stable-equilibrium dead state the temperature and pressure must remain constant for each specific entropy calculation, however Fraser and Kay (2003) state that even though it must remain constant during each instantaneous calculation of exergy, it need not, and most likely is incorrect to assume that it remains constant over different periods of time.

Equation (3-6) makes it quite clear that exergy is inherently a pseudo property which derives its value based on the gradients of properties at a current state and at some equilibrium state. While seemingly simple to calculate, Evans (1969) has shown that exergy actually incorporates a variety of thermodynamic concepts such as Helmholtz free energy, Gibbs free energy and enthalpy which makes it such a powerful thermodynamic concept.

3.4 Exergy destruction and lost work potential

From equation (3-4) it becomes apparent that any entropy production in the system, or by the system within the immediate environment will result in a loss of work potential, which is indicated by the minus sign in front of the entropy production term ($T_o đP_s$). This entropy production term as it relates to the loss in work potential has become known as the "Gouy-Stodola theorem" (Bejan, 1997) and is shown below:

$$đW_{lost} = T_o đP_s \quad (3\text{-}7)$$

In any real system, whether it be biological or mechanical, irreversibilities exist which impact the ability of the system to function as efficiently as possible and lead to an increase in entropy. Through the Gouy-Stodola theorem, these irreversibilities can be thought of as a degradation of work potential in which exergy is converted (or degraded, destroyed depending on the literature) into entropy until the system reaches equilibrium with its surroundings. Semantically, any loss in work potential will be termed as "exergy destruction" throughout this thesis and are taken to be equivalent. Therefore equation (3-7) can be re-written in terms of exergy destruction as follows:

$$đX_{Destroyed} = T_o đP_s \quad (3\text{-}8)$$

While the Gouy-Stodola theorem presents itself as quite a simple and convenient way of calculating the lost work potential, it should be stressed that the entropy generation term can be easily misused or miscalculated. Again, the common mistake is to only include the entropy production of the system and neglect to account for the entropy production within the immediate environment. One of the more well known examples of this was presented by Chambadal (1957) where he investigated a power plant where the temperature of the exit stream from the plant was higher than the surrounding equilibrium temperature T_o. Thus there is still a non negligible portion of entropy production within the immediate surrounds as the exit stream cools down, something that only investigating the entropy production of the plants internal processes would miss (Bejan 1996).

The other caution which should be solicited when utilizing the Gouy-Stodola theorem, much like when formalizing the exergy derivations, is to be aware that this relation only holds true when the surrounding equilibrium temperature is constant (T_o). While not likely to be much of a problem when utilizing the theorem over instantaneous segments, it is most likely a reasonable hypothesis to assume that the dead state temperature changes over various significant swings in temperature (winter vs summer as an example). This again is something that is addressed by utilizing the stable-equilibrium dead state where T_o is assumed to be constant, thus allowing the theorem to be applied.

Chapter 4. Solar Exergy

The objective of this chapter is to investigate 3 popular solar exergy models which apply the previously discussed exergy framework to the suns radiation incident on earth. First an overview of solar exergy will be presented and the merits of why the solar exergy content of the suns radiation is vital for life to exist on earth will be explained. Various different interpretations of the solar exergy equation will then be discussed along with their inherent assumptions. Finally the models will be summarized and the importance of surface temperature will be highlighted.

4.1 Overview

In one way or another, virtually all life on earth owes its existence to the radiation the earth receives from the sun. No matter how far up the food chain one finds oneself, its life depends on the photosynthesis of plants and micro-organisms to convert the incoming solar energy and utilize it in some form. While most practical terrestrial applications depend on the magnitude of the incoming solar radiation, it is actually due to the exergy content of the suns radiation that life is able to exist and sustain on earth (Schneider and Kay, 1994;Kay, 1984; Schrödinger, 1944).

Being a conserved quantity, the amount of energy that comes in contact with the earth, barring any extended periods of warming, will eventually get reflected or re-emitted back out into space. This energy however carries the high amount of potential useful work (high exergy

content) which, as mentioned above, is what drives the various flows of energy and matter throughout the earth, and more importantly, feeds the inherent irreversibilities of all the biological processes (Wall, 1977). This is shown graphically in Figure 4-1.

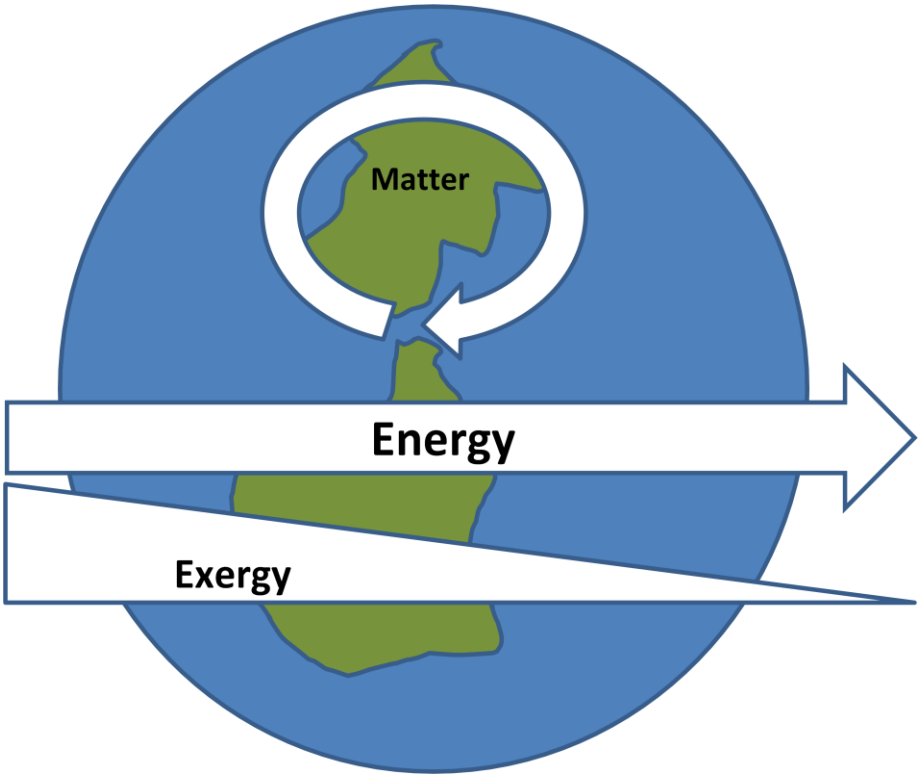

Figure 4-1 Flows of energy and matter on earth showing destruction of exergy
Adapted from Wall, 1977

When the solar radiation carrying the exergy comes in contact with the earth, it immediately starts to interact with matter and biological processes, and begins to degrade. Biologically, plants will be among the first to interact with the incoming exergy by utilizing photosynthesis to convert the solar exergy into various forms of chemical exergy. Again it should be noted that as a function of the second law of thermodynamics, exergy is only destroyed or degraded if

entropy is produced in either the system or surroundings. Crucially, the conversion of exergy into different forms does not inherently represent a degradation of energy quality; however since these processes are real and far from ideal, irreversibilities still exist. It is through these irreversibilities that entropy is generated and a destruction in work potential (exergy) is manifested (Wall, 1977; Schneider and Kay, 1994).

This destruction of the incoming solar exergy doesn't happen in one large chunk but instead happens gradually as the exergy transfers from the plants that initially photosynthesize it and then is continuously destroyed as it moves up through the various food chains. It is even suggested by Wall (1977) that any exergy which isn't utilized or cycled throughout the various food chains ends up as peat instead, this peat then gradually turns into coal and oil reserves. This shows how complex and far reaching the tracking of exergy is throughout complex systems, and how crucial and far ranging the effect of solar exergy has on life in general. While this will be further investigated next chapter, it has to be stressed that it is actually thanks to the high exergy content of the solar radiation, and not the magnitude, which allows life in almost any form to exist on earth (Schrödinger, 1944; Schneider and Kay, 1994)

4.2 Quantifying solar exergy

Due to the nature of how exergy is calculated, it is clear that depending on a number of different assumptions, one can arrive at a multitude of different answers for trying to quantify

solar exergy. This section will highlight the popular formulations of the solar exergy equation and explain the inherent assumptions that went into the formulations.

4.2.1 Type of system

Kabelac suggests that the various methods of classifying solar exergy can be largely divided into two distinct groups. The first group of analysis considers a “closed system” where “a certain volume is initially filled with equilibrium black-body radiation of a given temperature, and asks for the work which could ideally be extracted as the system reaches the dead state, as defined by a specified ambient”. The second group considers a “steady flow process” where “a steady flux of black body radiation of a given temperature is incident on an ideal conversion device… asked here is how much mechanical power (representing the high grade rate of energy) may be continuously drawn from the converter” (Kabelac, 1991).

The first group which considers a “closed system” has been thoroughly discussed by Bejan (1997) and won’t be discussed further since ecosystems are very much considered open thermodynamic systems and will be treated as such. Therefore the remainder of this chapter will focus on the second “steady flow process” open system group of solar exergy derivations.

4.3Explicit assumptions

All three of the models identified in the following section will utilize these explicit assumptions as part of their formulation.

4.3.1 Steady state-steady flow

Three competing derivations will be presented in the following sections which attempt to answer the maximum theoretical amount of work which can be extracted from the suns solar radiation. All three are modeled assuming a “steady state-steady flow” open system, which is depicted in the Figure 4-2:

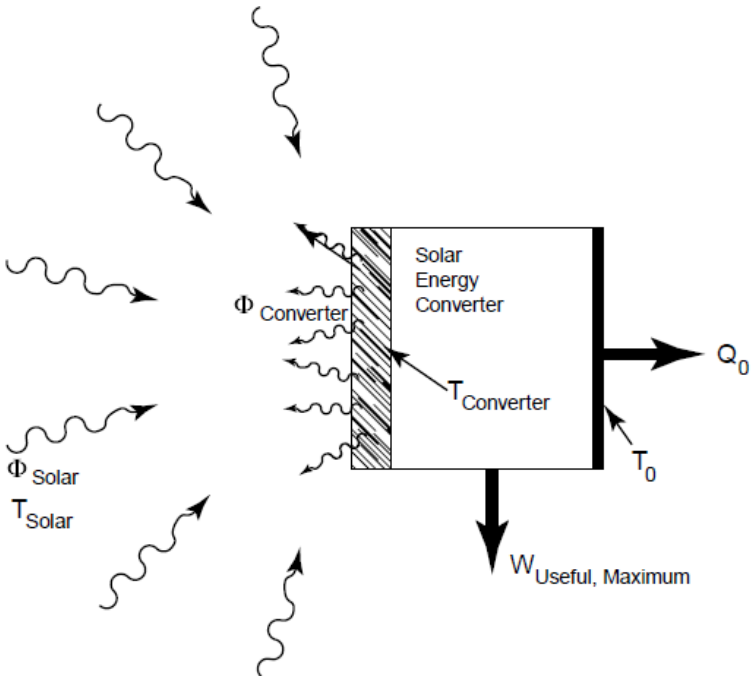

Figure 4-2 Steady flow solar exergy model for a solar energy converter
Source: Fraser and Kay (2003)

where ϕ represents the radiative flux and Q_o represents the heat flux. While this assumption is most likely sufficient to use over a small period of time, the cyclic nature of solar radiation, varying in intensity throughout the day (being most intense at solar noon and decreasing to 0 during the night) makes it likely unsuitable for longer periods of time.

4.3.2 Ideally concentrated solar radiation

It should be clear from Figure 4-2 that the solar converter which these models utilize to develop the derivation for solar exergy does not include any other sources of solar radiation, specifically the atmospheric background radiation. Also noted by Fraser and Kay is that while the sun only subtends a solid angle of 6.8×10^{-5} steradians, these models consider a full hemispherical (2π steradians) solid angle of incident solar radiation. This clearly represents an inherent maximization and any real case considering non-concentrated solar radiation (ie diffuse incident radiation) will produce necessarily less work output.

4.3.3 Diffuse blackbody radiation

While the radiation leaving the sun can be accurately modeled as blackbody radiation, by the time the radiation has reached the surface of the earth, its spectral distribution has changed significantly. This is largely due to the fact that various chemical molecules such as water, oxygen and carbon dioxide are highly interactive at various wavelengths. The effect of this interaction creates a decided impact on the amount of radiation which reaches the surface of

the earth in those specific absorption (or scattering) wavelengths. This is visualized in Figure 4-3 (Incropera and DeWitt, 2007).

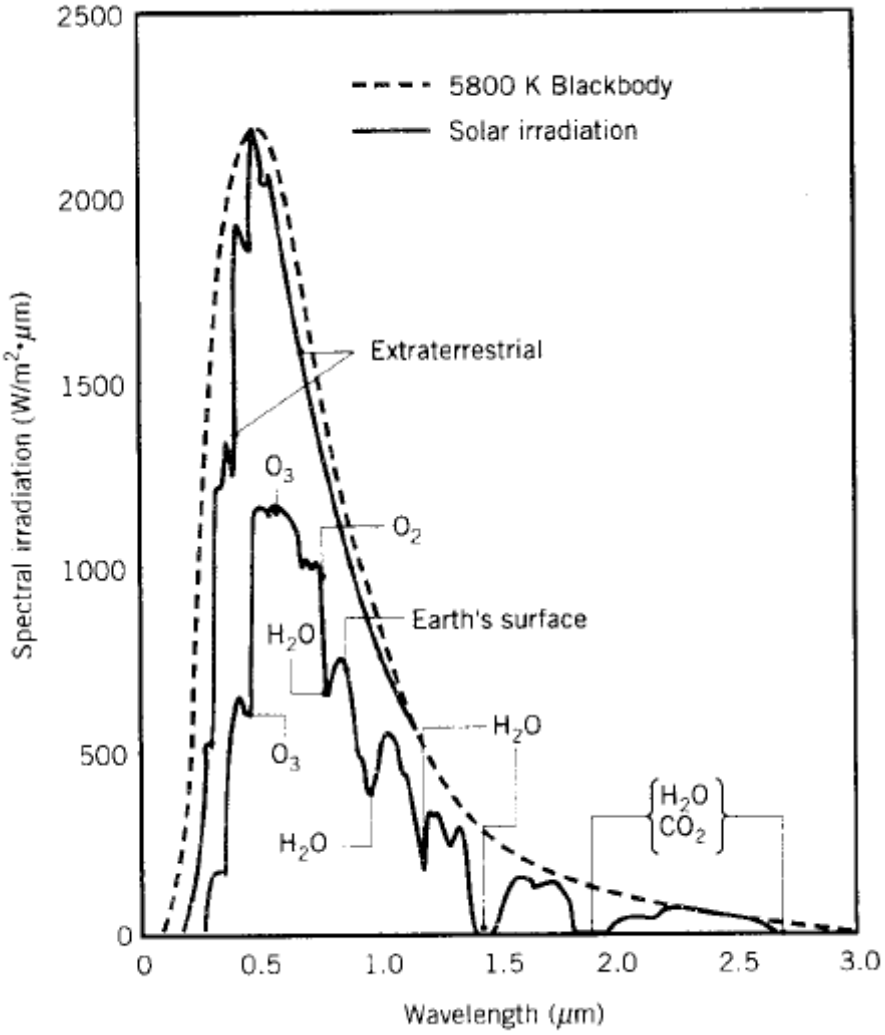

Figure 4-3 Spectral distribution of solar radiation
Source: Incropera and DeWitt (2007)

As Fraser and Kay point out, the main reason for invoking the diffuse blackbody radiation assumption is to utilize the expression developed by Planck for easily modeling the entropy content of solar radiation. This expression is shown in equation (4-1).

$$\Psi_{T,Radiation} = \frac{4}{3}\frac{\Phi_{T,Radiation}}{T_{Radiation}} \quad (4\text{-}1)$$

where $\Psi_{T,\,Radiation}$ represents the entropy flux and $\Phi_{T,Radiation}$ represents the energy flux of the incoming radiation.

4.3.4 Conduction or convection to the environment at T_o

The last explicit assumption which the following models utilize is that all convective or conductive heat transfer between the system and the environment will happen at the dead state temperature (T_o). This is to enable one to assume that the heat transfer between the system and the environment happens in a reversible fashion (no entropy production). The notion of reversible heat transfer stems from the concept of the Carnot cycle in which heat transfer occurs over a finite ΔT, or in other words, when the temperature difference approaches 0.

The reason why radiation is not included in this explicit assumption is that much like assuming reversible conduction or convective heat transfer, in order for the incoming radiation to be absorbed reversibly $T_{surface}$ must be equal to T_{solar}. While that alone seems like an impractical assumption to justify, assuming this to be the case would also make the efficiency of any solar

collector zero in the process since collector efficiency is governed largely by the difference in radiative flux (which equals the work rate). During finite ΔT heat transfer or infinite time, conditions for which reversible heat transfer is possible, the work transfer rate of the solar collector is inherently zero, and therefore the efficiency is zero (Fraser and Kay, 2003).

4.4 Model 1: Zero entropy – finite area solar exergy

The first equation investigated was independently derived by Landsberg and Mallinson (1976), Bošnjakovi (1988), and Press (1976). It should be noted that the versions of the equations presented in this thesis will differ slightly in form from which they were originally presented in their corresponding papers. This thesis will utilize the nomenclature of Fraser and Kay when presenting the aforementioned equations in order to stay consistent with the nomenclature used throughout this thesis. The equation (4-2) derived by the aforementioned authors will be referred to as Model 1.

$$W_{Maximum} = \Phi_{\mathrm{T,Solar}} \left(1 - \frac{4}{3} \frac{\mathrm{T_o}}{\mathrm{T_{Solar}}} + \frac{1}{3} \frac{\mathrm{T_o^4}}{\mathrm{T_{Solar}^4}} \right) \quad (4\text{-}2)$$

Where $\Phi_{\mathrm{T,Solar}}$ represents the rate of solar radiation given off by the sun according to the Stefan-Boltzmann law and $\mathrm{T_o}$ is taken as the ambient temperature representing the dead state temperature. Model 1 utilizes two main assumptions; first it assumes zero entropy production and second it assumes a finite system area. Fraser and Kay (2003) took the equation in Figure 4-5 one step further by inferring that in order for the maximum amount of work to be extracted from the solar radiation, the surface temperature of whatever object is in contact with the

radiation must eventually reach the dead state temperature. Therefore the ambient temperature (T_o) in (4-2) can be replaced with surface temperature ($T_{surface}$)and is shown in equation (4-3).

$$X^t_{Solar,Model\ 1} = \Phi_{T,Solar}\left(1 - \frac{4}{3}\frac{T_{Surface}}{T_{Solar}} + \frac{1}{3}\frac{T^4_{Surface}}{T^4_{Solar}}\right) \quad (4\text{-}3)$$

Fraser and Kay then point out that since this model includes zero entropy production and has no consideration for system size, processing time or system structure, that this model actually represents a specialized type of exergy, called transport exergy. Transport exergy is a restricted version of exergy which represents the amount of exergy which enters a system under steady-state-steady-flow conditions and does not take into account any exergy associated with any energy stored in the system (Fraser and Kay, 2003).

The main assumption with this model, and thus the difficulty with utilizing it, is that entropy production is zero. As discussed under the previous sections assumptions about reversible convective and conductive heat transfer, there is a large problem with assuming that a system can absorb the incoming radiation in a reversible fashion. In fact, as pointed out by Kabelac (1991) and first developed by Planck (1966) any conversion between radiation and a heat flux, or vise versa is inherently irreversible. This is shown via the following equation:

$$\dot{S_{irr,Q}} = \frac{1}{3}A_2\sigma T_2^3 + A_2\sigma T_o^3\left(\frac{T_o}{T_2} - \frac{4}{3}\right) = \frac{A_2\sigma}{3T_2}(T_2 - T_o)^2(T_2^2 + 3T_o^2 + 2T_2T_o) \quad (4\text{-}4)$$

Equation (4-4) represents the rate of entropy production which a modified Carnot heat engine produces if it operates between a constant heat flux and a constant radiation flux. In this particular representation of the equation, the Carnot engine receives a heat flux at some temperature T_1, and emits blackbody radiation out into the environment (T_o) at a temperature of T_2. By examining this equation it becomes clear that entropy production is always positive except for the case when $T_2 = T_o$, however when this happens the entropy production rate of the incoming heat flux becomes negative unless the incoming heat flux becomes zero, which obviously can't happen. Therefore it was deduced by Kabelac (1991) that there exists no possible operation mode of the modified Carnot engine which does not produce entropy, and is the basis for the fact that if T_{solar} and $T_{surface}$ are not equal, radiative energy transfer is an inherently irreversible process.

The major assumption which model 1 requires is that it assumes zero entropy production, especially when it has been proven that radiation cannot be absorbed in a reversible manner. The magnitude of how much this assumption overstates the amount of exergy carried by solar radiation has yet to be investigated.

4.5 Model 2: Non zero entropy production – finite area solar exergy

Model 2 has been the choice favored by Castańs (1976), Haughts (1980), De Vos and Pauwels (1981), and finally Bejan (1997). While model 2 also assumes a finite area solar collector, it differs from model 1 in that it does not assume zero entropy production. Here it is assumed

that the incoming solar radiation is converted to thermal energy, and as was stated in Section 4.4, this conversion is an inherently irreversible process. The mathematical expression of model 2 is shown in equation (4-5):

$$W_{Maximum} = \Phi_{\mathrm{T,Solar}}\left(1 - \frac{\mathrm{T}^4_{\mathrm{Optimum}}}{\mathrm{T}^4_{\mathrm{Solar}}}\right)\left(1 - \frac{\mathrm{T_o}}{\mathrm{T_{Optimum}}}\right) = \Phi_{\mathrm{T,Net}}\left(1 - \frac{\mathrm{T_o}}{\mathrm{T_{Optimum}}}\right) \quad (4\text{-}5)$$

Here $T_{Optimum}$ is the temperature which optimizes the power output from the equation (4-6) which was derived by conducting a first and second law analysis on a theoretical solar collector which converts all the incoming radiation into a heat flux, depicted in figure 4-4.

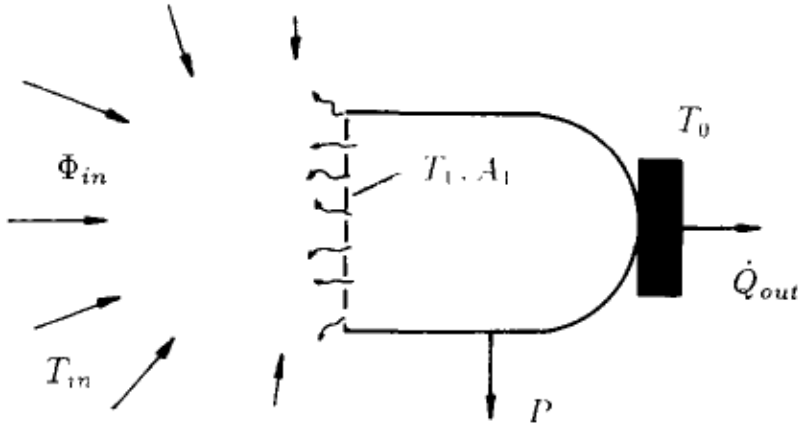

Figure 4-4 Ideal radiation to heat flux solar collector
Source: Kabelac (1991)

By utilizing this model to conduct a first and second law analysis, where the amount of entropy generated by radiation being converted into a heat flux is explicitly known (see Section 4.4), the first and second laws can be combined (by eliminating Q_{out}) to produce the following equation for maximum power output (Kabelac, 1991):

$$P = A_1\sigma\left(T_{in}^4 - T_1^4\right) - A_1\sigma T_o\left(\frac{T_{in}^4}{T_1} - T_1^3\right) \quad (4\text{-}6)$$

Here T_1 represents the temperature of the "radiation intercepting area" and T_{in} represents the temperature of the incoming radiation (source temperature). This represents the maximum power output which a device can generate assuming it converts all radiation into a heat flux. Here T_1 of the radiation intercepting area is an unknown quantity, and thus to determine the optimal mode of operation, equation (4-6) should be maximized with respect to this unknown temperature ($\frac{\partial P}{\partial T1}$ = 0). Solving this first order partial derivative equation yields the following result (Kabelac, 1991):

$$0 = 4T_1^5 - 3T_oT_1^4 - T_{in}^4T_o \quad (4\text{-}7)$$

Since T_o is known (T_{solar}) this equation can then be solved for T_1 which will then represent the optimal temperature for power maximization and can be substituted into equation (4-5) for determining the solar exergy.

As pointed out by Fraser and Kay (2003), if one is to assume a T_{solar} of 5762K and a ambient environment temperature T_o of 300K then the optimal temperature for an ecosystem to maintain ($T_{optimal}$) according to model 2 would be approximately 2465K, which clearly is unrealistic. It is also difficult to reasonably apply the assumptions to an ecosystem environment. While the finite area assumption, much like in model 1, places a structural requirement on the system whenever model 2 is utilized, the new constraint presented in

model 2 is that all the incoming radiation must be converted into a heat flux. This prompted Fraser and Kay (2003) to describe the exergy presented in model 2 as a form of “restricted exergy”.

Restricted exergy, by definition, represents the amount of exergy which can be generated while taking into account all the systems structural restrictions and any general operating restrictions to which the system must conform. An ecosystem for instance would be restricted in the range in temperatures which it can be at in order to conduct photosynthesis, or the strict requirement on specific wavelengths which it must utilize for photosynthesis are all examples of structural requirements which it must operate in (Fraser and Kay, 2003).

However the simple fact that the restrictions on photosynthesis have to be stated means that the main premise of model 2, being that all radiation must be turned into a heat flux, is clearly not suitable when modeling the solar exergy of an ecosystem. Combined with the fact that $T_{optimal}$ was such an outlandishly high value means that model 2 is most likely the least viable option.

4.6 Model 3 Zero entropy production – infinite area solar exergy

The final model was formulated by Jeter (1981) where he derived the maximum conversion efficiency (Carnot efficiency) for the utilization of solar exergy of a system, although it should be

noted that in the original paper the term essergy was used instead of exergy. The final mathematical efficiency which Jeter (1981) derived is shown in equation (4-8):

$$W_{Maximum} = \Phi_{T,Net}\left(1 - \frac{T_o}{T_{Solar}}\right) \quad (4\text{-}8)$$

In his derivation, Jeter assumed that the solar collector had infinite area and that it could operate in a reversible way, thus zero entropy production. However, the assumptions are almost mutually dependant on each other since the solar collector which Jeter depicts achieves reversible heat transfer by assuming that any heat transfer happens between a finite temperature difference and over an infinite area. This is shown mathematically in the equation (4-9) for net heat transfer (Φ_{net}) (Jeter, 1981).

$$\Phi_{Net} = \lim_{T_{Surface} - T_{Solar}} A(T)\,\sigma\left(T_{Solar}^4 - T_{Surface}^4\right) \quad (4\text{-}9)$$

The main outcome of this equation, just as in model 2 is that $T_{surface}$ becomes unrealistically large as it is forced to the stated limit which in this case is the blackbody temperature of the sun. By driving the surface temperature to the limit, one is in essence fixing the surface temperature, and seeing as ecosystems surface temperature is always changing, significantly between day and night, this might prove problematic.

Another main objection to this model is based on its assumption of infinite area. While the objection to why this could be unrealistic is clear, Kabelac (1991) addresses this issue stating that it can still be utilized as a theoretical maximum, much like the way in which Carnot engine

(when considering conduction and convection) is utilized as model for understanding the theoretical maximum. However, the usefulness of this model is disputed by both Fraser and Kay (2003) and Bejan (1997). Fraser and Kay (2003, p.51) state that there is a general misunderstanding of how the assumption of reversible heat transfer is formalized as they argue that infinite area and infinite time are not the only ways to achieve reversible heat transfer over finite temperatures. They state that “for conduction, for example, an infinite thermal conductivity also works to provide finite heat transfer rate across a finite area and an infinitesimally small temperature difference.” Thus, it would seem that some possibly more prudent ways of achieving reversible heat transfer have been overlooked. Bejan (1997) stated it more simply when addressing the infinite area assumption claiming that it was “totally unrealistic”. It is finally concluded by Fraser and Kay (2003) that due to these concerns model 3, specifically relating to equation (4-8) is “meaningless from an exergy perspective”.

4.7 Model summary

Now that all 3 models have been presented and characterized with respect to two parameters: incoming solar radiation energy and surface temperature, the models can be compared and contrasted to identify the best model for agricultural crops. While no sensitivity analysis has yet to be thoroughly conducted, a high level analysis still provides a large amount of insight to compare and contrast the models. Model 3 is best served as a theoretical "maximum efficiency" of solar radiation and not as a method of deriving a value of exergy. Model 2 on the other hand is the most conservative model for solar exergy as it is the only one to model the heat transfer

as a non reversible process, thus bringing an entropy term into the equation. This represents a somewhat fundamental problem with utilizing model 2, if exergy is to represent the *maximum* amount of work potential which can be extracted, then by definition it should not be modeled to inherently include entropy production.

Based on the assumptions presented in the Section 4.4, it would appear that model 1 does the best job at providing reasonable and realistic assumptions while also capturing the true definition of exergy. By assuming zero entropy production and a finite area, model 1 still represents a true "maximum" to-the-dead-state work potential while also staying within the confines of a realistic device, something which assumes an infinite area would have a hard time doing. This assertion that model 1 represents the best potential description of exergy is something that is also echoed by Fraser and Kay (2003).

4.8 The importance of surface temperature

The crucial thing to note from Model 1 is that the incoming solar exergy is dependent only on the incoming solar radiation flux and surface temperature. This establishes the importance of surface temperature as a plant has means to control its surface temperature whereas the incoming solar radiation flux is largely out of the control of the plant.

It is possible to measure surface temperature with relative ease on a large scale, either by land (handheld, tractors, etc.) or air (drones, satellites, etc.) making it potentially well suited for use within precision agriculture as a method to actively identify variability in crops. The next chapter, Chapter 5, looks at applying the exergy destruction principle using large scale remote sensing of agricultural crops.

Chapter 5.The Exergy destruction principle

While the previous chapters largely laid the foundation and mathematical framework for how exergy is described and modeled, the objective of this chapter is to introduce the exergy destruction principle and examine how exergy can be utilized to describe ecosystem health, development and stress. As briefly alluded to in chapter 1, the first attempt to utilize the laws of thermodynamics to quantify ecosystem development came from Schrödinger (1944) when he developed his "order from disorder" premise which tried to account the fact that, in apparent contradiction of the second law of thermodynamics, ecosystems exist in a highly ordered state and appear to actually increase in complexity over time.

Schrödinger was able to rectify this by turning to non-equilibrium thermodynamics to model ecosystems. By utilizing a non-equilibrium model, Schrödinger was able to describe how a highly complex organism can feed off of an incoming energy flow from a larger encompassing system, and utilize it to produce a more organized and lower entropy state. Thus it was shown that ecosystems are able to become more complex by lowering their local entropy level at the expense of increasing the entropy of the surrounding environment, thus still leading to a total (entire system) entropy increase.

The exergy destruction principle builds upon this idea of examining ecosystems under the lens of non equilibrium thermodynamics and examines how it can be applied to gain insight into the

functioning of the ecosystem. As mentioned in the previous chapter, surface temperature has a large effect on the exergy flows in and out of an ecosystem. Applying this reasoning further, this chapter will explain how surface temperature can be utilized as an analog (at least relatively) to measure the maturity or complexity of the system, and crucially as a way to infer plant stress. The focus of this chapter is to investigate the exergy destruction principle and develop an understanding for the various implications, specifically with regard to surface temperature, this principle has for understanding ecosystem development.

5.1 Background

An important shift in thermodynamics, specifically as it relates to the foundations of the exergy destruction principle, occurred when Caratheodory proved that the second law can't always be strictly depicted as a "increase in entropy" (Caratheodory, 1909). He went on to state in an axiom the following with regard to the interpretation of the second law:

> *In any arbitrary neighborhood of an arbitrarily given initial point there is a state that cannot be arbitrarily approximated by adiabatic changes of state.*

As Schneider and Kay (1994) pointed out that unlike previous formulations of the second law, Caratheodory's interpretation was important as it showed geometrically that entropy didn't always dictate and increase in local entropy.

Hatsopoulos and Keenan (1965), and Kestin (1966) then further expanded this formulation to include the first law and developed what they called the "Law of Stable Equilibrium (Hatsopolous and Keenan)" and/or "The Unified Principle of Thermodynamics (Kestin)" which is stated below (adapted from Schneider and Kay 1994):

> *When an isolated system performs a process after the removal of a series of internal constraints, it will reach a unique state of equilibrium: this state of equilibrium is independent of the order in which the constraints are removed*

This introduces the concept of *equilibrium states* and of special importance to the exergy destruction principle is how this is applied to systems which are open to energy or mass flows and thus exist in stable states at some distance away from equilibrium. Nicolis and Prigogine (1977, 1989) were the first ones to formally utilize this new framework when investigating complex open systems, such as that of an ecosystem, which are moved away from equilibrium due to fluxes of energy and matter across their given system boundary.

Nicolis and Prigogine then showed that these systems are able to maintain their complexity and form by continually dissipating (utilizing) the energy flux, which they described as "dissipative structures". While it will be more thoroughly described in the subsequent section, dissipative structures are able to maintain or even reduce their local entropy level when exposed to an influx of energy by dissipating the flux at the cost of increasing the global (total) entropy of the entire system that the structure is located within (Schneider and Kay, 1994; Nicolis and Prigogine, 1977; 1989). Thus since the total entropy of the global system still increases in

relation to the dissipation of the system, the second law isn't violated as would first appear, especially when considering the pre-Caratheodory view of the second law.

One important thing to note is the different nomenclature which is used throughout various literary sources to represent a variety of different concepts with regard to the second law and dissipative structures. This will become increasingly important as the exergy destruction principle is introduced, as seemingly slight variations in definition, ie. dissipation vs destruction, take on increased significance. Also, previously mentioned is the idea of complexity, and specifically how it relates to the idea of form or structure of a system, which will be investigated later in this chapter. For the scope of this thesis, increased structure will always correspond to a increase in complexity and thus a decrease in local entropy.

5.2 Dissipative Structures

As alluded to in the subsequent section, dissipative structures in essence represent the bridge or transition from the more generalistic description of the second law, to a more complete model which accounts for self organizing systems. And while Nicolis and Prigogine were the first to shed light on dissipative structures and their mathematical description, it represents a significantly limited case where the system in question is still adequately close to equilibrium that a linear expansion of the entropy function with respect to equilibrium can be assumed (Schneider and Kay, 1994; Nicolis and Prigogine, 1977). This however represents a problem when considering living systems which operate significantly far away from equilibrium.

In order to deal with this restriction, Schneider and Kay (1994) proposed a corollary which builds upon the work of Kestin and his "Unified Principle of Thermodynamics" (Kestin, 1966). While the mathematical formulation is out of the scope of this thesis, their conclusion is of significant importance:

> *The thermodynamic principle which governs the behaviour of systems is that, as they are moved away from equilibrium they will utilize all avenues available to counter the applied gradients. As the applied gradients increase, so does the system's ability to oppose further movement from equilibrium.*

Schneider and Kay went on to call this the "Restated Second Law" and correspondingly any statements with regard to the second law pre-Caratheodory (ie. "increase in entropy") are referred to as the "Classical Second Law". While the importance of this statement will be evident as the chapter goes on, it should be noted that this really represents the fundamental driving force that dissipative structures utilize in order to increase their structure or form when exposed to gradients (such as but not limited to energy).

Perhaps the best example of the restated second law and a good illustrative example of how dissipative structures operate in far from equilibrium settings is the Bénard cell. The Bénard cell represents Rayleigh-Bénard convection which form structured cells when exposed to a high enough heat gradient. The schematics of the Bénard cell is shown below:

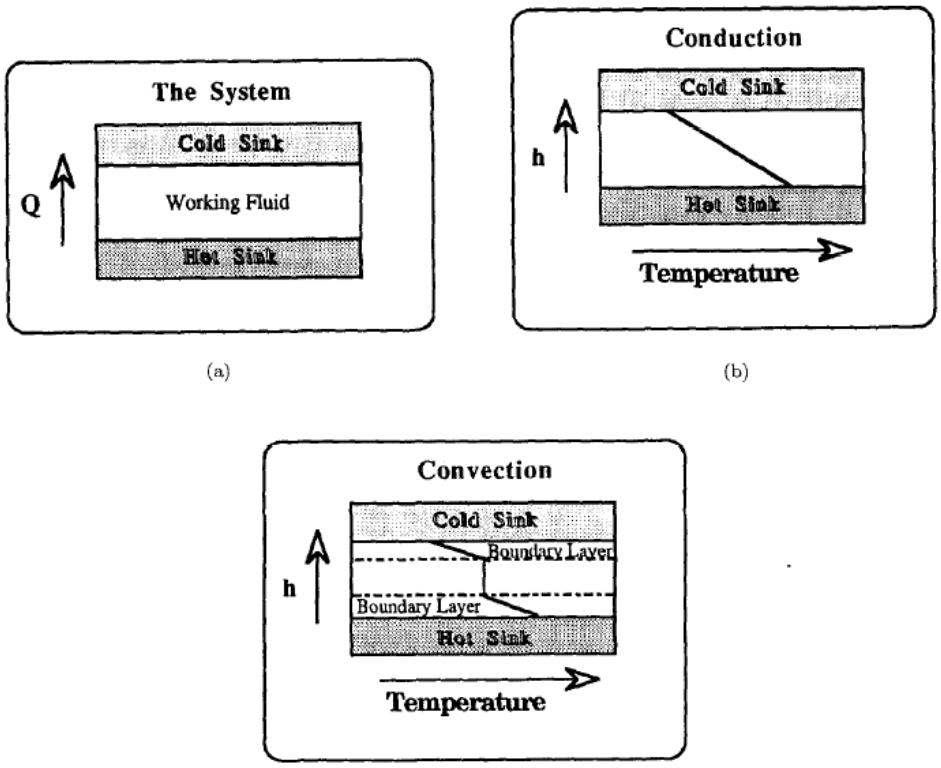

Figure 5-1Bénard cell schematic
Source: Schneider and Kay (1994)

As Figure 5-1 illustrates, a liquid (usually of high viscosity) is placed in between two sinks and energy is supplied in order to generate a temperature gradient (ΔT) across the liquid. As per the restated second law, when exposed to a gradient, the fluid will be resist the gradient and act to mitigate the degree to which it is moved away from equilibrium and thus act to dissipate the imposed energy gradient. At low gradients, this dissipation occurs through conduction, however as the gradient increases, the mode of dissipation will change to convection and Bénard cells will eventually start to form (Chandrasekhar, 1981).

The gradient of the Bénard cell is measured via the Rayleigh number which is a dimensionless number that allows the mode of heat transfer to be accurately predicted in this case (such as the transition from conduction to convection). The container is also highly insulated so accurate measurements of temperature, heat transfer etc. are able to be taken. Below are the adapted results from Schneider and Kay (1994) in which they utilized experimental data generated by Silveston (1957) where he accurately measured heat transfer in horizontal flow in silicon 350 oil.

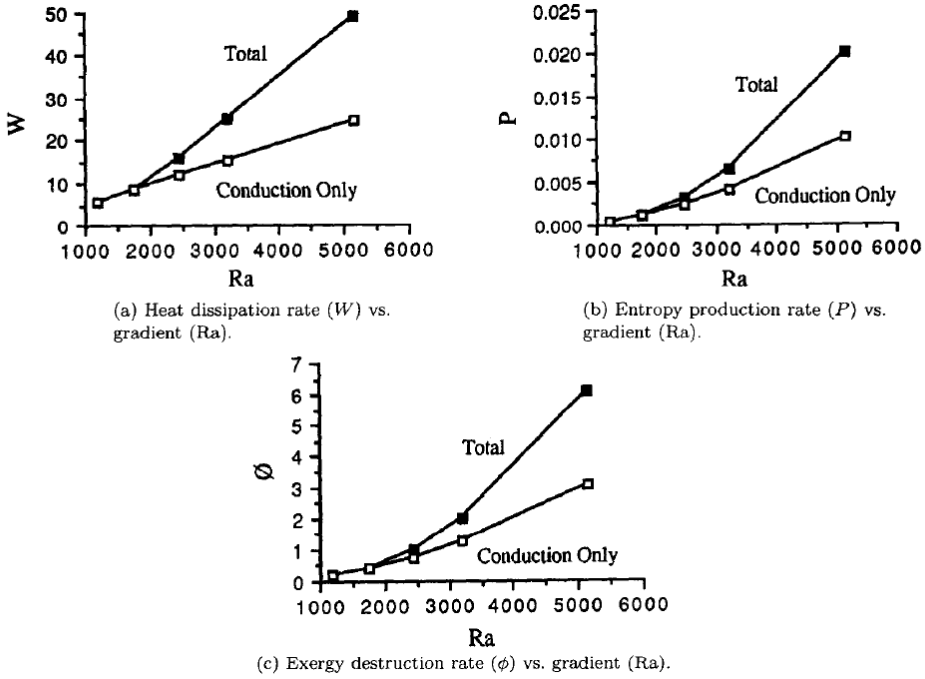

(a) Heat dissipation rate (W) vs. gradient (Ra).

(b) Entropy production rate (P) vs. gradient (Ra).

(c) Exergy destruction rate (ϕ) vs. gradient (Ra).

Figure 5-2 Adapted Bénard cell results
Source: Schneider and Kay (1994) adapted from Silveston (1957)

The three graphs represent the heat dissipation (top left), entropy production rate (top right) and finally the exergy destruction rate (bottom centre) all in relation to the Rayleigh number which serves as a measure of the temperature gradient across the fluid. At a Rayleigh number of approximately 1760 convection starts and Bénard cells begin to form, and as the gradient increases (increasing Rayleigh number) convection becomes the dominant mode of heat transfer.

In all three graphs conduction has been shown separately from the total as to clearly illustrate the effect which Bénard cells have on all 3 measures. By examining the first graph (top left) it also becomes clear that with the formation of structured Bénard cells, dissipation increases substantially, which is in agreement with the restated second law. Also of particular interest is graph 3, which measures exergy destruction as a function of the applied temperature gradient. Since the second graph shows that the entropy production rate increases with increased gradient, it should be of no surprise that exergy destruction also increases with increased gradient (recall the Gouy-Stodola theorem) and that both curves are of the similar shape. An interesting outcome of graph 3 is that as the gradient increases, it will correspondingly take a larger amount of supplied work in order to maintain the fluid structure (which in this example takes the form of a Bénard cell).

It is interesting to look at these graphs in relation to the restated second law which was defined in the previous section. The restated second law states that as a system is pushed away it will

take advantage of all possible pathways in order to counter the applied gradient and return itself back to equilibrium. As a function of this statement two important observations can be made, firstly, as a system is pushed farther away from equilibrium, it will organize itself in a way to increase dissipation (in the case of an energy gradient). This is not only evident in the first graph which shows dissipation rate linearly increases with applied gradient, but also in the fact that dissipation increases when the mode of heat transfer changes from conduction to convection. While Bénard cells clearly exhibit a highly organized structure, the fact that the heat transfer mode changes from conduction to convection is also a very clear case of structures becoming organized.

The second important point and a reflection of the restated second law is that as complexity increases, the structure will require increasingly more applied work in order for complexity to be maintained (as depicted in the third graph of Figure 5-2). This is crucial as it means that the complexity of the structure highly depends upon the amount of work available to the system and provides the basis for the vital connection between exergy and complexity which will be examined in the next section.

5.3 The Exergy Destruction Principle

As a clear by-product of the restated second law, it has been shown that as a system is pushed away from equilibrium, it will act in a way to oppose this movement (Kay, 2000; Schneider and Kay, 1994;Nicolis and Prigogine, 1977 etc.). When examining this statement through the lens of

energy (as a magnitude) it is clear that the response of the system is to begin dissipating the applied energy gradient. When examining the restated second law in terms of the exergy which the applied energy gradient is carrying however, the terminology has to be slightly adjusted. If energy is said to be dissipated by a system, then exergy can be said to be degraded or destroyed by a system. Under this premise, the restated second law can be rewritten in terms of exergy as follows:

> *A system exposed to a flow of exergy from outside will be displaced from equilibrium. The response of the system will be to organize itself so as to degrade the exergy as thoroughly as circumstances permit, thus limiting the degree to which the system is moved from thermodynamic equilibrium. Furthermore, the further the system is moved from equilibrium, the larger the number of organizational (i.e. dissipative) opportunities which will become accessible to it and consequently, the more effective it will become at exergy degradation. This is the exergy degradation principle for nonequilibrium thermodynamic situations. (Kay, 2000)*

Since this statement is so fundamentally important for the theory presented in this thesis it is imperative that each sentence be adequately explained and each is broken down individually below:

> *A system exposed to a flow of exergy from outside will be displaced from equilibrium*

This first statement should come as no surprise, as exergy fundamentally represents how far away from equilibrium a system is from its environment, it should implicitly follow that as a

system is imparted with a flux of exergy that it should then be pushed at least some distance away from equilibrium.

> *The response of the system will be to organize itself so as to degrade the exergy as thoroughly as circumstances permit, thus limiting the degree to which the system is moved from thermodynamic equilibrium*

Again, this line is fairly similar to that of the restated second law for energy dissipation, however this is where the change in terminology is first adjusted to fit within the lens of exergy analysis. Instead of the structure dissipating the energy, the structure acts to utilize the exergy and in return the exergy can be said to be destroyed or degraded. It should be noted that these 3 terms: degradation, destruction and utilization are often and mistakenly used interchangeably when they can all mean something slightly different. For the purposes of this thesis, the following definitions will be used:

- Utilization: This term is used to describe situations in which exergy is used by the system to convert energy into different forms or drive internal processes.
- Degradation: This term is used to describe situations in which the work potential from the incoming exergy stream is reduced. It is usually used to describe situations in which a small portion of the total exergy stream is destroyed as exergy is transferred and cycled throughout the system feeding irreversibilities.
- Destruction: This term is used to describe the actual process of exergy being destroyed and converted into entropy. This is either due to the irreversibilities in the processes

> which make up the system, or a product of the re-radiation of the incoming short wave solar radiation in the form of long wavelength thermal radiation (waste heat).

One of the most important aspects of the above excerpt and correspondingly the work conducted by Schneider and Kay (1994) as represented in the third graph (graph c) in Figure 5-2, is the fact that dissipative structures are no longer classified just with regards to their dissipative capabilities, but also their ability to dissipate gradients. Of clear interest to the scope of this thesis is the ability of ecosystems to not only dissipate the incoming radiative energy, but also to degrade the associated exergy gradient which is being carried by the energy flux.

> *Furthermore, the further the system is moved from equilibrium, the larger the number of organizational (i.e. dissipative) opportunities which will become accessible to it and consequently, the more effective it will become at exergy degradation.*

Perhaps the best way to visualize this statement is again by referring to the curves depicted in Figure 5-2 and realizing that all curves show a positive slope with respect to the applied gradient. As predicted by this statement, as the system is moved farther away from equilibrium (as depicted by moving right along the x-axis) the amount of exergy which is destroyed (as depicted by the curve in the third graph c) is greatly increased. Conversely, the third graph can be interpreted in a slightly different way. Instead of depicting it as a system becoming more effective at destroying exergy, it can also be taken to show how much work potential must be applied to the system in order to maintain its structure. This not only infers a more complex structure, but allows serves as an indicator that the farther the system is pushed away from equilibrium, the more it will resist further movement.

Perhaps the most important aspect of the aforementioned statement is the ramifications it has for attempting to measure the complexity of systems. Since the exergy flows in and out of a system can be theoretically calculated, the difference between the incoming and outgoing flows (assuming steady-state where no storage occurs) will represent the amount of exergy destroyed by the system. By extension, this allows the complexity of the system (or maturity when examining ecosystems), at least comparatively speaking, to be inferred remotely. Examples of which will be investigated in subsequent sections.

The final statement comes to the conclusion on which this chapter has been focused and formally introduces this exergy specific restated second law to be the exergy destruction principle:

This is the exergy degradation principle for nonequilibrium thermodynamic situations.

Most interesting to note is the fact that the theory was originally named the "exergy degradation principle", the wording which was changed sometime after Kay (2000) first formulated the principle. Note that this is simply a change in semantics alone, as this thesis follows the definitions and nomenclature of Fraser and Kay (2003) in which destruction is more clearly defined and is thus preferred to the aforementioned degradation term.

However, somewhat lost in the various different theory names and interpretations is the fact that at the core, the exergy destruction principle simply represents a specialized form of the restated second law.

5.4 Life and the exergy destruction principle

Now that the exergy destruction principle has been stated in technical terms, its application to life and specifically ecosystems will be further investigated. Given that ecosystems and life on earth are exposed to an influx of both energy and exergy, by application of the restated second law (which will now be referred to as the exergy destruction principle), it is expected that these systems, much like the Bénard cell, will organize themselves in a way which optimizes its ability to negate the effect of any applied gradients. Again this highlights the shift in thinking between what would seem impossible under the structure of the "classical" second law and now what behavior is to be expected under the exergy destruction principle. Fraser and Kay (2003) stated it more succinctly:

> *Given the exergy destruction principle and the right conditions, the emergence of living systems should be expected as a means of furthering the mandate of exergy destruction. In particular, the earth is an open thermodynamic system with a large exergy flow impressed upon it by the sun. Consequently physical and chemical processes will emerge to destroy the incoming exergy. For example, energy shifts (conversion of short wave radiation to longer wave infrared), absorption, and meteorological and oceanographic*

circulation will degrade much of the incoming solar exergy. And, as argued elsewhere [Kay, 1984; Kay and Schneider, 1992; Schneider and Kay, 1994], life is simply another means of destroying solar exergy.

Interesting to note, Schrödinger (1944) first developed the framework to suggest that ecosystems, and all living systems for that matter, are able to be classified as non-equilibrium dissipative structures. In his initial formalization, Schrödinger utilized a concept of "negative entropy" or negentropy to describe how ecosystems were able to increase their relative complexity, however as pointed out by Fraser and Kay (2003) this was an incomplete and partially incorrect model. For instance negentropy is most importantly not a substitute for exergy destruction, and various inconsistencies with how negentropy handles information and observation of systems have been identified. For example, negentropy could sometimes produce Carnot efficiencies greater than 1, while this was clarified by Brillouin (1953), it is still not an advisable term for dealing with ecosystem complexity.

While the Bénard cell and organic life are both forms of dissipative structures, they clearly represent very different situations. As Wicken (1987) noted, living systems are a very specialized form of dissipative structures since unlike Bénard cells, they are self creating systems which don't depend on applied forces for the creation of higher ordered structures. Wicken also stated that the genetic mechanisms of replication and reproduction (ie. DNA) allow living systems to be "stable vehicles of degradation" with respect to any imparted gradients.

Specifically when dealing with ecosystems, the main gradient which is of critical importance is the exergy gradient which is imparted upon the system by the suns radiation. Shown in the Figure below is a conceptual model developed by Kay (2000) which depicts how self organizing systems can behave as a dissipative structure.

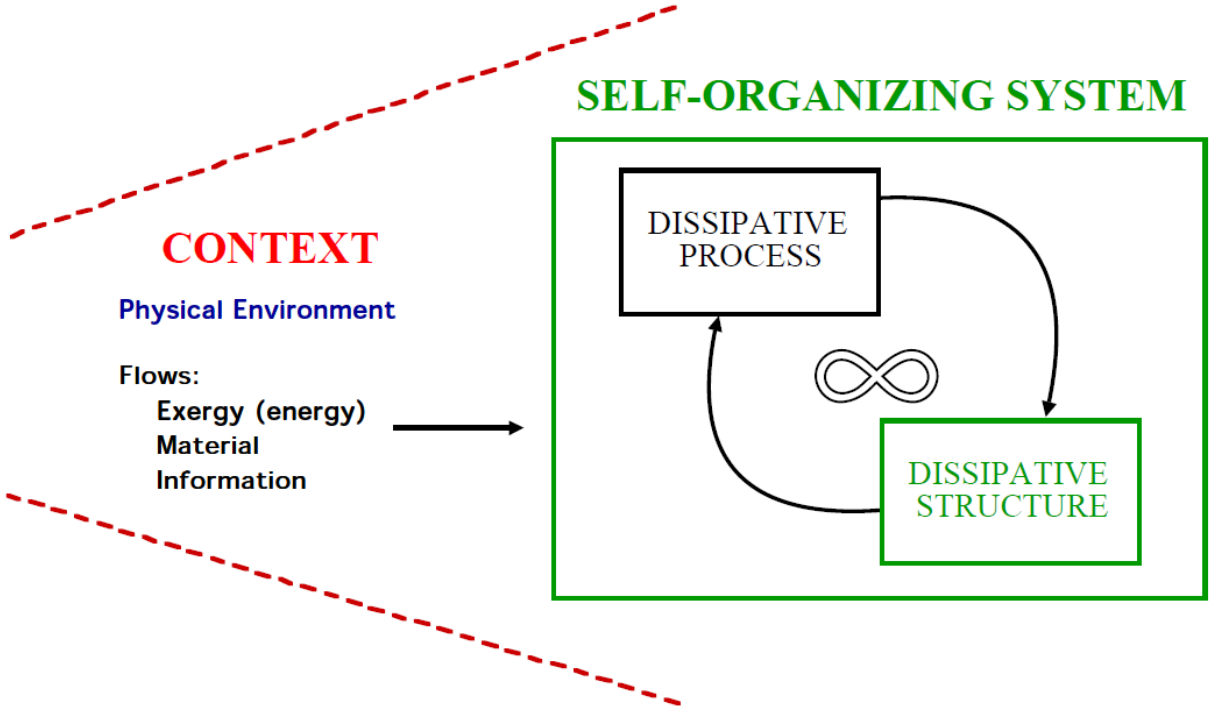

Figure 5-3 Self organizing system model
Source: Kay (2000)

As noted by Kay (2000), and by virtue of the restated second law, self organizing dissipative processes will emerge whenever a gradient with sufficient exergy exists to support them. These dissipative processes will then restructure any available raw materials (ie. biomass) in order to better destroy the exergy. While out of the scope of this thesis, it can be reasonably assumed that given various constraints imposed on the processes due to their surrounding environment

etc., that some processes will be favored or deemed more advantageous. Once these favored processes become established, they start to dissipate energy (destroy exergy) and can now be classified as dissipative structures. These initial structures form the groundwork or foundation for more dissipative processes to branch off and form, which then in turn form their own structures and the process continues. Thus the longer this process goes on, the more complex and thus, the better at dissipating exergy the structure as a whole becomes.

5.5 Exergy destruction principle and surface temperature

The exergy destruction principle hypothesizes healthy plants will strive to reduce the effect of any imparted exergy gradients, as an outcome of this hypothesis, measuring the dominating exergy inputs on the system becomes important when inferring plant health. As a consequence, the characterization of incoming exergy flows are hypothesized to be sufficient in characterizing the health and operation of plants.

Referring to Figure 1-1, it follows that the dominant exergy inputs should be identified.

$X_{\dot{M}water}$ (Exergy associated with mass flow of water)

$T_{water} = T_o$ (reference temperature) therefore,

$$X_{\dot{M}water} = 0$$

$X_{\dot{M}\text{fertilizer}}$ (Exergy associated with mass flow of fertilizer)

Average solar flux in Elora Ontario: 1325 W/m^2 (McIntyre, 2008)

Assume: 1m^2 surface area, 3 months of growing, 10 hour sunlight per day

Assume: Fertilizer is Ammonium Nitrate

Gibbs formation energy = -2.3 GJ/tonne (de Beer, 2000)

Total solar energy:

$$1325\ W\ \times\ (3\ months) \times \left(\frac{30\ days}{month}\right) \times \frac{10\ hours}{day} \times \frac{3600\ seconds}{hour} = 4.293\ \text{GJ}$$

Total fertilizer sprayed: 150 kg / hectare (Chapter 6)

$$\frac{150\ kg}{hectare} \times \frac{1\ hectare}{10000 m^2} \times 1m^2 = 0.015\ kg$$

Total amount of exergy contributed by fertilizer:

$$\frac{2.3\ GJ}{1\ tonne} \times \frac{1\ tonne}{1000\ kg} \times 0.015\ kg = 0.0000345\ GJ$$

$\frac{Gibbs}{\Phi} = \frac{0.0000345\ GJ}{4.293 GJ} = 0.00000803 \approx 0$ Therefore,

$X_{\dot{M}\text{fertilizer}} = 0$

X_Q (Exergy associated with heat transfer)

$T = T_o$ (reference temperature) therefore,

$X_Q = 0$

X_{solar} (Exergy associated solar radiation)

$X_{solar} = \phi_{solar} f(T_{surface})$

From Model 1: $W_{Maximum} = \Phi_{T,\text{Solar}} \left(1 - \frac{4}{3}\frac{T_o}{T_{\text{Solar}}} + \frac{1}{3}\frac{T_o^4}{T_{\text{Solar}}^4}\right) \neq 0$ therefore,

$X_{\text{solar}} = 0$

The incoming exergy flows of the water and heat transfer are 0 as they all occur at a temperature equal to that of the atmospheric or dead state temperature. The exergy associated with fertilizer is non-zero (1X is the standard application of fertilizer rate of 150 kg/hectare), but in comparison to the amount of exergy received from the sun it becomes a negligible amount and is assumed to be zero when considering an entire growing season. As described in Chapter 4, solar exergy is a non zero value and has a high dependence upon surface temperature. **Therefore, it is concluded that the only dominant incoming exergy flow for agricultural crops is the via the incident solar radiation.** It should also be noted, as explained in Chapter 4 and again stated as an assumption in Section 6.5, that the exergy received from the background radiation on clear sky days is negligible compared to that of the incident solar radiation.

By application of the exergy destruction principle, it is hypothesized that healthy plants will optimize their surface temperature in order to maximize the incoming solar exergy (Fraser and Kay, 2003; Schneider and Kay, 1994).

5.5.1 Maturity and surface temperature

In this ideal case, where various different maturity ecosystems are all exposed to the same amount of solar radiation, then the most mature ecosystem should re-radiate its energy at the lowest possible exergy level. As an extension of this, and of practical application to thermal

remote sensing, this means that the most mature ecosystem will have the lowest surface temperature (Kay, 2000; Fraser and Kay, 2003; Schneider and Kay, 1994).

This theoretical prediction has been confirmed by a number of different experiments. The first of which was conducted by Luvall et al. (1990) where they utilized a thermal infrared multichannel scanner (TIMS) to measure the thermal infrared radiation emitted (8.2µm - 12.2µm) over a tract of variable land covers in Costa Rica. Figure 5-4 shows the calculated canopy surface temperature over a 400m transact with the various land covers labeled.

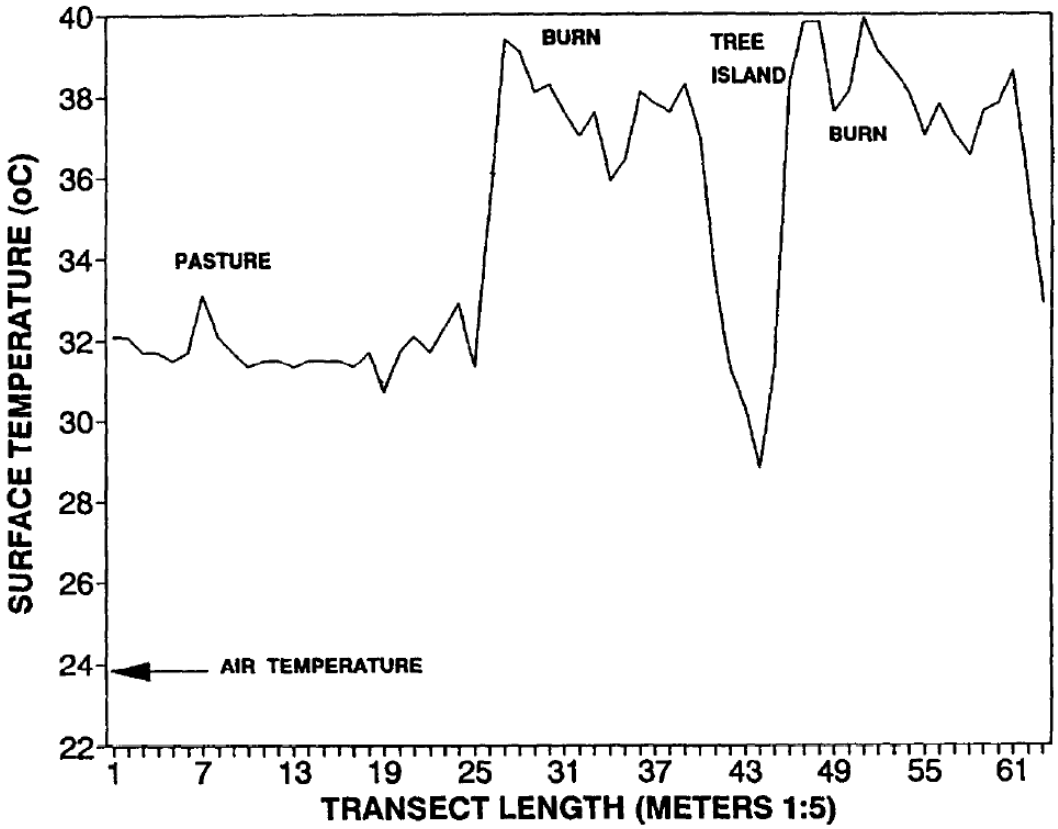

Figure 5-4 TIMS surface temperature data
Source: Luvall et al. (1990)

Perhaps the most notable observation from Figure 5-4 is the fact that the various different land covers have such a significant difference in surface temperature. The surface temperatures also follow the maturity level of the various land covers as predicted by the exergy destruction principle. From least mature to most mature: burn (highest temperature), pasture (middle temperature), tree island (lowest temperature).

Further experiments were carried out utilizing the TIMS in which the H.J. Andrews Experimental Forest was imaged. Again utilizing a similar setup where the TIMS was equipped to an aircraft and it was flown over a transact of approximately 1000m in length of variable land covers. Depicted in Figure 5-5 is the results of two passes over the same tract, one conducted at noon and the other taken post sunset.

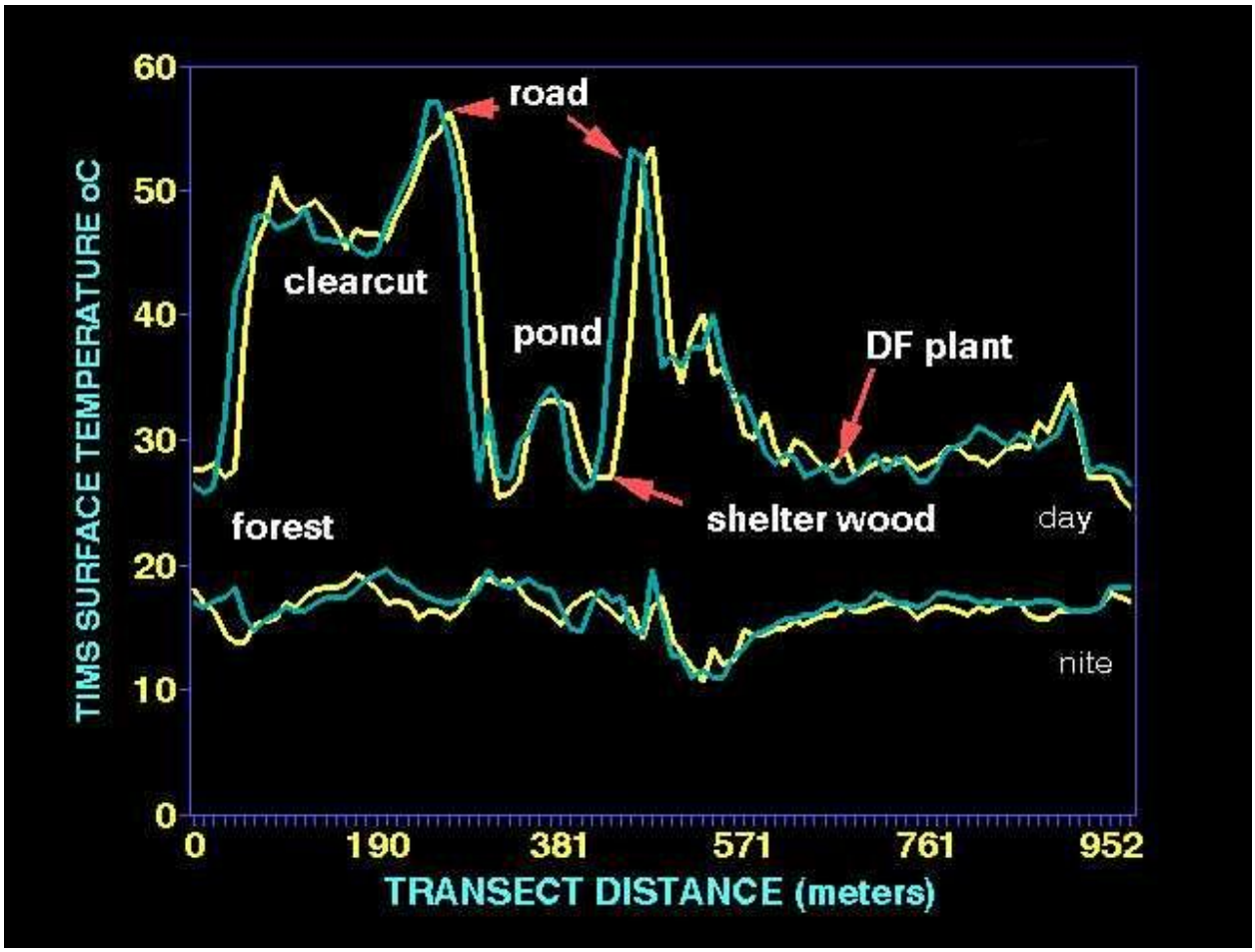

Figure 5-5 H.J. Andrews Experimental Forest TIMS data
Source: R. Fraser NASA Presentation March 2006 adapted from Luvall et al. (1990)

The same data shown with more specific labels is depicted in Figure 5-6.

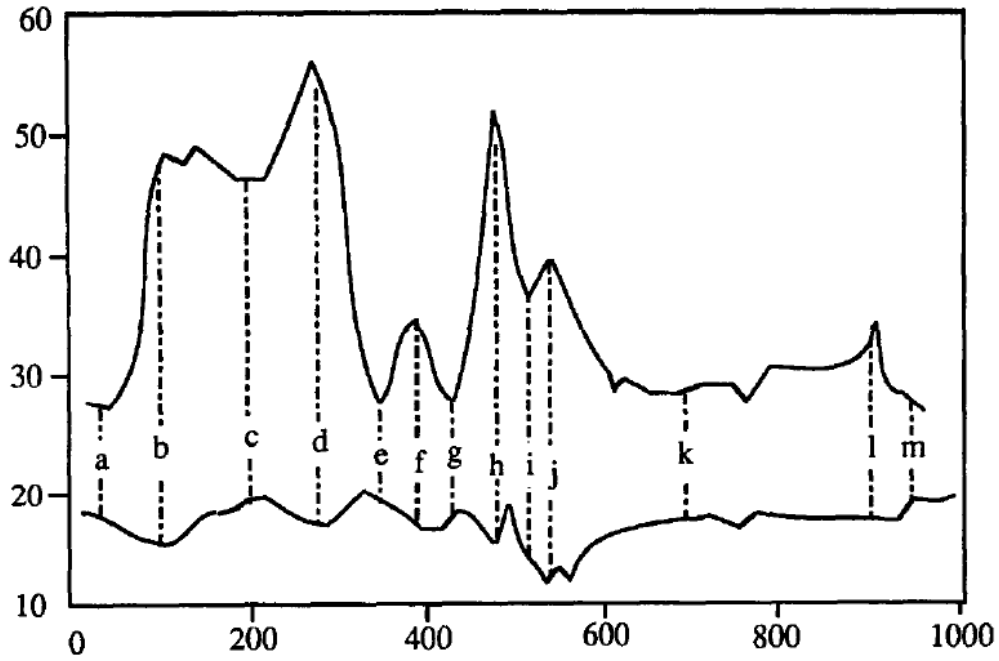

(a) edge of forest,
(b) narrow road,
(c) somewhere in a clear cut,
(d) a wider road,
(e) one side of a small shelter wood of Douglas Fir,
(f) a pond within the shelter wood,
(g) the other side of the shelter wood,
(h) a wide road,
(i) trees along the road,
(j) in a flat part of a clear cut,
(k) somewhere in a 15 year old Douglas Fir plantation,
(l) a trail,
(m) an old stand of Douglas Fir regrowth.

Figure 5-6 H.J. Andrews Experimental Forest land covers
Source: Schneider and Kay (1994) adapted from Luvall et al. (1990)

The two lines in Figure 5-6 depict the same data as Figure 5-5, where the top line represents the surface temperature of measurements taken at noon and the bottom line represents the surface temperature of measurements taken after sunset. The data is in agreement with the exergy destruction principle and its prediction that the most mature ecosystems should re-radiate their energy at the lowest possible exergy level, which corresponds to a lower surface temperature, especially when considering succession from non vegetated land to forests. This is

clear in the data when comparing the surface temperature of a section of clear cut verses that of a Douglas fir plantation which almost amounts to a 20 degree Celsius temperature difference.

While the decreasing surface temperature with respect to maturity has been well observed when measuring different land covers, the results are less clear when examining how surface temperature correlates with maturity within the same land cover. For instance, various studies such as the one presented by Maes et al. (2011) have shown that while dissipation increases with increasing maturity when comparing various different land covers (forests > agricultural > buildings), they observed no appreciable difference when comparing the dissipation of various maturities (for example when comparing medium and old forests of the same type) or even the reverse trend in some cases. A excerpt of their results is shown in the Figure 5-7 where "Po" represents poplar trees, "OD" represents other deciduous, and "Pi" represents pine. Also below the tree type is the symbol to represent age "Y" being young, "M" being medium and "O" being old.

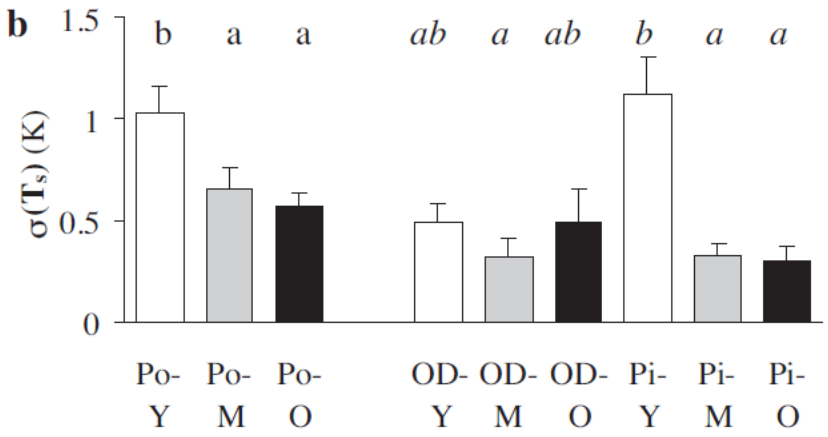

Figure 5-7 Effect of age on similar tree type
Source: Maes et al. (2011) pg. 15

While the poplar trees seem to be in agreement with the exergy destruction principle, the same cannot be said for the other deciduous or pine trees which show a reverse in surface temperature trend and no significant difference. This presents a potential question that the exergy destruction principle must provide further clarification on, or provide adequate reasoning for; however more specifics about how they generated their data (sample size of trees in their land cover map, sensor details etc) need to be known in order to fully understand the significance and implications of the results.

While issues like this still need to be investigated further, largely due to a lack of quality data, there exists a few possibilities which could account for why increased maturity does not always correlate with a lower surface temperature. Maes et al. (2011) suggest that due to a linear relationship between surface temperature and evapotranspiration, the lowest surface temperature with regard to forest succession would not necessarily occur with the most

mature forest but instead when the forest goes through the aggradation phase of development when the trees are rapidly accruing biomass and evapotranspiration is high. In fact, It is a well known fact that fast growing tree types that experience aggressive aggradation phases have the highest levels of evapotranspiration (Licata et al., 2008; Calder, 2007), and therefore it is suggested by Maes et al. (2011), skew the relative temperatures in trees of a similar type.

Similarly, while surface temperature can be a good indicator of the exergy flows at least relatively speaking when comparing various land covers, there are still a multitude of other factors which can affect the flows such as emissivity, leaf surface area, roughness etc. This issue was also identified by the Maes et al. (2011) study as being a potential source of error, as studies have recently shown the effect which structure and size can have on surface temperature. Leuzinger and Körner (2007) went on to suggest that "...canopy and leaf characteristics (branching, leaf density, angle, thickness, canopy roughness, surface specific energy absorption, instantaneous wind pattern) are causing the final canopy temperature pattern, which can only be determined empirically".

Also of interest is the effect which surface temperature has on the incoming exergy flows. By referring back to solar exergy model 1 in Figure 4-5 it is clear the effect which surface temperature has on the incoming exergy flow. Inferred from the equation in Figure 4-5, as surface temperature decreases, the ecosystem will receive more exergy from the suns radiation, and correspondingly, as surface temperature increases, it will receive less. This again

points to how exergy, at its core, is simply a measure of how far away from equilibrium a system is with its environment. Much like the Bénard cell, this signals the fact that as complexity increases, a larger and larger amount of work input potential is required in order for the structure to be maintained.

5.5.2 Surface temperature and stress

While the correlation between surface temperature and maturity is a fundamental pillar of the exergy destruction principle, this section lays the foundation of how the exergy destruction principle can be applied to measure and monitor stress in plants, specifically with regard to agricultural crops. Surface temperature has long been utilized as a indicator for a variety of applications within the agricultural sector, including: irrigation and water stress management, crop yield prediction, and evapotranspiration monitoring (Idso et al., 1977; Idso et al., 1981; Luvall and Holbo, 1989a; Luvall and Holbo, 1989b; Luvall and Holbo, 1991;Bastiaanssen et al., 2000; Pinter et al., 2003).

While the underpinnings of how stress effects plant physiology is out of the scope of this thesis, a basic understanding of stress and what it means thermodynamically is still of importance. While at least somewhat counter intuitively, perhaps the most concise way to define stress is to first define what an optimal system would look like (for the purposes of this discussion optimal will be taken as a system devoid of any stress).After establishing an optimal system, the definition of stress can then be "reverse engineered" .

In an optimal environment every plant would be afforded the required amount of nutrients (sunlight, nitrogen etc) as to never be a limiting factor in ecosystem growth. Also, while competition exists within the ecosystem between species in order to gain a larger and larger share of potential resources, this is still deemed as a natural phenomena and an integral part of a healthy functioning ecosystem. Therefore it can be deduced that “stress” in the extremely broad sense is anything that brings an ecosystem out of this optimal state, the most common example being stress caused by a lack of resources such as water or nitrogen.

As it was previously hypothesized, optimal systems will act to develop pathways to further destroy or degrade any gradient imparted upon them. If stress is taken as a departure from this optimal state, then this departure will undoubtedly affect those pathways, and by doing so it will reduce the ecosystems ability to resist gradients that push it away from equilibrium. Impairing an ecosystems ability to degrade the incoming exergy will have a decided effect on the exergy flows, both incoming and outgoing (Schneider and Kay, 1994). It is also suggested by Kay (1991) that in the presence of stress a plant or ecosystem would return to a previous stage of development or succession, interestingly enough on the same development path or "thermodynamic branch" with which it came. This is depicted in Figure 5-8.

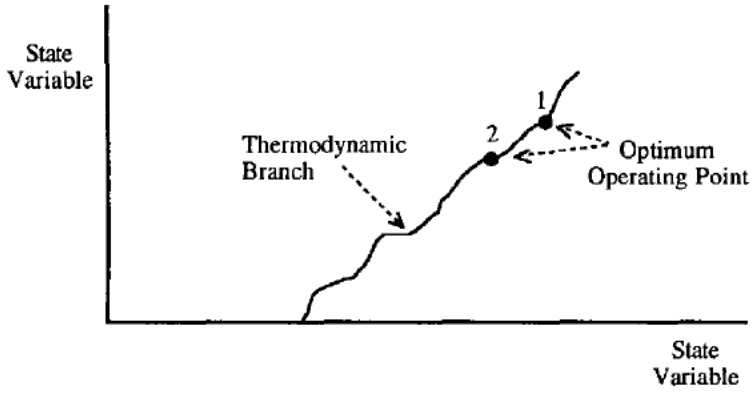

Figure 5-8 Effect of stress on thermodynamic pathways
Source: Kay (1991)

While the language utilized in Figure 5-8 is somewhat uncommon at least in engineering practice. It should be noted that here "state variable" refers to Odum's representation in which state variables are things such as photosynthesis, total biomass etc. as opposed to the thermodynamic description of state variables such as temperature, pressure etc. (Odum, 1969). Regardless of the definition of "state variables", the image depicted in Figure 5-8 can be taken as a thermodynamic diagram of sorts which shows how an ecosystem develops over time as depicted by the "thermodynamic path". In Figure 5-8 the system continues to develop under optimal conditions until it reaches point 1 at which point the system experiences stress and reverts to a previous succession stage on its thermodynamic path (point 2). Of note is how point 2 is still labeled as an optimum operating point, which illustrates that even though a system will be negatively impacted by stress, it will always act in a way which it optimizes the circumstances it is in (Kay, 1991).

As various pathways get hampered due to the applied stress, the ecosystem will be unable to effectively resist or degrade the same amount of exergy which it once could and thus will get pushed farther from equilibrium. This once previously destroyed exergy will now instead have to be re-emitted back into the surroundings, which it will do by increasing its surface temperature so that it can re-radiate its energy into the surroundings at a higher exergy level (Fraser and Kay, 2003).

Not surprisingly, in stark contrast to how a healthy system will utilize the available exergy in order to develop more pathways so that it can more effectively destroy the incoming exergy, and as a byproduct reduce its surface temperature, a system under stress will do the exact opposite. The stressed systems existing pathways will either become blocked or be less effective at destroying exergy and as a byproduct will increase its surface temperature. Either way surface temperature plays a huge role in how the ecosystem operates, which is why remote sensing is primed to play such an important role in ecosystem characterization going forward.

5.5.3 Building on previous work

While there is a clear precedent in the literature to conduct further research on a number of different topics with regard to surface temperature and the application of the exergy destruction principle, the main findings and experiments conducted in this thesis and presented in the following chapter will be an extension of the masters work conducted by Mohammad

Akbari (Akbari, 1995) at the University of Guelph. With specific focus on how remote sensing can be utilized by the precision agriculture industry for identifying stress in crops.

5.5.3.1 Akbari Thesis overview

Even though Akbari's work was more focused on the agronomy aspect of measuring stress in agricultural crops such as corn and soybeans, much of his findings are unsurprisingly consistent with the results predicted by the exergy destruction principle. Of specific interest to Akbari was the relationship between the canopy surface temperature and air temperature differential which he predicted would be of crucial importance to how stress can be identified (Akbari, 1995).

While the focus was on identifying stress in agricultural crops, Akbari did conduct a few experiments which measured the surface - air temperature differential for non-agricultural sites of various successions (maturities) in a local area, much like the results presented in the previous section. An example of his results are shown in the Figure 5-9.

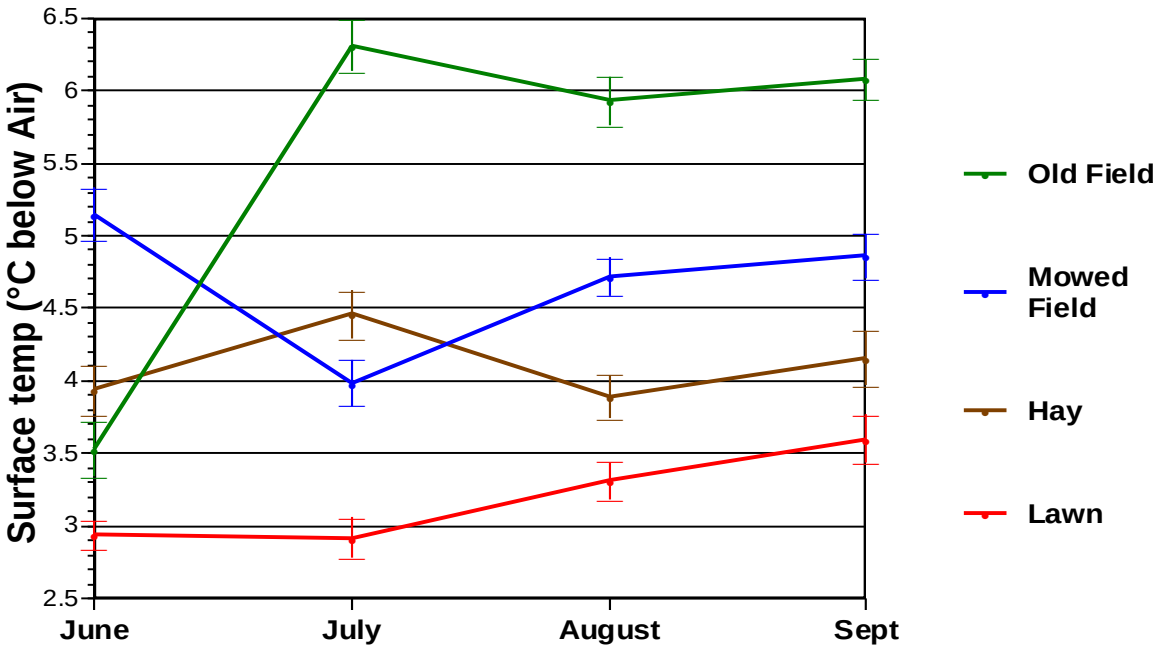

Figure 5-9 Surface - air temperature differential for various ecosystems
Source: R. Fraser NASA Presentation March 2006 adapted from Akbari (1995)

The 4 ecosystems shown in Figure 5-9 are all of different succession or maturity, sorted by increasing succession: Lawn, Hay field, Mown field, Old field (20 years old). Since the left axis here is a measure of the surface - air temperature differential, the ecosystem which has the lowest surface temperature (assuming a similar air temperature) will have the highest differential. These results are again consistent with the exergy destruction principle and highlight an important point about not just studying surface temperatures in isolation, but instead utilizing things like air temperature to get a more accurate description of the surroundings in which an ecosystem operates. This is crucial when comparing ecosystems of different locations with different atmospheric conditions.

The importance of air temperature is also something which is reiterated by Fraser and Kay (2003) and is inherently a significant factor when it comes to calculating solar exergy. While the past sections have been spent describing how surface temperature effects how much exergy the plant receives from the solar radiation, one must not forget that exergy is a measure of how far away from equilibrium a system is with its *environment*, and thus the surroundings must not be neglected. This again becomes implicitly clear by referring back to the solar exergy equations presented in Chapter 4.

By examining the equation of model 1 (Figure 4-5), it is clear that the reference state (T_o) has just as much impact on solar exergy as does the plants surface temperature. However not shown in Section 4.4 as it is out of the scope of this thesis is the fact that in the derivation of model 1 the surface temperature approaches the reference temperature when the limit of the exergy equation is taken (Landsberg and Mallinson, 1976; Bošnjakovi, 1988; Press,1976). As a byproduct of this, and as identified by Fraser and Kay (2003), this means that the ecosystem surface temperature is correlated with the reference temperature, where the reference temperature can be properly assumed to be the atmospheric air temperature. If these two temperatures are correlated, then that ultimately means that it is in fact the reference temperature which has the final say in terms of determining the incoming solar exergy, which Akbari's data also suggests.

5.5.3.2 Focus on agriculture

While Akbari's work included some trials measuring surface temperature of ecosystems representing different successions (corresponding to the first outcome of the exergy destruction principle which hypothesizes that exergy destruction increases with maturity), his work largely focused on monitoring the impact that stress has on surface temperature of agricultural crops (corresponding to the second outcome of the exergy destruction principle that stress inhibits the ability of ecosystems to degrade exergy) and how it could be utilized in a precision agriculture management regime. The main experiments Akbari conducted which the experiments in this thesis will build on are those which dealt with variable nitrogen rates in corn. In these experiments various different nitrogen rates were applied (0, 50, 100, 125, 150 and 200 kg per hectare) in order to generate a variable stress profile within the corn plots. Further specific details about the planting practices and herbicidal treatments can be found within Akbari's thesis (Section 3.2 page 46).

In the main experiments Akbari conducted, surface temperature was remotely sensed via a handheld infrared thermometer which operates in the 8-14 micrometer range and was held approximately 50cm above the surface of the leaf at a 90 degree angle above the canopy. The emissivity of the leaf was set at an average value of 0.98 (Akbari, 1995 Section 3.3.1 page 48). Figure 5-10 is an excerpt of his results:

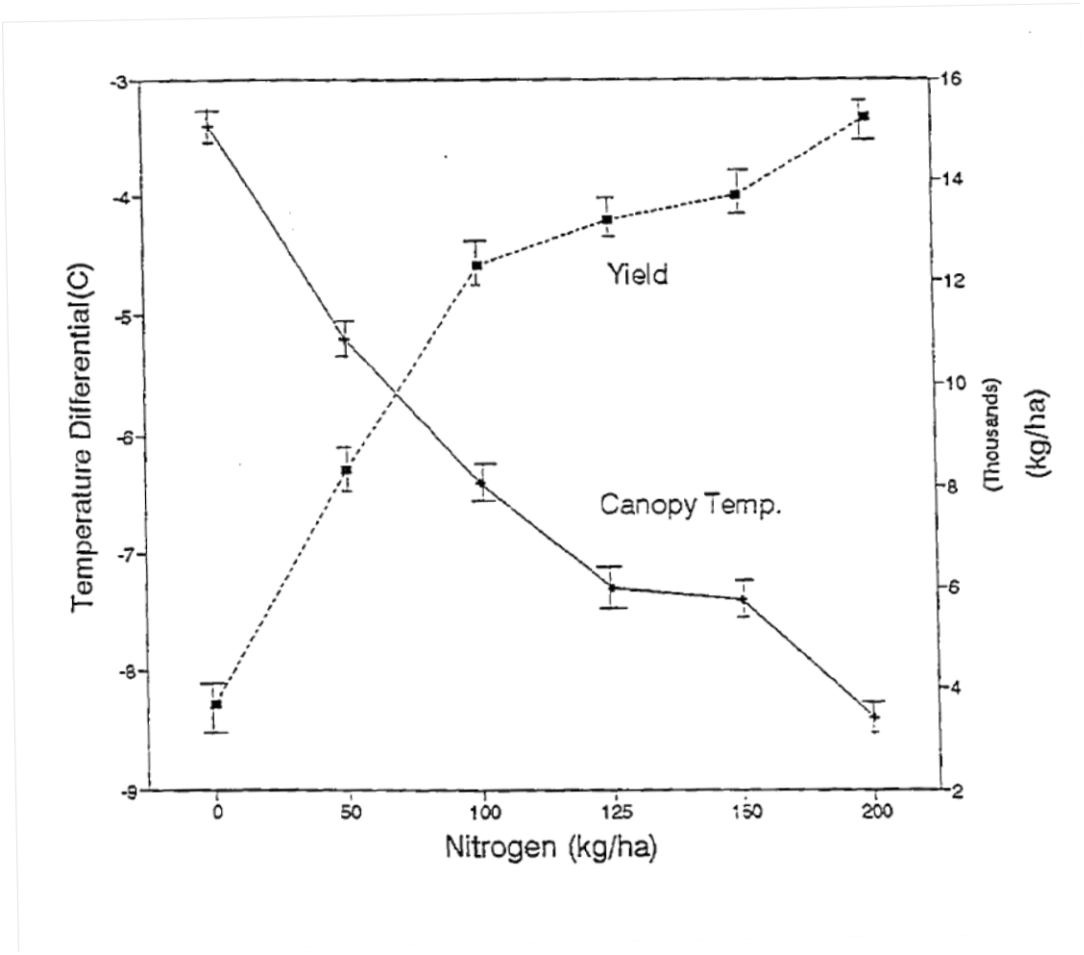

Figure 5-10 Surface temperature and yield as a function of nitrogen rate
Source: Akbari (1995)

In this experiment, the nitrogen represents an "analog" stress which is variably applied in order to generate a range of stress levels within the corn, from the extremely severe case of 0 kg/ha applied nitrogen to the more standard application rate of approximately 125 kg/ha. As predicted by the exergy destruction principle, any stress imparted upon the system will begin to hinder the pathways which the ecosystem had developed to destroy the incoming exergy. This should in turn reduce the amount of exergy destroyed by the system and cause the system to re-radiate its energy at the highest exergy level which it accomplishes by raising its surface

temperature. This hypothesis is clearly supported by the results shown in Figure 5-10, as evidence of the increasing air-surface temperature differential with decreasing stress (increasing nitrogen rate).

The yield data shown on this graph serves two distinct purposes. Firstly, and perhaps more important to the agronomist than the thermodynamicist, is to see the physical effect which stress has on the morphology and structure which will then manifest itself in the yield of the crop. Secondly, yield can be taken in the literal form as a measure or extension of the crops level of development, something which the exergy destruction principle has clear theories about as it pertains to surface temperature. In fact the mapping of yields in crops by utilizing remotely sensed data pre-harvest has already been investigated quite extensively with varied degrees of success (Bhatti et al., 1991; Timlin et al., 1998)

A main objective of this thesis is to confirm these results and further expand the data set which study the thermodynamic effect of plant stress and identify its suitability as a tool for the precision agriculture industry. The next chapter will outline the experimental methods and procedures of the trials conducted as part of this further research.

5.6 Theory into practice

While the exergy destruction principle hypothesizes that healthy plants want to utilize exergy more effectively so that it can gain more exergy from the suns radiation, in practice, healthy plants have to optimize their surface temperature in relation to their surroundings. For example, while ideally they would want to maintain a surface temperature as low as possible, there are a number of different factors which a plant is effected by, such as needing to maintain a certain temperature for photosynthetic processes to occur.

As discussed in Section 5.5.2, stress will affect a plants ability to destroy exergy, thus throwing off their optimization, and pushing it farther away from equilibrium, thereby increasing its surface temperature. The trials presented in Chapter 6 will be centered around inducing a variable stress profile in both corn and wheat and observing to what degree surface temperature is affected.

Chapter 6. Materials and Methods

The various experiments which will be presented in this chapter can be split up into two distinct categories. First, much like the work conducted by Akbari, field trials took place during the summer growing season which represent realistic, albeit uncontrollable natural conditions. The second type of experiments were conducted in a more controlled environment within a greenhouse located at the University of Guelph which offered much more stringent control over input variables to the plants such as water and nitrogen. All experiments were made possible thanks to a joint venture with the University of Guelph's Department of Plant Agriculture. The objective of this chapter is to describe the materials and methods employed by both sets of experiments and lay the groundwork for the application of remote sensing surface temperature within the precision agriculture sector.

6.1 Field Trials

The field trials were located in 3 sites owned and operated by the University of Guelph: Elora research station, Arkell research station and the Woodstock research station. All planting, tillage, herbicide and pesticide treatments were completed by the technical staff in charge of the various locations and were conducted using standard procedures. All corn was planted utilizing a standard density of 9 plants per m^2 and each distinct treatment plot consisted of 4 rows of approximately 4 meters in length. An example of this spacing is shown in Figure 6-1.

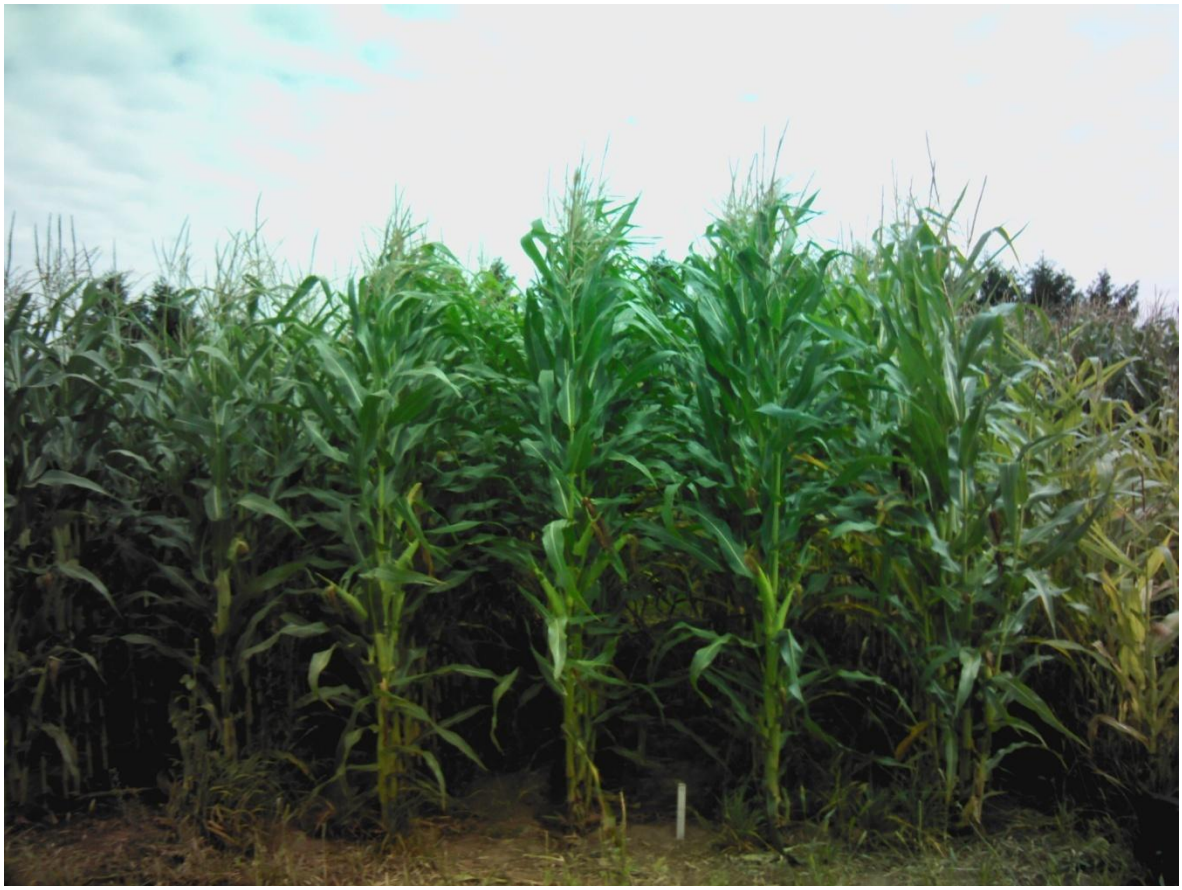

Figure 6-1 Spacing in corn trial

In Figure 6-1, the white peg sticking out of the ground represents the middle of one block, so the same treatment is applied to the two rows of corn on either side of the peg, and then the next treatment block begins. All treatments were replicated 4 times and planted according to a randomized block design. An example of what a trial would look like is shown in Figure 6-2.

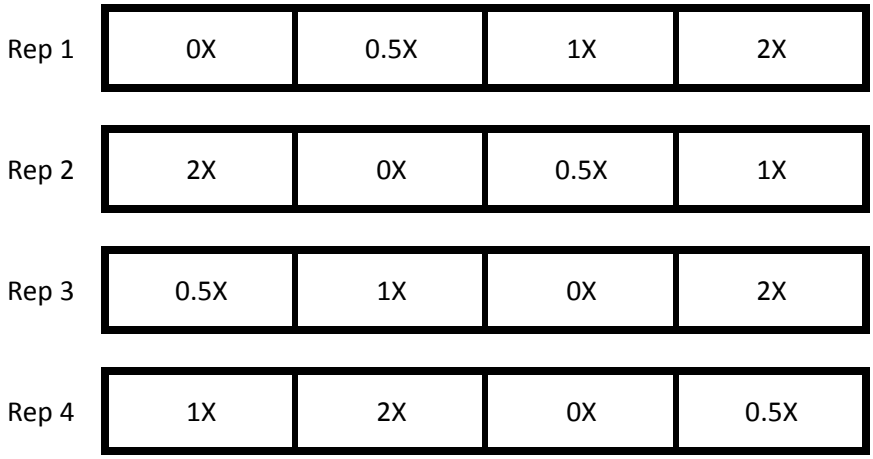

Figure 6-2 Example of randomized block trial scheme

Figure 6-2 is be an example of a nitrogen stress trial which was performed where 0X, 0.5X, 1X, 2X represent the amount of nitrogen applied to the crop relative to the industry standard or average which is applied in the specific area (ie. 1X represents the industry standard, 0.5X represents half that amount etc.). As mentioned, each block represents approximately 4 rows of corn each and thus it can be assumed that all corn in each 4 repetitions experience the same atmospheric conditions (such as relative humidity, precipitation, wind, soil condition, etc).

Two different types of field trials were conducted, the first type utilized variable applied nitrogen in order to simulate stress, the second utilized use of an analog weed which was removed at different stages of corn development in order to induce stress. Both types will be more accurately explained in the section below.

6.1.1 Nitrogen stress trials

These trials are largely a continuation of the stress studies first initiated by Akbari (1995) and the University of Guelph Department of Crop Science. Stressing the plants with nitrogen, or lack thereof, is chosen as it provides the advantage of accurately controlling the stress input on the crop even in an outdoor and largely uncontrolled environment, something which would be extremely difficult if stressing the crop via water or photon exposure.

Trials consisted of both corn and winter wheat, which were identical in conceptual setup and execution. The setup consisted of a randomized block design of four treatments and four repetitions such as that depicted in Figure 6-2. The 4 treatments represent 0X, 0.5X, 1X and 2X times the amount of standard nitrogen which is applied to corn and winter wheat. Herbicide and pesticides were applied according to the standard procedure adhered to in industry, on a pre and post emergence basis depending on severity of weeds and required rainfall for chemical activation. An example of the treatment schedule which shows the random block design, specific strain of corn utilized, and herbicide log is shown in Appendix A.

The trials were completed in the summer of 2014 and 2015 at the Elora/Arkell and the Woodstock research stations, respectively. Corn was planted in May of both years and taken to harvest where yield data was manually collected by the technical staff at each location. Figure 6-3 and Figure 6-4 show the experimental setup of both the nitrogen corn and winter wheat trial in located in Arkell and Elora respectively.

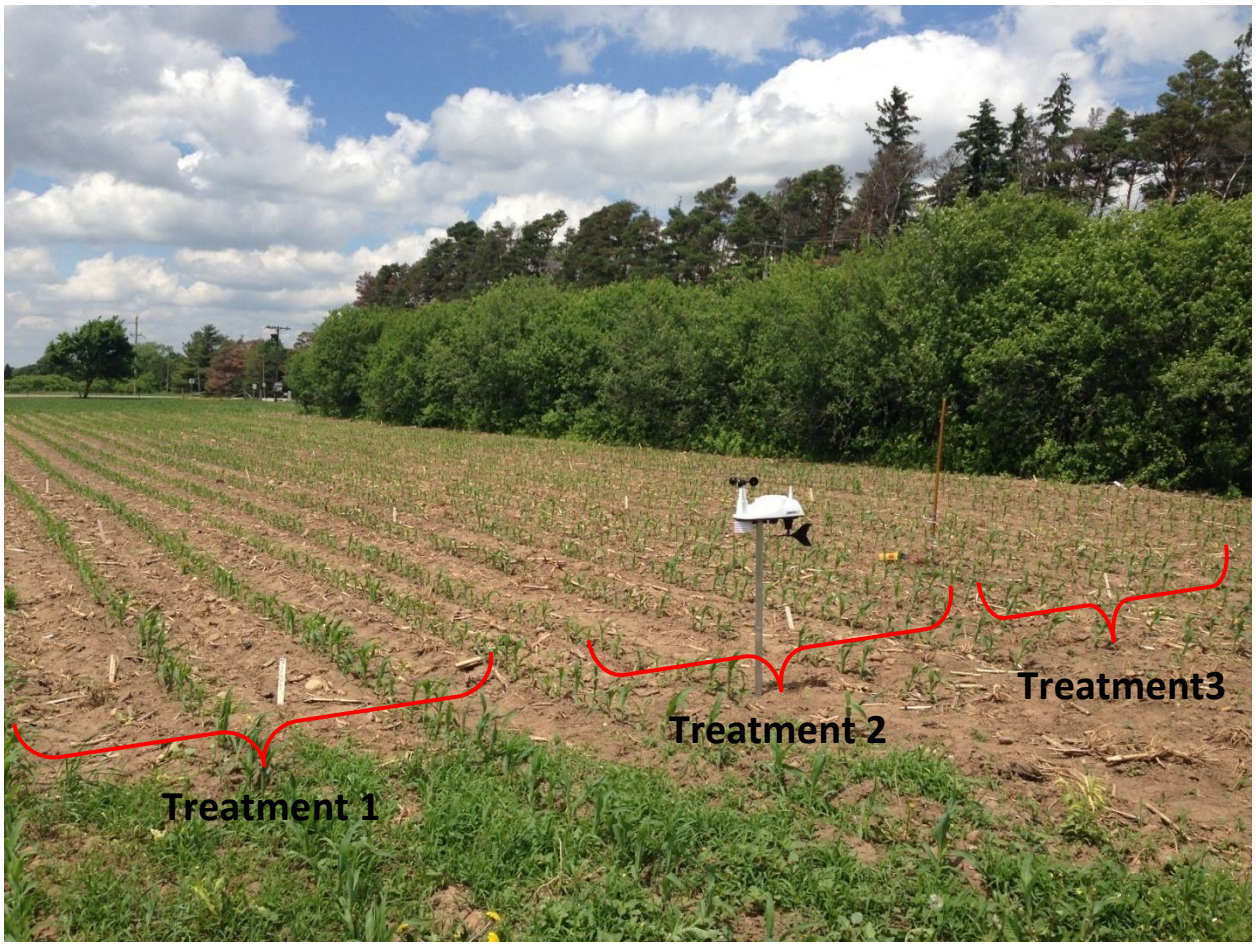

Figure 6-3 Nitrogen stress corn trial at Arkell
Photo taken June 13th 2014

The photo in Figure 6-3 was taken when the corn was approximately in the 5th leaf stage and depicts the spacing and layout of the experiment with the white stakes denoting each treatment plot. Note that the fourth treatment on the far right side isn't shown.

Figure 6-4 Nitrogen stress winter wheat trial at Elora
Photo taken June 13th 2014

Figure 6-4 shows the winter wheat trial which was located at the Elora research station and again shows the experimental setup where the pink flags indicate the individual treatment plots. The various nitrogen treatments produced a noted effect on both the biomass and color of the wheat as indicated in the visual difference between treatment 1 (2X nitrogen) and treatment 3 (0X nitrogen).

6.1.2 Weed stress trial

The second type of field trials conducted utilized the presence of a competing species ("weed") planted in close proximity to the corn plants in order to generate stress. Wheat was chosen as the analog weed as it would grow at approximately the same rate early on in the corns development as to not completely dominate and wipe out the corn early on. The wheat was then removed at different stages of the corns growth according to the leaf stage of the corn with one plot experiencing a full season of stress (weeds never removed until harvest) and one being a control (weed free check). A picture taken of the full season stress plot is shown below.

Figure 6-5 Full season weed stress corn
Picture taken July 18 2014

The timings of the removals corresponding to the corn leaf stage were as follows: 2-3, 4-5, 6-7, 8-9. When the corn reached the corresponding leaf stage a herbicide which was specifically selected for its negligible effect on corn was hand sprayed and typically destroyed all weeds within 5 days. A similar randomized block design was utilized to position the 4 repetitions of 6 treatments which is shown in Figure 6-6.

Figure 6-6 Weed stress trial layout
Photo taken June 18th 2014

Figure 6-6 shows the first of the four repetitions (the other 3 are to the left side) and illustrates the herbicide in action which was just sprayed on the 2-3 leaf stage plot. The herbicide acts

extremely quickly at this growth stage and take a few days longer as everything increases in biomass.

6.2 Nitrogen stress greenhouse trials

While the field trials represent a realistic case to study crop stress, they are often subjected to a number of uncontrollable variables which have a decidedly unknown effect on the stress levels of the crop. For example: droughts can occur, resistant weeds, pests, wind and air temperatures etc. all can have a significant impact on crops which are grown in an outdoor environment. By utilizing a greenhouse a number of these variables can be more accurately controlled or even eliminated, which will allow for more acute stress control, in this case being nitrogen, and improve the integrity of the measurements.

The light source in the greenhouse is set to operate in a "supplemental sunshine" setting in order to simulate 16 hours of sunlight. In this supplemental setting, the lights will turn on at dawn when the sun rises and will begin to supplement the incoming sunlight for the next 16 hours at which point they will turn off. The system is GPS based with a light meter in order to coordinate when the lights are fully on, half on, or completely off as would be the case during a clear sunny day. There's also an air conditioner on one side of the greenhouse in order to regulate the temperature and prevent overheating, especially during the summer.

Corn was chosen as an ideal candidate for greenhouse trials as it had been known to grow extremely well in previous greenhouse trials conducted at the University of Guelph. Each corn plant is potted individually in a gravel based soil and fed via drip with water and a nitrogen based liquid fertilizer. The drips work on a timer based system with an intake pump from a gallon tub of nitrogen which gets mixed into the flow of water and delivered to the respective pots. There were 3 nitrogen treatments (low, medium and high) consisting of 30 plants per treatment which was repeated for 2 repetitions. The experimental layout is shown in the Figure 6-7:

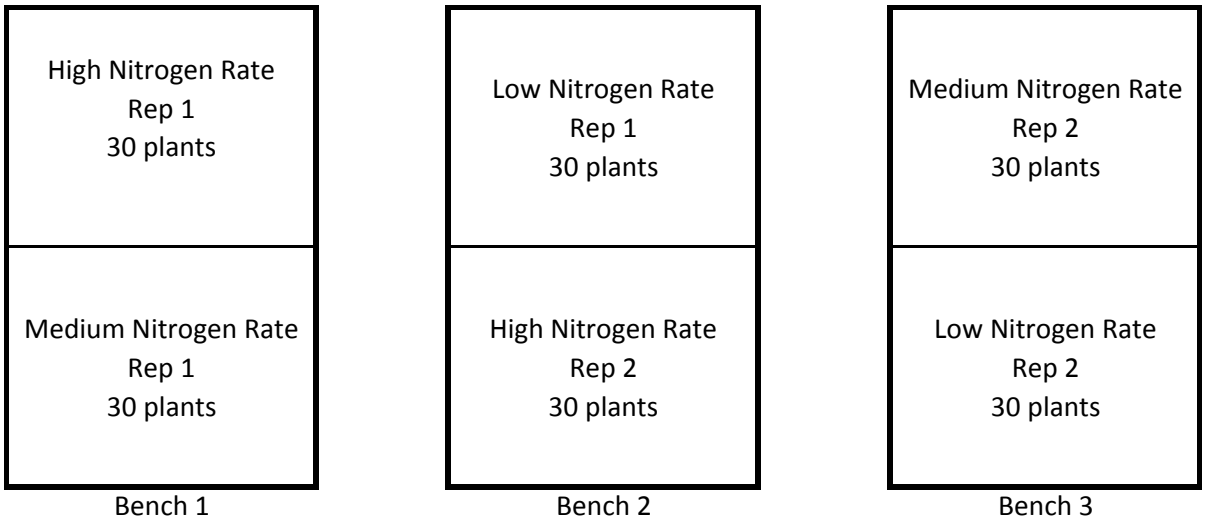

Figure 6-7 Greenhouse layout

Figure 6-8 shows a picture of the high nitrogen rate (rep 1) corn in the background and the low nitrogen rate (rep 1) in the foreground. Figure 6-8 also shows the drip mechanisms which delivers the nitrogen and water to each pot (black rod sticking into the pot) and the planting density of the corn.

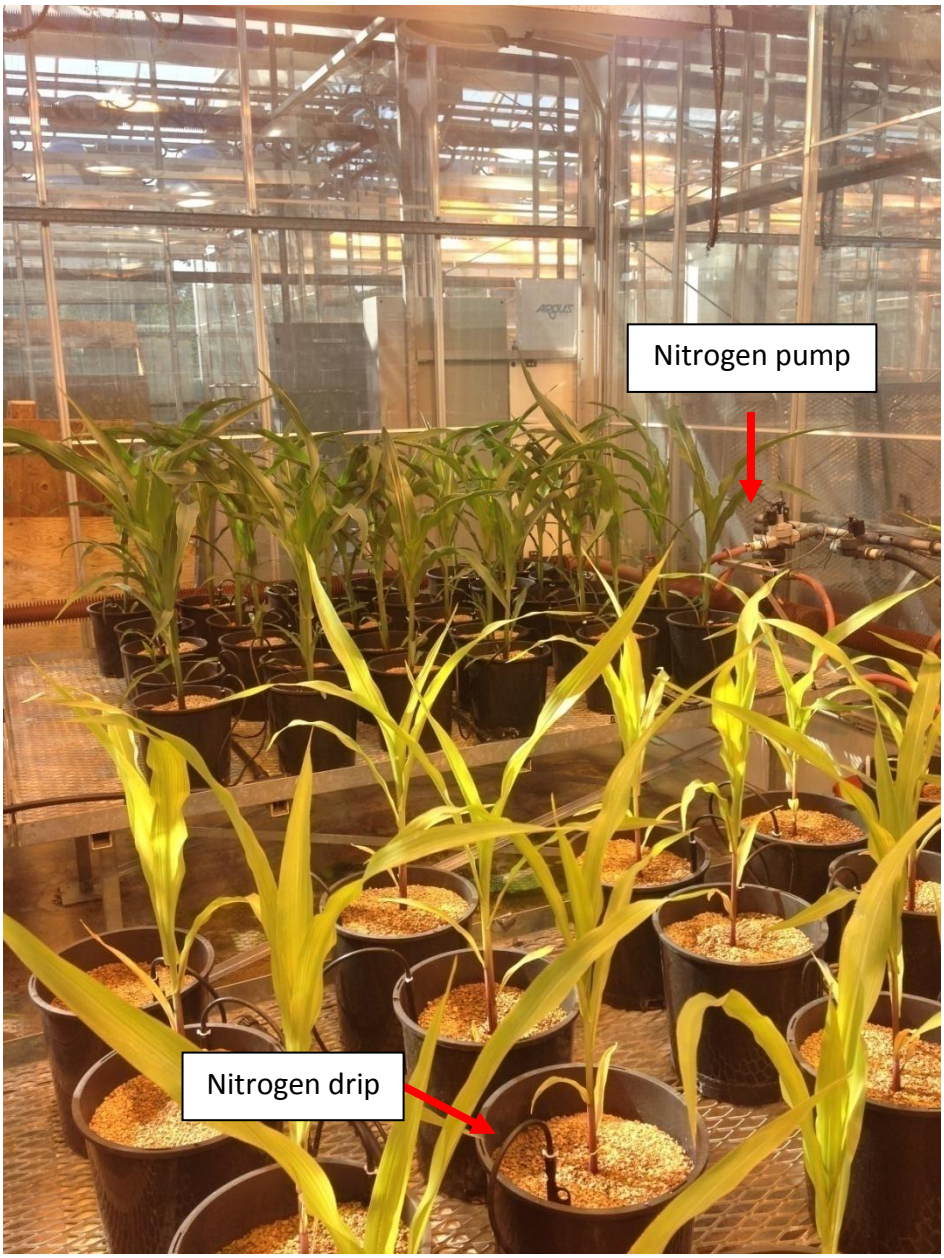

Figure 6-8 Low and high nitrogen corn
Picture taken June 29 2015

It is interesting to note, that visually there already exists a substantial difference between the low nitrogen and high nitrogen treatments, not only in color but also in biomass. Seen on the far right of the picture is the pump which delivers the liquid nitrogen mixture into the individual

pots. Flow rates were tested before every experimental run in order to ensure even distribution of liquid amongst all pots.

The corn was grown until it reached approximately 3 feet in height at which point it was harvested by cutting the stem right above the soil. The leaves of each plant were then removed and run through a leaf area machine which records the surface area. After collecting the surface area measurements each corn plant (leafs + stem) was individually bagged and dried. The drying process took approximately 5 days at 80°C in order to remove the moisture content so that the biomass can be accurately weighed. Biomass and leaf area results are shown in Appendix B.

6.3 Measurements and tools

The principle tool utilized for surface temperature measurements is a FLIR T620 thermal camera (640 x 480) which utilizes an uncooled focal array to measure temperatures in a range of -40°C to +150°C within an accuracy of +/- 2°C or +/-2%. When taking readings the camera was positioned approximately 0.5m away from the crop and readings were taken in a perpendicular direction away from the incident sunlight. A surface emissivity of 0.95 was utilized for all plant surface measurements. An example of the thermal image produced is shown in Figure 6-9.

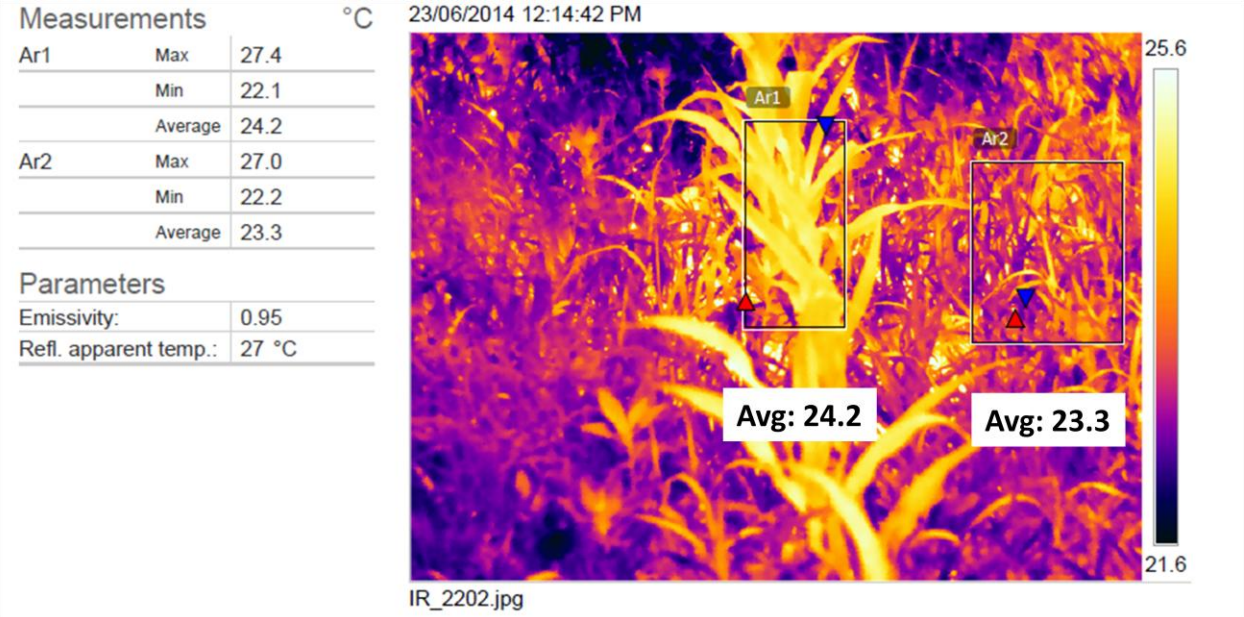

Figure 6-9 Example corn trial thermal image

Figure 6-9 shows an image taken of the corn field trials where the corn is stressed with an analog weed (wheat) which was planted throughout the plot, where yellow represents a hotter temperature and blue/purple represent colder temperature. In the image, the plants in the middle of the image with the box average of 24.2°C are the corn and all other plants in the image are the analog weed (average of 23.3°C). While the averages indicated on the image show almost a full degree of temperature difference between the corn and the weed, it should be noted that as this is a thermal image, the fact that the corn can be resolved visually means that a non zero temperature difference between the corn and weed exist.

Field measurements were always taken near noon hour under consistent clear sky conditions and temperatures were always taken from the middle rows of the plots to avoid any edge

effects which might occur between treatment types. A mobile weather station was also utilized in order to measure atmospheric conditions such as humidity, air temperature and wind speed. Measurements of each trial took approximately 1 hour and it can be assumed that there were no significant changes in incoming radiation level or atmospheric conditions over that time.

In combination with thermal imaging, thermocouples were utilized in both the field trials and the greenhouse. Type T FEP insulated thermocouples were chosen which have a temperature range of -200°C to +204°C and an accuracy of +/-0.5°C or +/-0.4% of the stated reading. In the field trials, thermocouples were affixed to the leaves of mature corn which could support their weight and not damage the plant, in the greenhouse thermocouples were affixed in the whorl of the corn as the leaves were too small to support the weight without damage as shown in Figure 6-10.

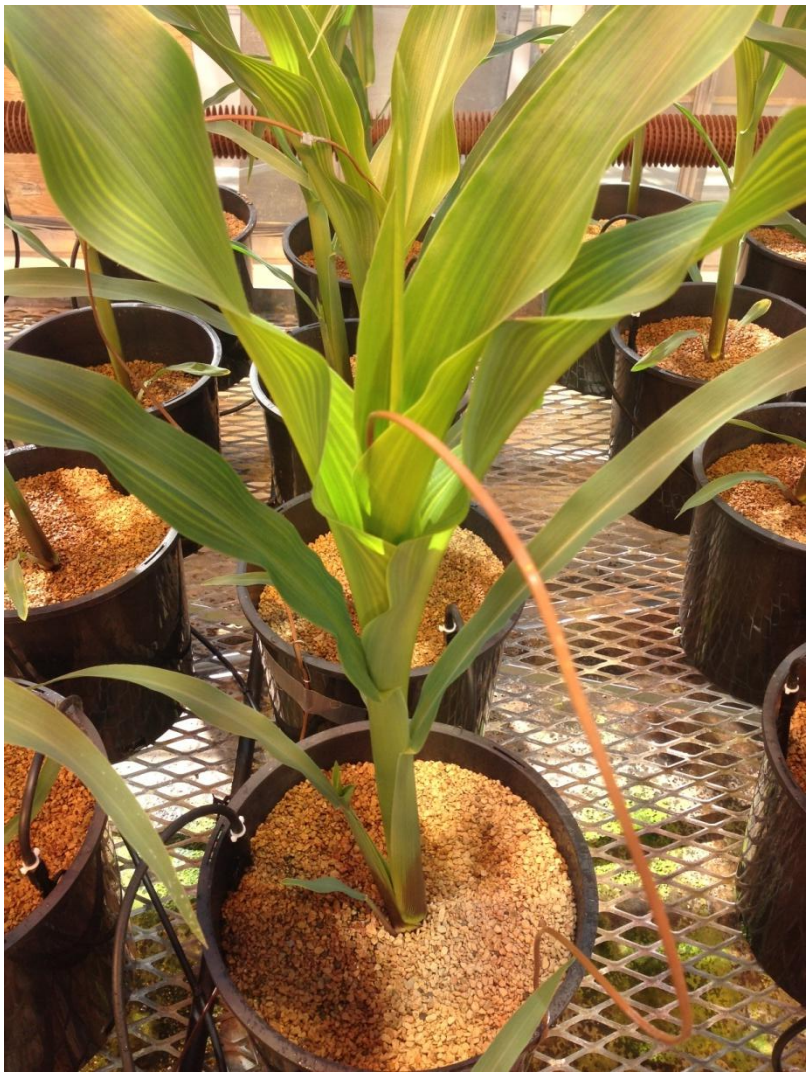

Figure 6-10 Whorl thermocouple setup
Picture taken June 29th 2015

All thermocouples were connected to a recording device which enabled 24 hour autonomous measurements.

6.3.1 Surface temperature averaging

While surface temperature is often mentioned as a singular quantity, by investigating a thermal image of corn (Figure 6-11), it is clear that the entire plant doesn't maintain a single temperature and there is a large amount of variability even across a small cross section of the leaf's surface.

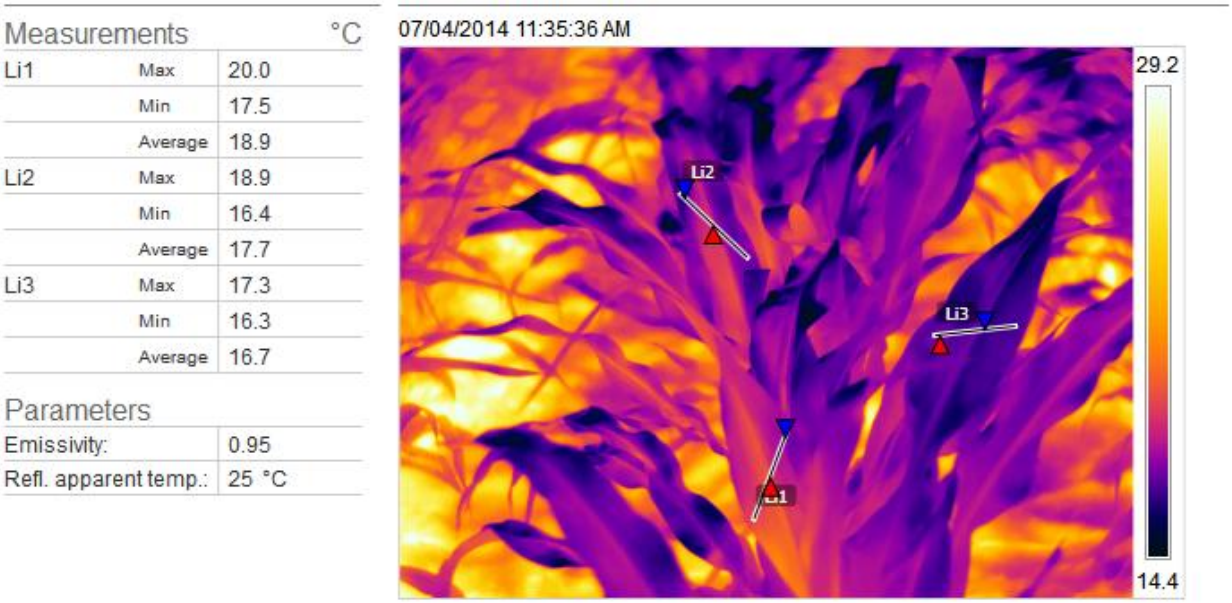

Figure 6-11 Surface temperature variability in corn

In Figure 6-11, 3 lines have been drawn across the leaf's surface which output the max, min, and average temperature over the line's span. By investigating Line 1 (Li1) it shows a 2.5°C temperature difference between the max and min temperatures, all of which occur over a roughly 10 centimetre distance. In order to produce a "singular" surface temperature which can be used to compare corn in different stress conditions a average surface temperature is calculated from the thermal images.

6.3.2 Image processing

Thermal images were processed utilizing FLIR image software "ResearchIR 4" which converted the bulk radiance data into surface temperature given various input factors such as atmospheric temperature, surrounding temperature etc. Most post processing techniques utilized a box averaging to determine an estimated crop surface temperature. The software also allowed for temperature segmentation as to exclude temperatures (such as those of the hot soil) and thus generate a realistic "average surface temperature" measurement. An example of the segmentation software to remove the hot soil is shown in Figure 6-12.

Figure 6-12 Image segmentation

The image on the left represents a standard thermal image without the use of any processing, the image on the right represents an adjusted image where anything which is white has been segmented out enabling accurate surface temperature averages to be taken.

6.4 Methodology

Now that the experiments have been outlined, a brief methodology of both the field and greenhouse trials will be discussed. **Refer to Appendix C for the complete methodology detailed for each individual trial**.

6.4.1 Field trial methodology

Beginning approximately one week after corn emergence from the soil or late may for the wheat trials, measurements would begin to be collected. Thermal images would be taken by standing on the edge of the plot as to not disturb the growing conditions of either the corn or the weeds. The thermal camera would be positioned towards the center of each treatment plot and held approximately 1m away from the corn. Measurements were always taken at a consistent time (12pm), under consistent weather conditions and would be taken in a timeframe of approximately 10 minutes to ensure relatively constant atmospheric conditions.

Measurements were always taken with clear skies, and in the case of a small amount of cloud cover which could interfere with the direct sunlight, measurements would stop and only resume once clouds passed. A small weather station was also utilized in order to monitor local air temperature accurately. Visits to the field sites happened 2-3 times a week to collect data and ensure all experiments were functioning properly.

As mentioned in Section 6.1, all spraying of herbicides for the weed stress trial were conducted by the University of Guelph field staff. All chemicals (herbicides, pesticides, fertilizers) were sprayed by hand utilizing a backpack spraying system which sprayed one treatment plot at a time with minimal intrusion to the plants. The field staff also completed the yield gathering once the growing season was over. The yield was gathered from each individual plot by hand and then weighed on a scale to infer the total gross yield of all trials.

6.4.2 Greenhouse trial methodology

As mentioned in Section 6.2, the corn in the greenhouse was planted by hand into individual pots (1 gallon) filled with approximately the same amount of gravel. Water from a garden hose was then slowly sprayed on the top of each pot for approximately 1 minute to ensure removal of dust and debris from the gravel. In order to ensure a consistent planting depth, a stick was pushed into the top surface of the gravel until a line was reached (2 inches) and a single seed was dropped into the crevasse formed by the stick. The hole was then filled back up and patted down to ensure that the seed remained in position. The nitrogen/water delivery nozzle was then inserted approximately 1 inch into the soil on the inner edge of each pot.

The corn took approximately 1 week to emerge from the gravel. During that week the pots are only being supplied with water and no nitrogen as its not yet needed by the plant. The nitrogen compound was mixed and prepared by the greenhouse staff at the University of Guelph. Once the corn emerged from the gravel, the nitrogen pumps were turned on and would deliver fixed

amounts of nitrogen mixed in with the water. The water/nitrogen mixture was delivered on a timed basis, which started at approximately 5 minutes per hour and would scale up as the corn grew to approximately 10 minutes per hour.

The greenhouse was checked on daily to ensure that all pumps/lights were functioning properly. Whorl temperatures were taken on a semi daily basis utilizing a hand held thermal gun. Thermal images were taken from the side of each bench looking down on the corn and would gather temperature information of approximate 6 corn plants per picture and were taken approximately twice per week. Thermocouples were also utilized to take 24 hour measurements. Each trial took approximately 1 month at which point the corn grew too large for the greenhouse, which corresponded to a corn plant of approximately 10 leaf stage in development.

At the conclusion of a trial, each corn plants stem would be cut with shears right above the gravel. All of the leaves would then be cut off and bagged individually with the corresponding stem. The leaf surface area was then taken for each plant by running all the leaves through a leaf area machine which calculated total surface area. Each bag (containing leafs and stem) was then dried in a specialized plant drier located at the University of Guelph for approximately 5 days to remove all water content from the plant biomass. Once dried, the biomass of each plant was weighed.

6.5 Field trial assumptions

As stated in Section 4.3.2, the solar exergy model with which the exergy destruction principle builds upon assumes that only direct solar radiation is taken into account, thus ignoring other sources of radiation such as background radiation that is present within the earth's atmosphere. The effect of this assumption is limited by only collecting data on days with entirely clear skies.

As calculated in Section 5.5, the only dominant incoming exergy flow when examining agricultural crops is the incoming solar exergy (refer to the flow diagram in Figure 1-1 to see all flows). As such, the exergy destruction principle as hypothesizes about surface temperature (Section 5.5.1) focuses entirely on the relationship between plant health and the incoming exergy which the plant receives from the incident solar radiation. It should be stressed that, when studying the application of the exergy destruction principle as it pertains to precision agriculture in the field trials, the results should not be taken as an analysis on the exergy balance of the plants, but rather a testing of the hypothesis of the effect of stress on surface temperature.

Chapter 7. Results and discussion

The objective of this chapter is to present and discuss the results of the trials conducted. Unless otherwise stated, any temperature listed within this chapter is calculated as an average of all four repetitions of the same treatment.

7.1 Field Trials

7.1.1 Nitrogen stress winter wheat

First the summary of the surface temperatures taken during the 2014 summer trial will be shown. These results represent a bulk averaging rectangle over the wheat plants surface temperature data as to avoid the soil which would be similar to any aerial imaging application such as a drone or low flying aircraft.

	Nitrogen Rate			
	0X	0.5X	1X	2X
	0	60	120	240
June 6	21.0	19.8	19.6	19.4
June 10	24.8	23.4	23.2	23.5
June 13	20.1	18.7	19.2	18.9
June 18	20.2	19.7	19.8	19.8
June 20	19.9	18.9	18.4	18.4
June 23	23.8	22.5	22.4	22.4
June 26	21.4	21.0	20.6	20.7
July 4	19.0	18.4	18.1	18.2
July 10	19.9	19.0	18.8	18.9
July 18	24.7	24.8	23.5	23.9
July 23	24.6	24.7	23.4	23.8

Table 7-1 Surface temperature summary

where 1X is the standard "normal rate" (approximately 120kg/hectare) applied to winter wheat. While Table 7-1 doesn't involve much detail, it does serve the purpose of showing the variation of temperature which can exist due to stress and the clear trend of how increasing the stress level has a significant impact on the surface temperature, as evident by the 0X nitrogen temperatures. An interesting trend which will be observed throughout all the trials is the fact that the 2X nitrogen treatments do not produce the lowest surface temperatures, instead, much like what is observed in Table 7-1 the 1X rate produces the lowest temperature. It is theorized that this is due to excess nitrogen inducing stress into the plant, much like the phenomenon that is observed when too much fertilizer burns a lawn.

Winter wheat was the least responsive in both temperature and yield with respect to nitrogen rate compared to the other trials. It is theorized that this is most likely due to the small leaves which do not facilitate the same amount of evapotranspiration and dissipation as does corn. This is shown in Figure 7-1 which compares surface temperature and yield data with respect to the nitrogen treatments which was generated from images taken by the thermal camera.

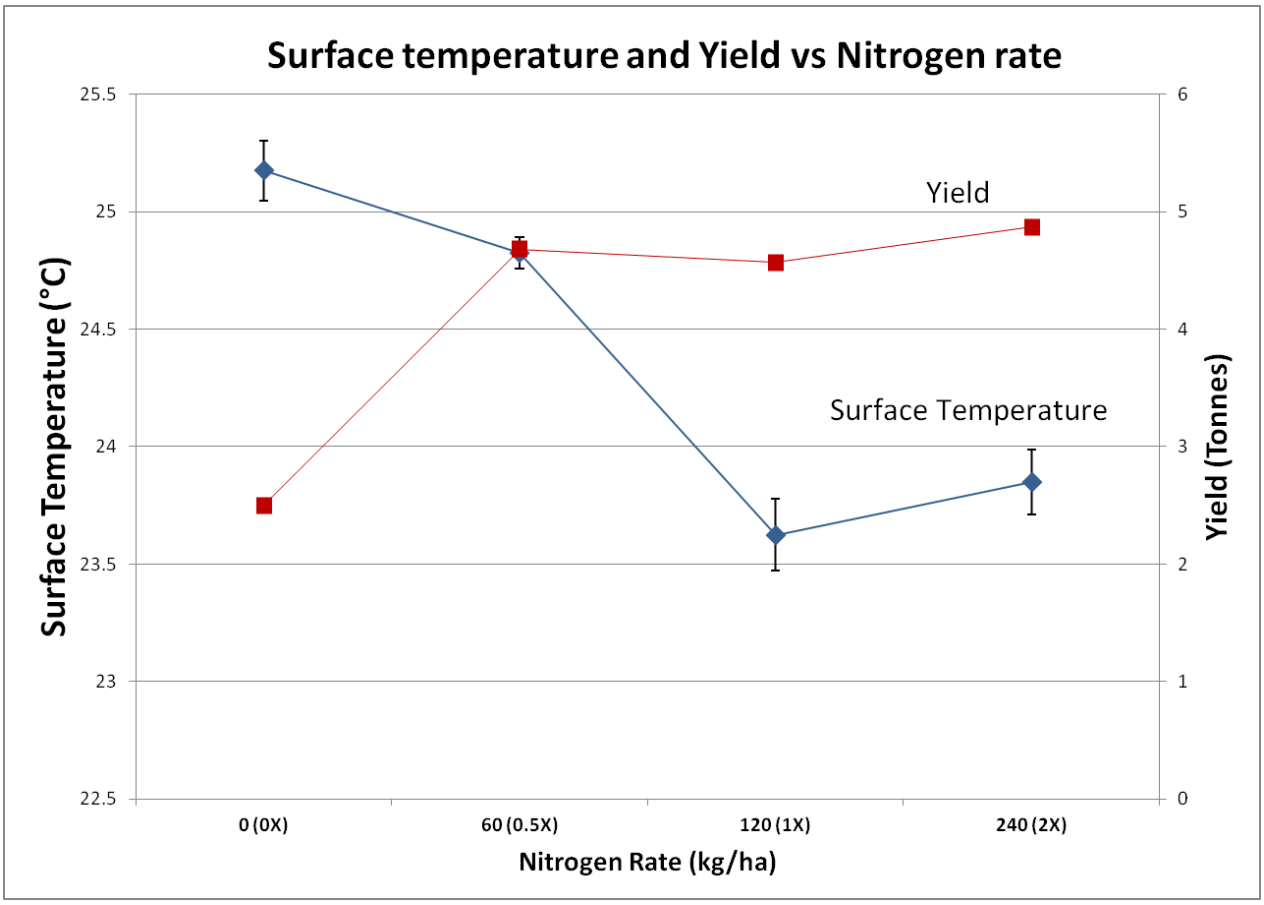

Figure 7-1 July 18 nitrogen wheat data

The temperature data in Figure 7-1 represents the average surface temperature of the wheat after segmentation where the soil and shadow temperature were removed. On July 18th the wheat was on the verge of browning and thus was in its fully mature state, however a similar temperature trend was observed throughout the lifespan of the wheat. The temperature trend between the 0, 60 and 120 kg/ha conforms with the predictions of exergy theory well, however as mentioned earlier, the 240 kg/ha treatment tending to be a higher surface temperature was a little unexpected. However too much nitrogen can also have damaging effects on the plants

operation and is a likely reason for the surface temperature increase. There also wasn't as much of a yield response to the nitrogen as was expected, however the reason why it didn't respond in a more linear fashion isn't entirely clear. The entirety of the yield data can be found in Appendix D.

7.1.2 Nitrogen stress corn

The results for the nitrogen stress corn will be presented in a similar fashion to the nitrogen wheat trials, however the size of the corn leaf compared to that of the wheat allows for better imaging and the chance for thermocouples to be mounted directly onto the leafs. First, much like the data presented by Akbari in Figure 5-10, a surface temperature and yield graph is shown which was generated from images taken by the thermal camera, shown in Figure 7-2.

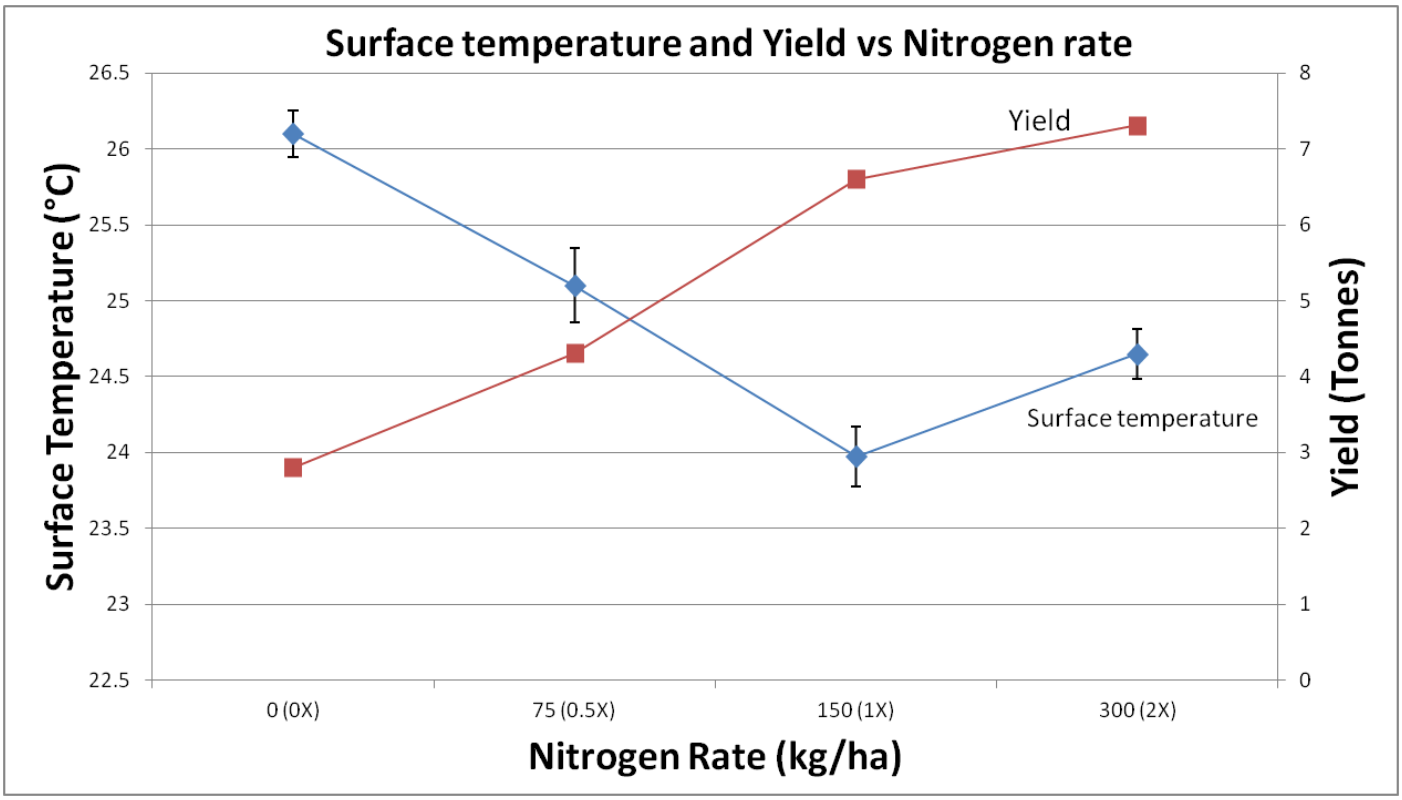

Figure 7-2 July 18th nitrogen corn data

Not surprisingly the overall trends of both the yield and surface temperature curves are quite similar to that of the wheat, however the slope of both curves with regard to the nitrogen rate are much less dramatic when compared to the graph in Figure 7-1. The error bars on the surface temperature represent the standard error associated with the data set, and thus the temperature differences between each treatment shown in Figure 7-2 are taken as being statistically significant. The data shows quite a linear temperature trend between the 0X, 0.5X and 1X treatments (where 1X is approximately 150 kg/ha) with each treatment back to normal levels representing approximately 1°C reduction in surface temperature as stress is decreased. These results support the trend predicted by the exergy destruction principle.

Again of particular interest is the behavior of the corn subjected to the 2X nitrogen rate, as it produces a higher surface temperature compared to the 1X rate but produces a slightly higher yield. It is predicted that in this extreme case of supplying the plant with such an excess of nitrogen, while it will still stress the plant which is reflected in the surface temperature, the yield produced represents an outlier case which is driven higher due to the abundance of nitrogen. This phenomena is observed in both the corn and wheat trials.

7.1.3 Weed stress corn

The final field trial which was conducted was the weed stress corn, where wheat was utilized as an analog weed to induce stress and was removed at various corn leaf stages with the use of herbicide. Shown in Figure 7-3 is the temperature-yield curve which was generated from images taken by the thermal camera.

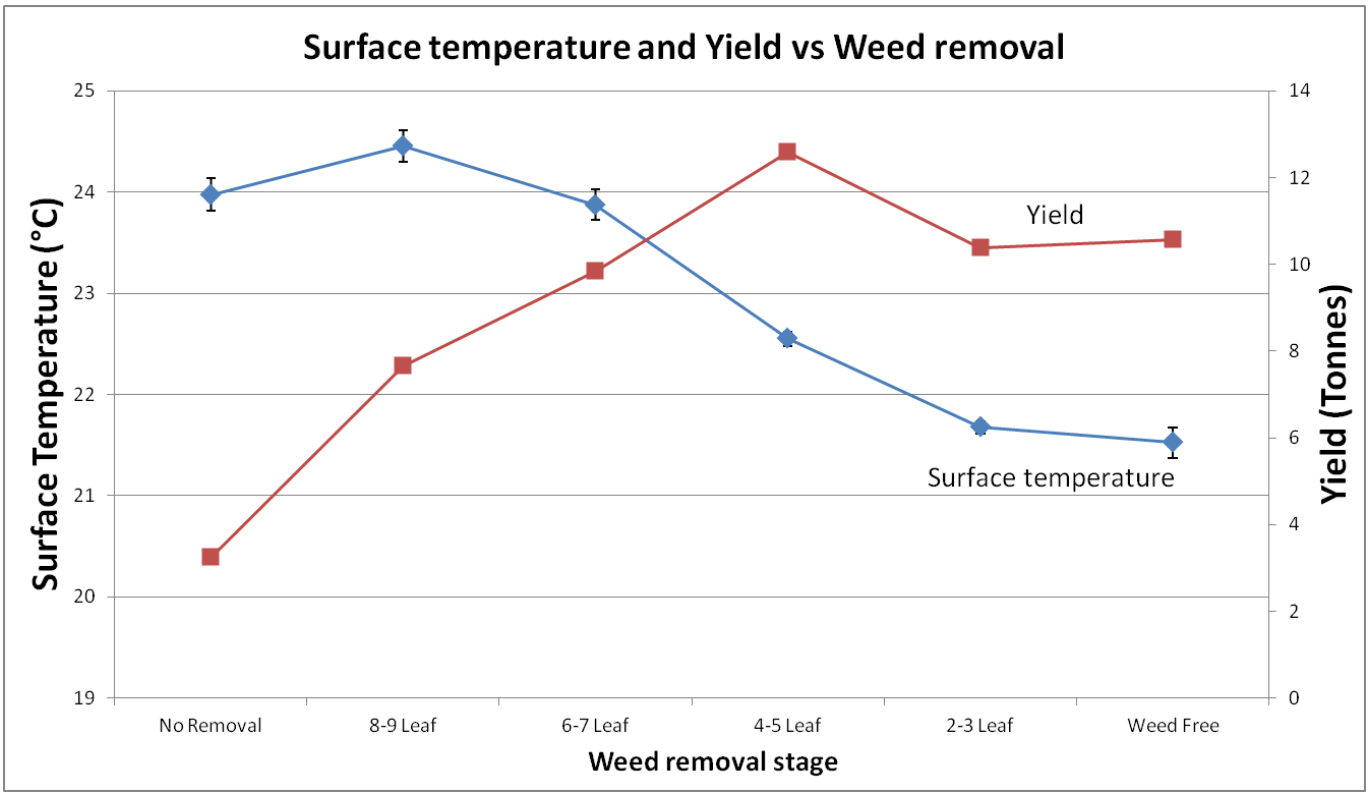

Figure 7-3 July 18th weed removal corn data

The weed removal stage is arranged according to the level of perceived stress on the corn as shown by the weed removal stage on the x-axis. This data is taken approximately a week after the last weed removal (8-9 leaf stage) so the only weeds left in the trial were on the full season stress or "no removal" plots. The surface temperature profile is again decreasing with decreased stress in a rather consistent manner, with the exception of the 8-9 leaf stage removal plots which had just received herbicide a week prior. It is hypothesized that this is due to the fact that the plants experience a significant amount of stress as the weeds which grew around the corn from emergence are taken away, which represents a significant change to its local environment and thus a large amount of induced stress.

The yield curve is quite responsive in the regions of extremely high stress and levels off as stress diminishes to the control "weed free" treatment, although the yield for the 4-5 leaf stage removal was a little higher than expected. As hypothesized by the exergy destruction principle, stress will impact the pathways which a plant utilizes to destroy exergy and as a consequence will be pushed farther away from equilibrium, resulting in a higher surface temperature. The temperature results are in agreement with that hypothesis. It is also hypothesized that healthier plants will generate more pathways for destruction and therefore become more complex systems which manifest itself in an increased yield. These results appear to generally follow this trend but more data is needed to come to any meaningful conclusions.

Along with the images taken with the thermal camera, thermocouples were utilized in order to record 24 hour temperature measurements. The thermocouples were secured to the top of the mature corn leaf of both the weed free control and the full season weed stress plots. Shown in Figure 7-4 is a 2 day excerpt of those results, air temperature was recorded via a mobile weather station on location.

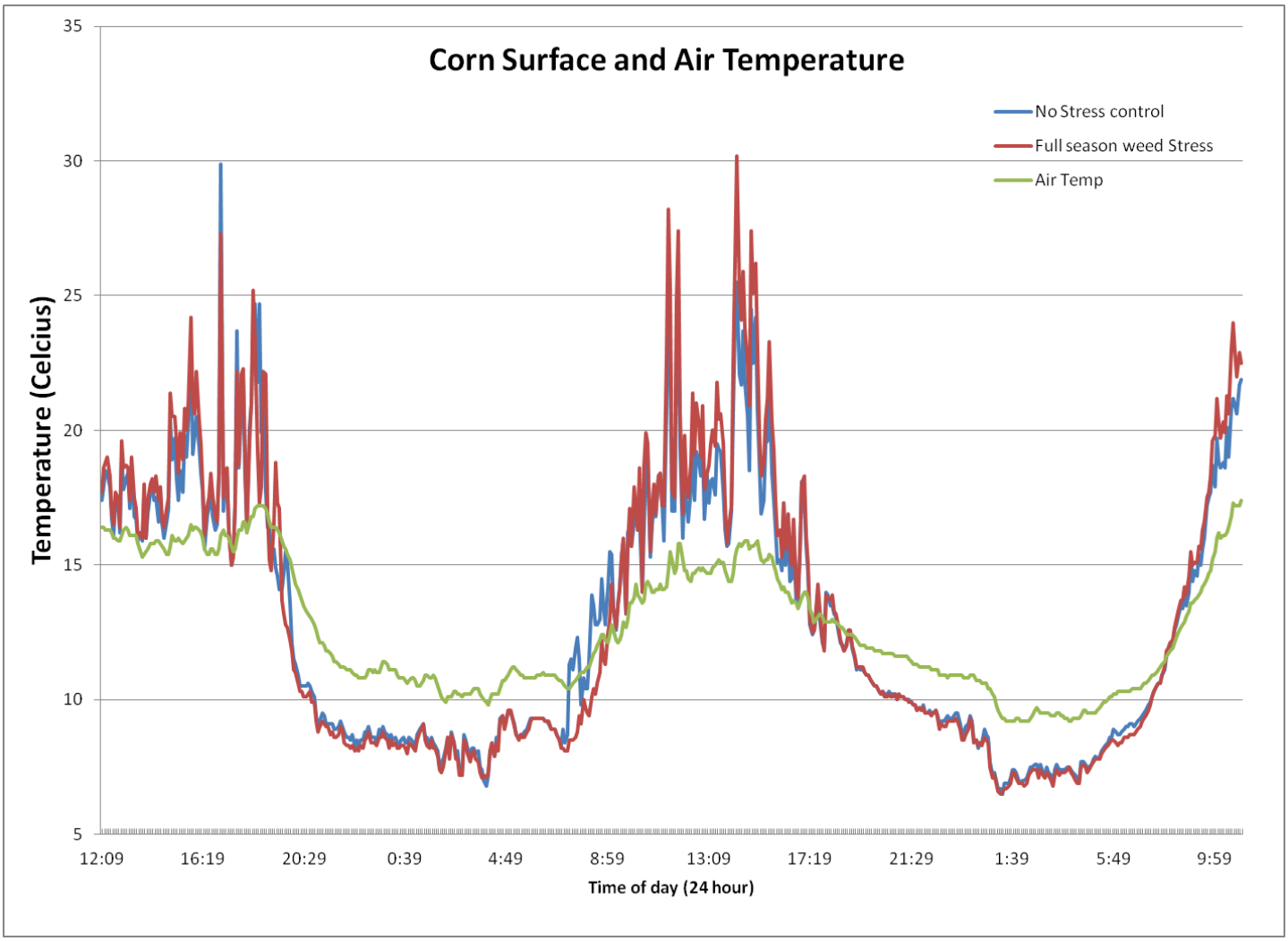

Figure 7-4 Weed stressed corn 24-hour thermocouple data

The thermocouples were hooked into a data recording device which recorded temperatures every 5 minutes. While the temperature difference between the stressed (blue line) and non stressed corn (red line) appears to be smaller than the difference picked up by the thermal camera in the Figures shown before, this isn't the case and is only a function of the resolution of the graph in combination with the many data points of which it is comprised. By graphing the difference between the stressed and non stressed corn data points the results come more in line with what was generated by the thermal camera. This is shown in Figure 7-5.

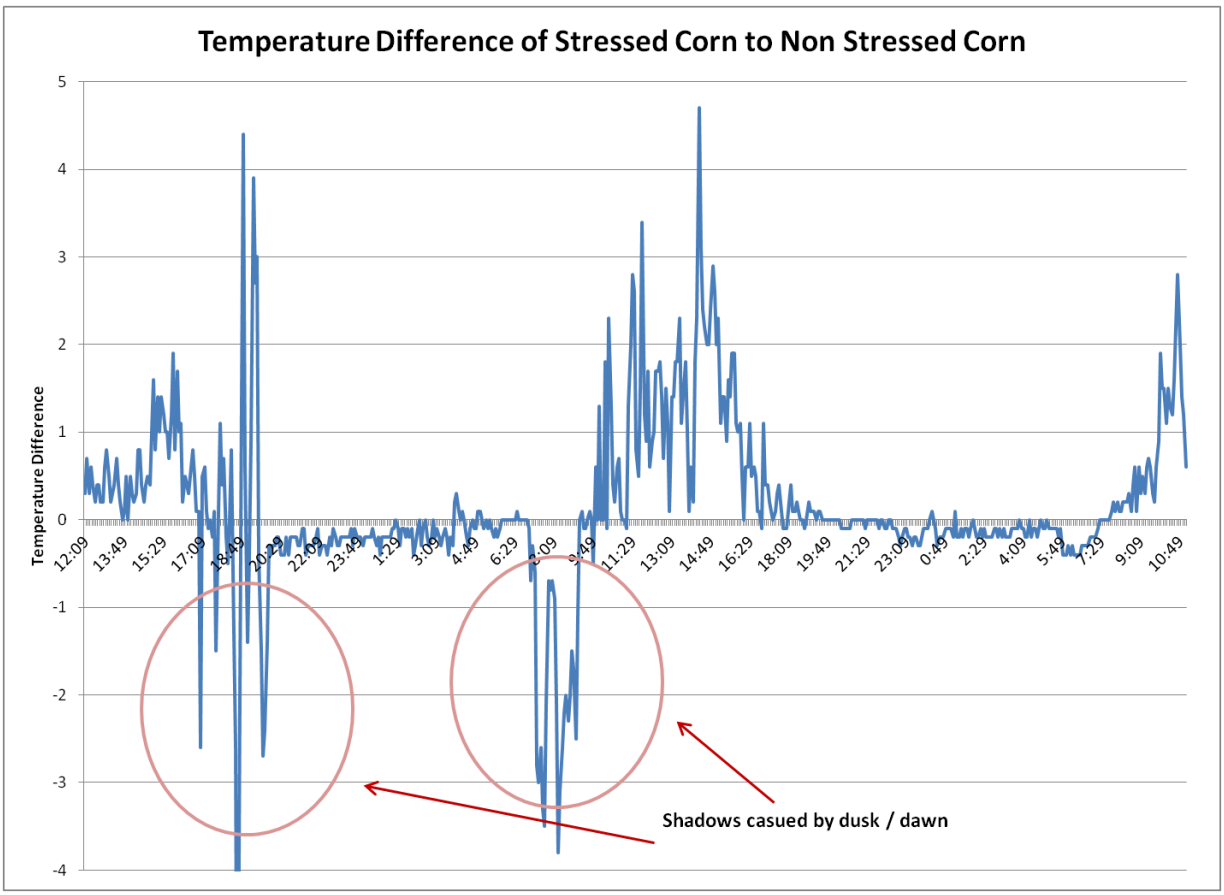

Figure 7-5 Temperature difference isolation

By investigating the graph in Figure 7-5, the temperature difference between the stressed and unstressed corn becomes much more clear, with the stressed corn being roughly 1 to 2 degrees hotter during the day than that of the control. However, this trend is reversed during the night, with the stressed corn appearing to be cooler than that of the control. While more work is needed to investigate this phenomenon, an initial hypothesis is that much like a desert which fluctuates wildly between the day and night due to the small heat capacity of the sand, a stressed plant will be less effective at buffering the temperatures of its surroundings, which appears to be the case in this data.

7.2 Effect of air temperature

As mentioned in Section 5.5 and observed in Akbari's experiments, plants will always try to optimize themselves according to their surroundings, which is largely impacted by the surrounding air temperature. Shown in Figure 7-4 is the relation that air temperature has on the surface temperature of both the stressed and non-stressed corn, where the surface temperature is well correlated with air temperature not only during the day but also during the night.

Figure 7-6 shows data from the weed stress corn trial over 4 days in July (approximately a week between days) while also plotting the air temperature.

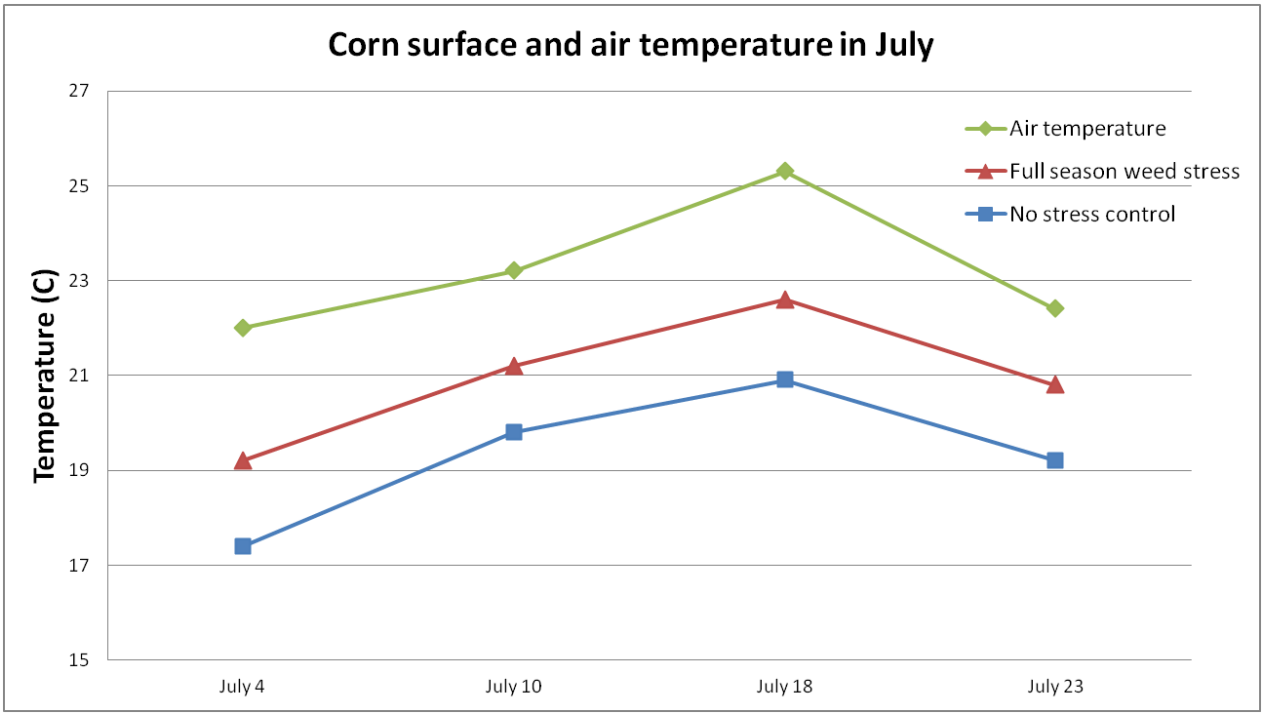

Figure 7-6 Corn surface and air temperatures in July

The data for Figure 7-6 was taken from the same two stress treatments as the extended thermocouple data shown in Figure 7-4 representing the control (zero stress) and the full season stress case where the weeds were never removed. The data depicted in Figure 7-6 was generated via thermal imaging and represents an average surface temperature. Much like in Figure 7-4, the data is well correlated with the air temperature. The corn appears to hold a relatively constant air to surface temperature differential which is approximately 3.5 - 4.5°C for the control corn and 2 - 2.5°C for the full season stress corn.

7.3 Greenhouse trials

Since the thermal images of the greenhouse nitrogen trials don't differ in substance or results to that presented in the nitrogen field trials, the results shown in this section will represent data which has been collected via a extended thermocouple test and also by a handheld infrared gun which enabled temperature readings from directly in the whorl. The following whorl temperatures, shown in Table 7-2, were taken when the corns leaf stage was approximately 9 and utilized a standard hand held infrared gun where 10 plants were measured per treatment.

	Whorl temperature (°C)										
Plant Number	#1	#2	#3	#4	#5	#6	#7	#8	#9	#10	Average
High Nitrogen	21.7	21.1	21.7	21.8	22.1	21.6	21.6	20.4	22.2	20.7	21.49
Medium Nitrogen	22.4	23.2	22.6	22.4	22.9	21.9	22.5	22.5	23.3	22.5	22.62
Low Nitrogen	22.4	25.3	25.1	23.6	24.6	23.6	23.9	24.8	22	21.6	23.69

Table 7-2 Greenhouse corn whorl temperatures

While somewhat unrealistic to compare these nitrogen rates to that experienced in the field trials due to the fact that it was continuously dripped, the "high" nitrogen rate was approximately equivalent to the 1X or standard nitrogen rate which is experienced in the field. Similarly with the leaf surface temperatures, the whorl temperatures confirm the hypothesis of the exergy destruction principle in that surface temperature (in this case being the inner whorl and not the leaf) increases with increasing stress.

These results were confirmed through the use of an extended thermocouple trial. Since the corn leafs were still quite small and fragile the thermocouples were placed inside of the whorl and left in place for 10 days to record every hour. The results shown in Figure 7-7 represent the average of 4 whorl temperatures for both the high and low nitrogen application rates.

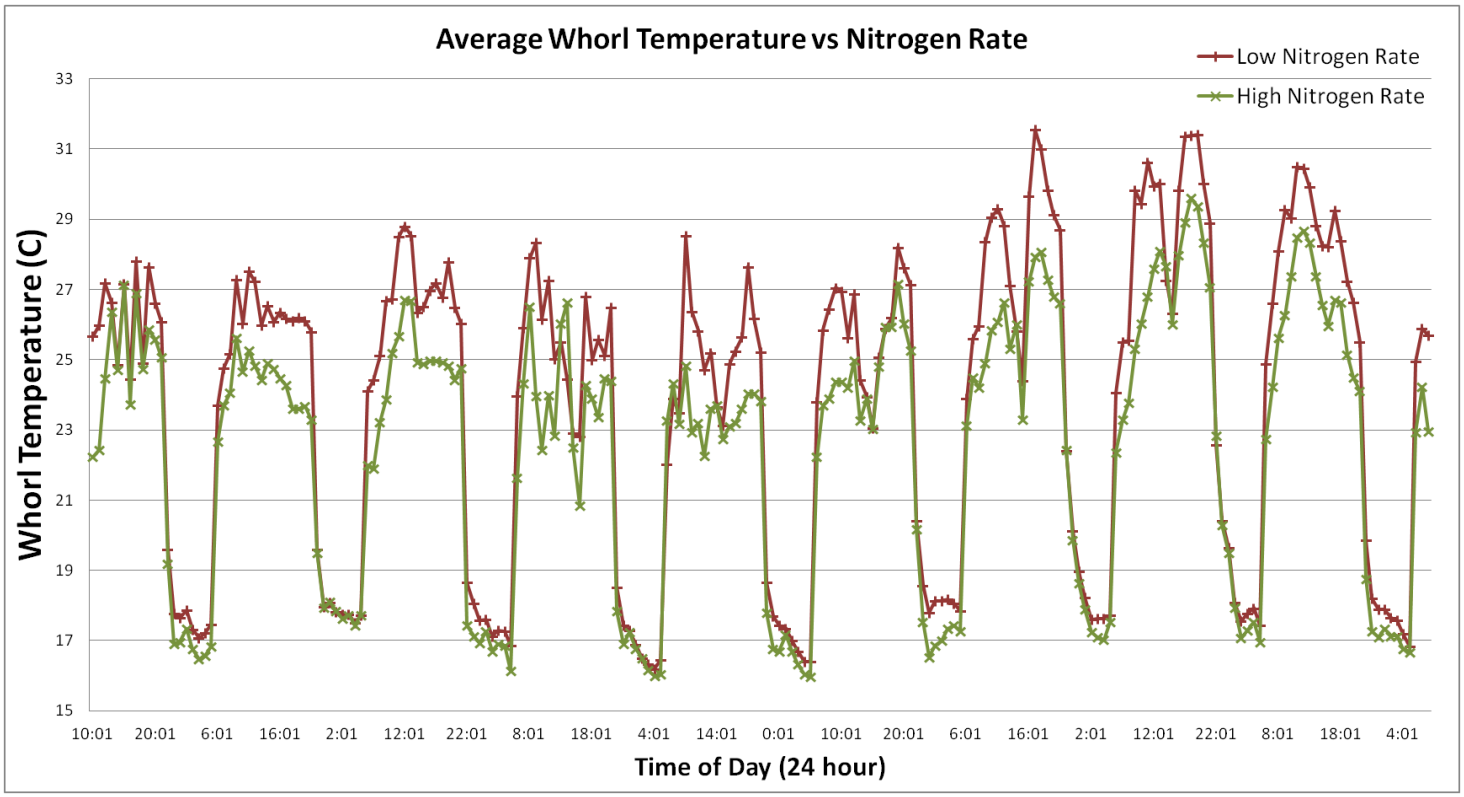

Figure 7-7 Extended greenhouse whorl temperatures

While the thermocouples were mounted inside the whorl of the corn, as opposed to on the leaf surface like the other trials, it still produced a similar temperature result with respect to the induced stress regime. These findings again reinforce the evidence that through the theoretical framework of the exergy destruction principle, surface temperature can be an effective tool for measuring and monitoring plant stress.

One particular point of interest is what happens to the temperatures at night. In this specific trial the high nitrogen (low stress) corn was actually cooler than the low nitrogen (high stress) corn, something which was not expected. The hypothesized result, which was explained in the

previous section, (refer to Figure 7-4 and the subsequent explanation) was that the stressed plant would be less able to buffer the surrounding temperatures and thus should be cooler at night when compared to the healthier plant, which was not the case in this trial.

This could be due to the fact that the thermocouples measured the whorl temperature and not the temperature of the leaf, however, it might point to a flaw in just examining surface temperature. As it was hypothesized in the previous chapters, surface temperature can be used as a proxy to estimate the exergy flows of the plant, especially comparatively, however it is just an estimate. Exergy requires a total energy balance of the system and the surroundings in order to be accurately calculated, which means that depending on the amount of radiation reflected within the greenhouse, heat transfer through the walls etc., temperature might not be an effective exergy proxy in a confined greenhouse setting. This could explain why the temperatures are reversed during the night in the above data, however more work needs to be conducted on the subject.

While these results still represent a preliminary investigation into the utilization of remote sensing into monitoring plant stress for utilization in precision agriculture, it is clear that a foundation exists to suggest that through the framework of the exergy destruction principle, surface temperature can be an effective measure of crop stress.

Chapter 8. Conclusions

Exergy is a representation of energy quality, work gradients, and distance with which a system is away from equilibrium. It is exergy and not energy that is the driving force for biological and thermodynamic processes on earth.

Exergy represents the *maximum* useful to-the-dead state work and derives its value based on how far away from equilibrium a system is with its environment, as such it requires that both the system and environment be well defined.

When systems are continuously exposed to outside gradients, structures will form which will act to dissipate the gradient and return the system to equilibrium.

Exergy carried by the suns incident solar radiation is the dominant exergy flow for agricultural crops and therefore is crucial to understanding how plants optimize their incoming exergy.

Through the exergy destruction principle, it is hypothesized that healthy plants will optimize their surface temperature and therefore maximize the amount of exergy they receive from the sun.

The exergy destruction principle hypothesizes that stress impacts the effectiveness of plants ability to destroy the incoming exergy, thus pushing stressed plants farther away from equilibrium. An effect that can be observed in their surface temperature and which preliminary data appears to confirm.

By remotely sensing plant and specifically crop surface temperature, one is able to identify crops under stress, at least on a comparative basis. This suggests that thermal remote sensing can be an effective tool for precision agriculture in identifying crop variability and allowing for rectification of the stress before any visual indicators are present.

References

Adl, Ammar., "Precision Agriculture", Faculty of Computers and Information, Cairo University, 2014.

Akbari, Mohammad H., Energy-based Indicators of Ecosystem Health, Master of Science, Dept of Crop Sciences (Advisor: Dr. Clarence J. Swanton), University of Guelph, Guelph, Ontario, 1995.

Atkins, P., 2001The Elements of Physical Chemistry ed., Oxford University Press, Oxford,.549 p.

Baehr,H. D. “Energie und Exergie”, VDI-Verlag, Düsseldorf, 1965

Bastiaanssen, Wim G.m, David J. Molden, and Ian W. Makin. "Remote Sensing for Irrigated Agriculture: Examples from Research and Possible Applications." *Agricultural Water Management*, 2000.

de Beer, Jeroen. "Potential for Industrial Energy-Efficiency Improvement in the Long Term", Eco-Efficiency in Industry and Science". 2000

Bejan, Adrian., Entropy Generation Minimization: The Method of Thermodynamic Optimization of Finite-size Systems and Finite-time Processes. Boca Raton: CRC, 1996. Print.

Bejan, Adrian., Advanced Engineering Thermodynamics, 2nd Edition, John Wiley and Sons,Inc., Toronto, Ontario, 1997.

Bhatti, A.U., D.J. Mulla, and B.E. Frasier., Estimation of soil properties and wheat yields on complex eroded hills using geostatis-tics and thematic mapper images. Remote Sens. Environ. 37, 1991.

Bošnjakovi. And Knoche K.F., Technische Thermodynamik, Teil 1. 7th ed., Steinkopff-Verlag, Darmstadt, 1988.

Brase, Terry., Precision Agriculture, Delmar Publishers, 2005. Online

Brillouin, L., The Negentropy Principle of Information, American Institute of Physics, 1953.

Calder, Ian R. "Forests and Water—Ensuring Forest Benefits Outweigh Water Costs." Forest Ecology and Management 251.1-2, 2007.

Caratheodory, C., Examination of the foundations of thermodynamics, “Untersuchungen über die Grundlagen der Thermodynamik,” Math. Ann. 67, 355-386. 1909, Web.

Castafis, M., Bases fisicas del aprovechamiento de la energiasolar, *Rev. Geofis.* 35, 227-239, 1976.

Cengel, Yunus A. and Michael A. Boles, Thermodynamics An Engineering Approach, ThirdEdition, McGraw Hill, Toronto, Ontario, 1998.

Chandrasekhar, S., Hydrodynamic and hydromagnetic stability, Dover Publications, 1961.

Cornelisson, R.L., Thermodynamics and sustainable development; The use of exergy analysis and the reduction of irreversibility. PhD Thesis, University of Groningen, 1997.

De Vos, A. and Pauwels, H., On the thermodynamic limitof photovoltaic energy conversion, *Appl. Phj,s.* 25, 119-125, 1981.

Evans, R. B.,A Proof that Essergy is the only Consistent Measure of Potential Work,Thesis, Dartmouth College, Hanover, New Hampshire, 1969.

Fraser, R. A. and Kay, J., Exergy Analysis of Ecosystems: Establishing a Role for Thermal Remote Sensing. *Thermal Remote Sensing in Land Processes*. Dale A. Quattrochi and J. Luvall, 2003

Hatsopoulos, G. N., and Joseph Henry Keenan. *Principles of General Thermodynamics*. New York: Wiley, 1965.

Haught,A. F., Physics considerations of solar energy conversion.Int. Conf. on Photochemical Conversion andStorage of Solar Energy, Boulder, CO, 1980.

Incropera, F. P. and DeWitt, D. P., Fundamentals of Heat and Mass Transfer, Sixth Edition, John Wiley& Sons, Toronto, Ontario, 2007.

Idso, S. B., R. J. Reginato, and R. D. Jackson. "Albedo Measurement for Remote Sensing of Crop Yields." *Nature* 266.5603, 1977.

Idso, S.b., R.d. Jackson, P.j. Pinter, R.j. Reginato, and J.l. Hatfield. "Normalizing the Stress-degree-day Parameter for Environmental Variability." *Agricultural Meteorology* 24, 1981.

Jeter,S. J.,Maximum conversion efficiency for the utilizationof direct solar radiation, *Solar Energy* 26, 231-236, 1981.

Jørgensen, Sven Erik. "Use of models as experimental tool to show that structuralchanges are accompanied by increased exergy." Ecological Modelling Issues 1-2:117-126. 1988

Jørgensen, Sven Erik, Søren Nors Nielsen, and Henning Mejer. "Emergy, Environ, Exergy and Ecological Modelling." *Ecological Modelling* 77.2-3, 1995.

Jørgensen, Sven Erik. *Eco-exergy as Sustainability*. Southampton: WIT, 2006.

Jørgensen, Sven Erik. *Evolutionary Essays: A Thermodynamic Interpretation of the Evolution*. Amsterdam: Elsevier Science, 2008.

Kabelac, Stephan. "A New Look at the Maximum Conversion Efficiency of Black-body Radiation." *Solar Energy* 46.4: 231-36, 1991.

Kay, James., Self-Organization in Living Systems, Ph.D. Thesis, Systems DesignEngineering, University of Waterloo, Waterloo, Ontario, Canada, 1984.

Kay, James J. "A Nonequilibrium Thermodynamic Framework for Discussing Ecosystem Integrity." *Environmental Management* 15.4, 1991.

Kay, James., Ecosystems as Self-Organizing Holarchic Open Systems: Narratives and the Second Law of Thermodynamics, Handbook of Ecosystem Theories and Management, University of Waterloo, 2000.

Kestin, Joseph., *A Course in Thermodynamics*. Waltham, MA: Blaisdell Pub., 1966.

Landsberg, P.T. and Mallinson, J.R., Thermodynamic Constraints, Effective Temperatures and Solar Cells, Int. Colloquium on Solar Electricity, CNES, Toulouse, pp. 27-46, 1976.

Leuzinger, S. and Körner, C., Tree species diversity affects canopy leaf temperatures in a mature temperate forest. Agric. For. Meteorol. 146, 29–37. 2007.

Licata, Julian A., Javier E. Gyenge, Maria Elena Fernández, Tomás M. Schlichter, and Barbara J. Bond. "Increased Water Use by Ponderosa Pine Plantations in Northwestern Patagonia, Argentina Compared with Native Forest Vegetation." Forest Ecology and Management 255.3-4, 2008.

Luvall, J. C. and Holbo, H.R., "Measurements of Short-term Thermal Responses of Coniferous Forest Canopies Using Thermal Scanner Data." *Remote Sensing of Environment*, 1989a.

Luvall, J. C. and Holbo, H.R., "Modeling Surface Temperature Distributions in Forest Landscapes." *Remote Sensing of Environment*, 1989b.

Luvall, J. C. and Holbo, H.R., “Thermal Remote Sensing Methods in Landscape Ecology,”Quantitative Methods in Landscape Ecology, Turner, M. and Gardner, R. H., Eds.,Springer-Verlag, Berlin, Germany, Chapter 6, 1991.

Luvall, J.C., Lieberman, D., Lieberman,M., Hartshorn, G.S., and Peralta,R., Estimation of tropical forestcanopy temperatures, thermal response numbers, and evapotranspiration using an aircraft-based thermalsensor, Photogrammetric Engineering and Remote Sensing 56 (lo), 1393-1410 (1990).

Maes, W.h., T. Pashuysen, A. Trabucco, F. Veroustraete, and B. Muys. "Does Energy Dissipation Increase with Ecosystem Succession? Testing the Ecosystem Exergy Theory Combining Theoretical Simulations and Thermal Remote Sensing Observations." *Ecological Modelling* 222.23-24, 2011.

McIntyre, Joseph. "Photovoltaic Potential in the City of Guelph", Department of Engineering, University of Guelph. 2008.

Nebraska Crop Watch, "Yield Monitoring and Mapping", University of Nebraska-Lincoln, Online: http://cropwatch.unl.edu/ssm/mapping

Nicolis, G., and I. Prigogine., *Self-organization in Nonequilibrium Systems: From Dissipative Structures to Order through Fluctuations*. New York: Wiley, 1977.

Nicolis, G., and I. Prigogine., *Exploring Complexity: An Introduction*. New York: W.H. Freeman, 1989.

Odum, E.P., "The strategy of ecosystem development" *Science,* April 1969.

Pinter, Jr. Paul J., Jerry L. Hatfield, James S. Schepers, Edward M. Barnes, M. Susan Moran, Craig S.t. Daughtry, and Dan R. Upchurch. "Remote Sensing for Crop Management." *Photogrammetric Engineering & Remote Sensing Photogramm Eng Remote Sensing*, 2003.

Planck, M., Theorie der Wärmestrahlung. 6th ed., Barth Verlag, Leipzig, 1966.

Press, W.H., Theoretical Maximum for Energy from Direct and Diffuse Sunlight. Nature,London, Vol. 264, pp. 734-735, 1976.

Rant, Z. Forschung Ing.-Wesens, vol. 22, 36, 1956.

Reynolds, William C. and Henery C. Perkins, Engineering Thermodynamics, McGraw-HillInc., Toronto, Ontario, 1977.

Risius, Nathan W., "Analysis of a combine grain yield monitoring system" Digital Repository, Iowa State University, 2014

Rosen, Marc A., and Dincer, I,. "Exergy as the Confluence of Energy, Environment and Sustainable Development." *Exergy, An International Journal* 1.1, 2001.

Rosen, Marc A., and Dincer, I,. "Thermodynamic Aspects of Renewables and Sustainable Development." *Renewable and Sustainable Energy Reviews* 9.2, 2005.

Schrödinger, Erwin.,*What Is Life?*. Cambridge University Press, 1944.

Schneider, E.d., and J.j. Kay. "Life as a Manifestation of the Second Law of Thermodynamics." *Mathematical and Computer Modelling* 19.6-8,25-48. 1994

Silveston, P.L., “Warmedurchange in Horizontalen Flassigkeitschichtem.” Heat Changes in Horizontal Silicon Oil, PhD thesis, Techn. Hochsch. Muenchen, Germany. 1957

Susani, L., F. M. Pulselli, et al. (2006). "Comparison between technological and ecological exergy." Ecological Modelling **193**(3-4): 447-456.

Timlin, D.J., Ya. Pachepsky, V. A. Snyder, and R. B. Bryant., Spatial and Temporal Variability of Corn Grain Yield on a Hillslope. Soil Sci. Soc Am J. 1998.

Valero, A. "Exergy Accounting: Capabilities and Drawbacks." *Energy* 31.1, 2006.

Wall, G. "Exergy - A Useful Concept Within Resource Accounting" *Institute of Theoretical Physics* Report no. 77-42, 1977

Wark, Kenneth Jr. and Donald E. Richards, Thermodynamics, Sixth Edition, McGraw-Hill,Toronto, ON, 1999.

Wicken, J. S., Evolution, Thermodynamics, and Information: Extending the Darwinian Program, Oxford University Press, 1987.

Appendix A: Weed stress experimental design

A.1 Randomized block design

Shown in Figure A.1 is an example of the randomized block design which is computer generated by the University of Guelph for the weed stress trial. The row in which the plot location is shown corresponds to the treatment received and the plot number corresponds to the location in the field. For example, "301" is located in the third row in the trial, planted in the 1st plot from the left side and received the "Wheat removal T2, 4-5 leaf stage corn" treatment.

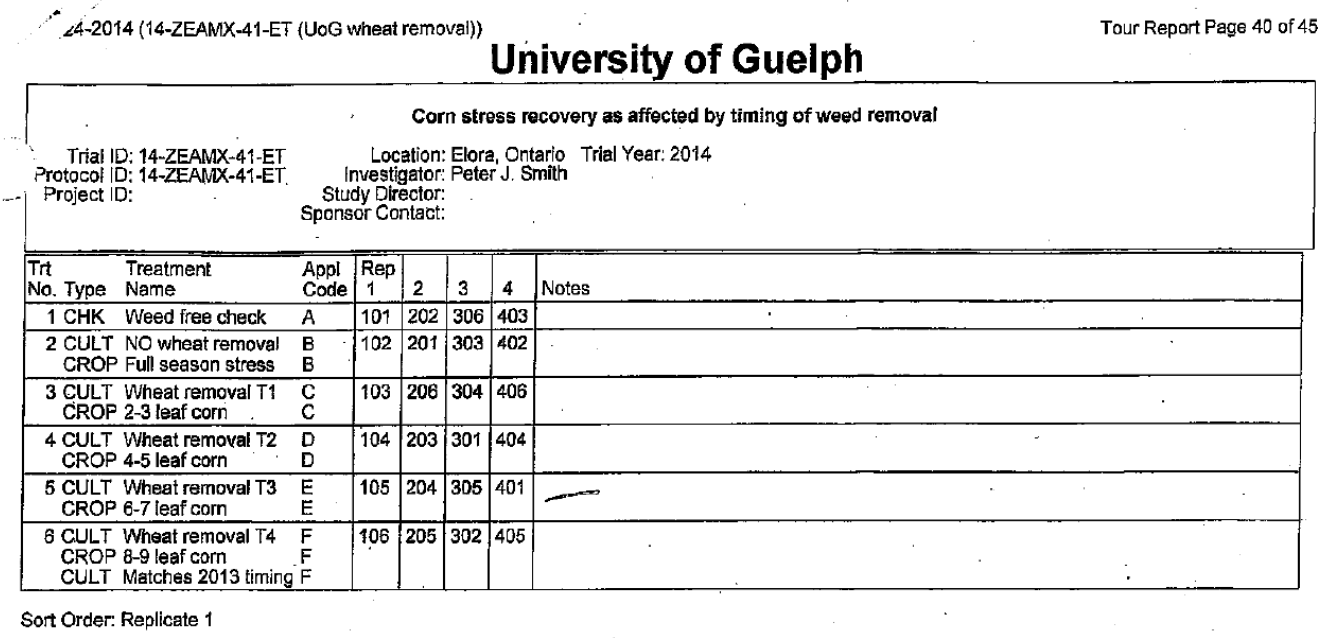

4-2014 (14-ZEAMX-41-ET (UoG wheat removal)) Tour Report Page 40 of 45

University of Guelph

Corn stress recovery as affected by timing of weed removal

Trial ID: 14-ZEAMX-41-ET Location: Elora, Ontario Trial Year: 2014
Protocol ID: 14-ZEAMX-41-ET Investigator: Peter J. Smith
Project ID: Study Director:
Sponsor Contact:

Trt No.	Type	Treatment Name	Appl Code	Rep 1	2	3	4	Notes
1	CHK	Weed free check	A	101	202	306	403	
2	CULT	NO wheat removal	B	102	201	303	402	
	CROP	Full season stress	B					
3	CULT	Wheat removal T1	C	103	206	304	406	
	CROP	2-3 leaf corn	C					
4	CULT	Wheat removal T2	D	104	203	301	404	
	CROP	4-5 leaf corn	D					
5	CULT	Wheat removal T3	E	105	204	305	401	
	CROP	6-7 leaf corn	E					
6	CULT	Wheat removal T4	F	106	205	302	405	
	CROP	8-9 leaf corn	F					
	CULT	Matches 2013 timing	F					

Sort Order: Replicate 1

Figure A.1 Randomized block design (6 treatments x 4 repetitions)

A.2 Herbicide application log

Figure A.2 depicts the log which was generated by the field staff for the weed stress trial. The columns in the log "A,B, C..." represents each time herbicide was applied and shown in the "crop stage" row is the corn leaf stage at which time the herbicide was applied. Other factors such as humidity, air temperature, wind speed were documented during each application.

Contact: U of G

Trial ID: ZEAMX - 41

Planting date:	May 19 2014	Emergence date:	~ May 27, 2014
Harvest date:		Seed variety	Pioneer P9906 AM

Special notes: Timing of wheat removal in corn

Application	A	B	C	D	E
Assessment schedule				Planted May 19 2014 – TRZAW variety – Pioneer 25R39	
Application date	May 19 @ planting	Jun 8	June 14	Jun 22	
Time of day	7:00 PM	12:00 noon	5:00 PM	3:00 PM	
Application timing	PRE	E post	M post	M POST	
Air temp (C)	17.1	17.6	21.9	29	
% RH	61	44	36	30	
Wind speed (Kph)	Ø	5 Kph	3 kph	Ø	
Wind direction	–	S	SW	–	
Dew presence (y/n)	N	N	N	N	
Soil temp (C)	14	21	23	30	
Soil moisture	adequate	adequate	adequate	adequate	
Cloud cover %	Ø	Ø	50	30	
Crop stage	PRE	3 lf	5 lf	7 lf	

Weed Leaf and /m2 (per metre square) at application

Weed		A	B	C	D	E
TRZAW	leaf	Ø	2-3 tillers	4-5	boot	
	/m2			+ tillers		
	leaf					
	/m2					
	leaf					
	/m2					
	leaf					
	/m2					
	leaf					
	/m2					
	leaf					
	/m2					
	leaf					
	/m2					
	leaf					
	/m2					
	leaf					
	/m2					

Figure A.2 Herbicide application log

Appendix B: Biomass and leaf area results

Located in Figure B.1 is the leaf area and biomass weights for the greenhouse trial. This data was collect after the trial was completed and was originally collected at the request of the University of Guelph. As explained in Section 6.4.2, after the corn was cut directly above the soil, the individual leaves were cut off and ran through a leaf area machine which calculates the total surface area of all the leaves representing the number shown.

The weights shown represent the total dry weight of the above ground biomass (stem + leaves) after being dried for approximately 5 days.

	Leaf Area Index (cm2)	
	Zone 1 (High Nitrogen)	Zone 3 (Low Nitrogen)
	3570	720
	2592	705
	3036	692
	2521	680
	2484	681
	2640	731
	2850	685
	2440	664
	2931	566
	2916	627
AVG	2798	675.1
	Weights (grams)	
	Zone 1 (High Nitrogen)	Zone 3 (Low Nitrogen)
	28.17	3.2
	19	4.1
	25.98	3.6
	20.98	5
	21.61	3.9
	22.6	4.8
	23.74	5.2
	21.7	4.5
	15.01	2.9
	23.5	4.3
AVG	22.229	4.15

Figure B.1 Greenhouse trial weights and leaf areas

The results indicate a significant effect which the low nitrogen rate had on plant physiology which is shown by the large drop in leaf area (approximately 4X reduction) and total biomass weight (approximately 5X reduction) between the high and low nitrogen treatment rates.

Appendix C: Experimental Methodology

C.1 Corn weed stress trial methodology

Utilizing a randomized block design generated by the University of Guelph, all 6 treatments were planted in mid May (corn + analog weed which was a wheat hybrid) which was replicated 4 times. All herbicide and pesticide controls not pertinent to the stress trial were handled by the field staff as part of their crop management program. Approximately 1 week after planting, both the corn and weed would emerge. Starting approximately 1 week after emergence (2 weeks after planting) corn would be large enough to start taking thermal images. Thermal images would be taken on the edge of the plot pointed at the middle of the treatment as to avoid any edge effects which might be present. The thermal camera was held approximately 1m above the corn surface. The thermal camera was calibrated according to the atmospheric conditions such as air temperature and humidity. The air temperature and humidity was monitored in real time with the use of a small (1.5m height) mobile weather station which outputs data to a handheld console.

Measurements would always be taken at a consistent time of day throughout the growing period (May - August) with consistent weather conditions in mind. Ideally measurements would always be taken on an entirely cloudless day, however in the case small amount of cloud cover which would block the direct sunlight, all measurements would stop and only resume once cloud cover had passed. All data collection would take approximately 10 minutes to take 1-2

pictures of each treatment plot (6 treatments X 4 repetitions = 24 treatment plots). This was done with speed in mind to ensure relatively consistent atmospheric conditions and radiative flux during data collection.

The University of Guelph field staff were responsible for spraying the herbicide to kill the analog weed at the predetermined corn leaf stage. This was done by hand utilizing a backpack spraying system which reduced the interference on the corn that would occur by utilizing various tractor delivered systems. Date and time of herbicide spray would be noted in a log (Appendix A). The field staff had someone on location everyday to ensure continued operation of all fields. Thermal imagery was collected 2-3 times per week on average throughout the growing season.

The thermal images were processed utilizing a block averaging tool after each image had been segmented, this was done to ensure only the corn surface temperature would contribute to the calculation (Section 6.3). Through segmentation, the surface temperatures of the weed, soil, and shadows would not contribute to any "average temperature" data. Once all images were segmented and averages taken the same treatments from each repetition would be averaged together. For example, referring to Figure A.1, to get the average surface temperature for the weed free control treatment on a specific day, the averages from the images taken for plot 101, 202, 306 and 403 would be averaged together.

Thermocouples were also affixed directly to the surface of the leaves and hooked up to a data recorder to provide 24 hour surface temperature measurements. The thermocouples were affixed to the plant by tying them to the stems and then taping them to the corn leaves. No tape was used close to the tip of the thermocouple to ensure it didn't affect the readings.

At the end of the growing season the corn was harvested by hand by the field staff and logged. After harvesting, the ears of each corn plant were removed and weighed to produce the actual yield amount.

C.2 Nitrogen stress corn trial methodology

All corn was planted in mid May utilizing a randomized block design for the 4 treatments (0,0.5X,1X,2X) which were replicated 4 times. The nitrogen treatments were sprayed by the field staff pre-emergence of the corn. All herbicide and pesticide controls were handled by the field staff as part of their crop management program. Approximately 1 week after planting, the corn emerged. Starting approximately 1 week after emergence (2 weeks after planting) corn would be large enough to start taking thermal images. Thermal images would be taken on the edge of the plot pointed at the middle of the treatment as to avoid any edge effects which might be present. The thermal camera was held approximately 1m above the corn surface. The thermal camera was calibrated according to the atmospheric conditions such as air temperature and humidity. The air temperature and humidity was monitored in real time with the use of a small (1.5m height) mobile weather station which outputs data to a handheld console.

Measurements would always be taken at a consistent time of day throughout the growing period (May - August) with consistent weather conditions in mind. Ideally measurements would always be taken on an entirely cloudless day, however in the case small amount of cloud cover which would block the direct sunlight, all measurements would stop and only resume once cloud cover had passed. All data collection would take approximately 10 minutes to take 1-2 pictures of each treatment plot (4 treatments X 4 repetitions = 16 treatment plots). This was

done with speed in mind to ensure relatively consistent atmospheric conditions and radiative flux during data collection.

The field staff had someone on location everyday to ensure continued operation of all fields. Thermal imagery was collected 2-3 times per week on average throughout the growing season. The thermal images were processed utilizing a block averaging tool after each image had been segmented, this was done to ensure only the corn surface temperature would contribute to the calculation (Section 6.3). Through segmentation, the surface temperatures of the soil and shadows would not contribute to any "average temperature" data. Once all images were segmented and averages taken the same treatments from each repetition would be averaged together. For example, the results of the 1X nitrogen rate treatment would be an average of all 4 repetitions of the 1X treatment plots to create a "congregate average".

At the end of the growing season the corn was harvested by hand by the field staff and logged. After harvesting, the ears of each corn plant were removed and weighed to produce the actual yield amount.

C.3 Nitrogen stress wheat trial methodology

The wheat utilized was a variety of "winter wheat". Winter wheat is planted in late September where it grows over the winter to be harvested a year later, usually early August.

All wheat was planted in late September (of the previous year) utilizing a randomized block design for the 4 treatments (0,0.5X,1X,2X) which were replicated 4 times. The nitrogen treatments were sprayed by the field staff pre-emergence of the wheat. All herbicide and pesticide controls were handled by the field staff as part of their crop management program. Approximately 1 week after planting, the corn emerged. Wheat measurements would usually commence early May when the winter wheat becomes active again and starts to turn a vibrant green. Thermal images would be taken on the edge of the plot pointed at the middle of the treatment as to avoid any edge effects which might be present. The thermal camera was held approximately 1m above the wheat. The thermal camera was calibrated according to the atmospheric conditions such as air temperature and humidity. The air temperature and humidity was monitored in real time with the use of a small (1.5m height) mobile weather station which outputs data to a handheld console.

Measurements would always be taken at a consistent time of day throughout the final growing period of the wheat (May - Mid July) with consistent weather conditions in mind. Ideally measurements would always be taken on an entirely cloudless day, however in the case small

amount of cloud cover which would block the direct sunlight, all measurements would stop and only resume once cloud cover had passed. All data collection would take approximately 10 minutes to take 1-2 pictures of each treatment plot (4 treatments X 4 repetitions = 16 treatment plots). This was done with speed in mind to ensure relatively consistent atmospheric conditions and radiative flux during data collection.

The field staff had someone on location everyday to ensure continued operation of all fields. Thermal imagery was collected 2-3 times per week on average throughout the growing season. The wheat would begin to brown in July at which point measurements would stop. The thermal images were processed utilizing a block averaging tool after each image had been segmented, this was done to ensure only the wheat temperature would contribute to the calculation (Section 6.3). Through segmentation, the surface temperatures of the soil and shadows would not contribute to any "average temperature" data. Once all images were segmented and averages taken the same treatments from each repetition would be averaged together. For example, the results of the 1X nitrogen rate treatment would be an average of all 4 repetitions of the 1X treatment plots to create a "congregate average".

At the end of the growing season (August) the corn was harvested by hand by the field staff and logged. After harvesting, the yielding portion of the wheat was removed and weighed.

C.4 Greenhouse nitrogen stress corn trial methodology

The corn in the greenhouse was planted in individual gallon pots which had holes in the bottom to allow for adequate drainage. The gallon pales were initially cleaned out thoroughly to remove any foreign material or chemicals / bacteria from previous trials. The pots were then lined with a thin mesh liner to ensure that the gravel utilized to grow the corn would not fall out of the drainage holes. The bagged gravel would then be individually scoped into the pots with care to not damage or move the liner inside, each pot was filled to approximately 3 inches below the top of the pot. As described in Section 6.2, the trial consisted of 3 nitrogen treatments (high, medium, low) each having a sample size of 30 corn plants, which was replicated twice for a total of 180 plants.

After all pots were filled and positioned on the benches in the greenhouse, water was administered to each pot for approximately 1 minute via a hose. This was done to remove the considerable amount of dust present in the gravel which would prevent even wetting of the nitrogen drip during the trial. The corn was then planted by hand into the centre of each individual pot utilizing a marked stick which would ensure that all seeds are planted at a consistent depth (2 inches). The spray nozzles for each plant were then inserted into the soil and hooked up to the main nitrogen/water line.

The corn took approximately 1 week to emerge from the gravel, during this time no nitrogen is being added to the pots and only fresh water is being supplied through the nozzles. Once the corn emerges, the nitrogen begins to be delivered with the water through a second pump which is connected directly to the nitrogen mixtures. The water/nitrogen delivery system works on a timer, where it initially turns on for approximately 5 minutes every hour and scales to approximately 10 minutes every hour as the corn grows.

The light source in the greenhouse is set to operate in a "supplemental sunshine" setting in order to simulate 16 hours of sunlight. In this supplemental setting, the lights turn on at dawn when the sun rises, and begin to supplement the incoming sunlight for the next 16 hours at which point they turn off. The system is GPS based with a light meter in order to coordinate when the lights are fully on, half on, or completely off as would be the case during a clear sunny day. There's also an air conditioner on one side of the greenhouse in order to regulate the temperature and prevent overheating, especially during the summer.

The greenhouse was checked on daily to ensure that all pumps/lights were functioning properly. Whorl temperatures were taken on a semi daily basis utilizing a hand held thermal gun. Thermal images were taken from the side of each bench looking down on the corn and would gather temperature information of approximate 6 corn plants per picture and were taken approximately twice per week. Thermocouples were also utilized to take 24 hour

measurements, and were placed directly into the whorl of the corn as the corn leaves were too weak to support the thermocouples without inducing stress or harm to the plant.

Each trial took approximately 1 month at which point the corn grew too large for the greenhouse, which corresponded to a corn plant of approximately 10 leaf stage in development.

At the conclusion of the trial, each corn plants stem would be cut with shears right above the gravel. All of the leaves would then be cut off and bagged individually with the corresponding stem. The leaf surface area was then taken for each plant by running all the leaves through a leaf area machine which would calculate total surface area. Each bag (containing leafs and stem) was then dried in a specialized plant drier located at the University of Guelph for approximately 5 days to remove all water content from the plant biomass. Once dried the biomass of each plant was weighed and recorded.

Appendix D: Yield data

D.1 Nitrogen stress wheat yield

Figure D.1 shows the yield breakdown for each plot in the nitrogen stress wheat trial. This is the raw data which is provided post processing of the wheat in the field. The data in the second column labeled "T-MET" represents the yield in metric tons.

University of Guelph

Variable nitrogen rates in winter wheat (U of Waterloo)

Trial ID:14-TRZAW-31-EN Location:Elora, Ontario Trial Year:2014
Protocol ID:14-TRZAW-31-EN Investigator:Peter J. Smith
Project ID: Study Director:
Sponsor Contact:

Crop Code	TRZAW	TRZAW
BBCH Scale	BCER	BCER
Crop Scientific Name	Triticum ae>	Triticum ae>
Crop Name	Winter wheat	Winter wheat
Rating Date	Aug-1-2014	Aug-1-2014
Rating Type	YIELD	YIELD
Rating Unit	G/plot	T-MET
Number of Subsamples	1	1
ARM Action Codes		TY1
Number of Decimals		2
Plot		
101	2721.3	2.61046143323765
102	4580.1	4.39355249710497
103	4918	4.71768982789945
104	4513.5	4.32966511553968
204	4982.7	4.77975459647714
203	2202.8	2.11307994162198
202	4552.5	4.36707664528512
201	4880.3	4.68152534914552
301	4842.5	4.6452651
302	4648.2	4.45887878366047
303	5552	5.32586700376123
304	2495.1	2.39347456071409
404	5107	4.89899185666582
403	6246.8	5.99236779522616
402	4046.3	3.88149417458917
401	2995.4	2.87339733844856

Sort Order: Assessment (Serpentine within blocks)

Figure D.1 Nitrogen stress wheat trial yield data

D.2 Nitrogen stress corn yield

Figure D.2 shows the aggregate yield data for the nitrogen stress corn trial. The data shown has already combined the 4 repetitions of each treatment, therefore the numbers shown in the columns labeled "1" and "2" represent the sum of all 4 repetitions for each treatment. The second column labeled "Yield T-MET" represents the yield in metric tons.

University of Guelph

Corn response to variable nitrogen rates

Trial ID:14-ZEAMX-37-AT Location:Arkell, ON. Trial Year:2014
Protocol ID:14-ZEAMX-37-AT Investigator:Peter J. Smith
Project ID: Study Director:
Sponsor Contact:

Trt No.	Treatment Name	Rate	Rate Unit	Appl Code	1	2
	Crop Code				ZEAMX	ZEAMX
	BBCH Scale				BCOR	BCOR
	Crop Scientific Name				Zea mays	Zea mays
	Crop Name				Corn	Corn
	Rating Date				Nov-10-2014	Nov-10-2014
	Rating Type				Yield	YIELD
	Rating Unit				G/sample	T-MET
	Number of Subsamples				1	1
	Footnote Number				1	1
	ARM Action Codes					TY1
	Number of Decimals					2
	10X NITROGEN			A	1387.55c	2.80c
	PRIMEXTRA II MAGNUM	4	l/ha	A		
	CALLISTO	0.3	l/ha	A		
	21/2X NITROGEN			A	2140.58b	4.31b
	PRIMEXTRA II MAGNUM	4	l/ha	A		
	CALLISTO	0.3	l/ha	A		
	31X NITROGEN			A	3276.50a	6.60a
	PRIMEXTRA II MAGNUM	4	l/ha	A		
	CALLISTO	0.3	l/ha	A		
	42X NITROGEN			A	3629.15a	7.31a
	PRIMEXTRA II MAGNUM	4	l/ha	A		
	CALLISTO	0.3	l/ha	A		
	LSD (P=.05)				746.801	1.504
	Standard Deviation				466.904	0.941
	CV				17.9	17.9
	Bartlett's X2				1.306	1.306
	P(Bartlett's X2)				0.728	0.728
	Skewness				0.2741	0.2741
	Kurtosis				-0.3624	-0.3624
	Replicate F				3.642	3.642

Replicate Prob(F)	0.0574	0.0574
Treatment F	19.557	19.557
Treatment Prob(F)	0.0003	0.0003

Crop Code
ZEAMX, BCOR, Zea mays, = US
Rating Type
Yield = yield
Rating Unit
T-MET = ton (metric=1000 kg)
ARM Action Codes
TY1 = 0.00201453*[1]

Footnote 1: Hvst area 3.03 m x 1.52 m

Means followed by same letter do not significantly differ (P=.05, Student-Newman-Keuls)
Mean comparisons performed only when AOV Treatment P(F) is significant at mean comparison OSL.

Figure D.2 Nitrogen stress corn yield data

D.3 Weed stress corn yield

Figure D.3 shows the aggregate yield data for the weed stress corn trial. The data shown has already combined the 4 repetitions of each treatment, therefore the numbers shown in the columns labeled "1" and "2" represent the sum of all 4 repetitions for each treatment. The second column "T-MET" represents the yield in metric tons.

University of Guelph

Corn stress recovery as affected by timing of weed removal

Trial ID:14-ZEAMX-41-ET Location:Elora, Ontario Trial Year:2014
Protocol ID:14-ZEAMX-41-ET Investigator:Peter J. Smith
Project ID: Study Director:
Sponsor Contact:

Trt No.	Treatment Name	Rate	Rate Unit	Appl Code	1	2
	Crop Code				ZEAMX	ZEAMX
	BBCH Scale				BCOR	BCOR
	Crop Scientific Name				Zea mays	Zea mays
	Crop Name				Corn	Corn
	Part Rated				GRAIN -	GRAIN -
	Rating Date				Nov-6-2014	Nov-6-2014
	Rating Type				MOICON	YIELD
	Rating Unit				%	T-MET
	Number of Subsamples				1	1
	Days After First/Last Applic.				171 130	171 130
	Trt-Eval Interval				171 DA-A	171 DA-A
	Plant-Eval Interval				171 DP-1	171 DP-1
	Days After Emergence				161 DE-1	161 DE-1
	ARM Action Codes					TY1
	Number of Decimals					2
1	Weed free check			A	28.78ab	10.56ab
	HALEX GT	2205	g ai/ha	A		
2	NO wheat removal			B	27.55b	3.25c
	Full season stress			B		
	HALEX GT	2205	g ai/ha	B		
3	Wheat removal T1			C	29.63ab	10.38ab
	2-3 leaf corn			C		
	HALEX GT	2205	g ai/ha	C		
4	Wheat removal T2			D	28.45ab	12.59a
	4-5 leaf corn			D		
	HALEX GT	2205	g ai/ha	D		
5	Wheat removal T3			E	30.43a	9.85ab
	6-7 leaf corn			E		
	HALEX GT	2205	g ai/ha	E		

6Wheat removal T4		F	31.03a	7.66b
8-9 leaf corn		F		
Matches 2013 timing		F		
HALEX GT	2205g ai/ha	F		
LSD (P=.05)			1.945	2.263
Standard Deviation			1.291	1.502
CV			4.41	16.59
Bartlett's X2			4.136	1.206
P(Bartlett's X2)			0.53	0.944
Skewness			-0.5752	-0.614
Kurtosis			1.8496*	0.0485
Replicate F			0.510	5.082
Replicate Prob(F)			0.6816	0.0126
Treatment F			4.035	18.749
Treatment Prob(F)			0.0161	0.0001

Crop Code
ZEAMX, BCOR, Zea mays, = US
Part Rated
GRAIN = grain
Rating Type
YIELD = yield
MOICON = moisture content
Rating Unit
Kg/plot = kilograms per plot
% = percent
T-MET = ton (metric=1000 kg)
Plant-Eval Interval
171 DP-1 = 1 ZEAMX May-19-2014
ARM Action Codes
TY1 = 1.144165*[1]*(100-[2])/84.5

Means followed by same letter do not significantly differ (P=.05, Student-Newman-Keuls)
Mean comparisons performed only when AOV Treatment P(F) is significant at mean comparison OSL.

Figure D.3 Weed stress corn yield data